

Hybrid Set-Seeking Systems

MODEL-FREE FEEDBACK OPTIMIZATION VIA HYBRID INCLUSIONS

JORGE I. POVEDA, ANDREW R. TEEL

J. I. Poveda (poveda@ucsd.edu) is with the Department of Electrical and Computer Engineering, University of California, San Diego, USA

A. R. Teel (teel@ucsb.edu) is with Department of Electrical and Computer Engineering, University of California, Santa Barbara, USA

Hybrid dynamical systems, which combine continuous-time and discrete-time dynamics, are pervasive in modern engineering. They naturally arise in cyber-physical systems (CPS) that integrate physical processes with digital components, spanning domains such as transportation [1], power grids [2], robotics [3], and power electronics [4]. Beyond cyber-physical systems, hybrid dynamics also appear in a wide range of applications, including mechanical systems with impacts [5], chemical process control [6], manufacturing systems [7], and synchronization mechanisms in biological systems [8, Ex. 1.2]. In the context of control and decision-making, hybrid systems can model algorithms that involve logic modes, timers, resets, impulsive actions, sampled-data structures, switching dynamics, event-triggered mechanisms, and general “if-then” rules, [8]–[10]. Hybrid systems are also closely related to frameworks widely studied in computer science and engineering, such as the well-known hybrid automata [11]–[13].

Despite the prevalence of hybrid systems in engineering and science, the development of extremum-seeking (ES) methods for systems with hybrid dynamics remained relatively unexplored until recently. ES systems are feedback control mechanisms designed to achieve real-time steady-state optimization in dynamical systems where both the plant dynamics and the cost function are unknown. This “model-free” characteristic makes ES an adaptable and powerful feedback control scheme for various

complex engineering applications where precise mathematical models are unavailable. As a result, ES has become widely adopted across different industries and areas, including engine optimization [14], wind turbine control [15], underwater vehicles [16], [17], ABS brake systems [18], autotuning systems [19], photolithography in semiconductor manufacturing [20], fuel cells [21], control of mobile robots [22], HVAC systems [23], model predictive control [24], biological systems [25], traffic control [26], [27], mechanical systems [28]–[30], sampled-data systems [31], [32], etc. For surveys on ES, we refer the reader to [33]–[35], as well as to [36, Sec. 13.3].

The idea of using feedback control mechanisms for real-time black-box optimization in dynamical systems dates back to the early 1920s with LeBlanc’s work [37], and was further advanced in the 1950s [38] and 1960s [39]–[42] in the adaptive controls’ literature under the name of “extremum control” [43, Sec. 13.3]. However, most of the stability results for ES nonlinear systems emerged in the 1990s and 2000s, utilizing multi-time scale methods for ODEs and identifying the appropriate time scales associated with the components of the algorithms [44]. Since then, different analytical tools for ES have been developed to solve model-free optimization and decision-making problems in single-agent systems [45]–[50], multi-agent systems [51]–[53], PDEs [54], stochastic systems [55], and more.

As the foundational theory behind ES relied on perturbation tools for locally Lipschitz ordinary differential equations (ODEs), particularly averaging [56], [57] and singular perturbations [57]–[59], the majority of the ES systems and algorithms were designed for applications with closed-loop smooth dynamics. In

particular, the study of ES systems that incorporate discrete-time behaviors—such as “events” triggered by specific conditions, abrupt state “jumps” or “resets” aimed at enhancing performance, or algorithms that “switch” between different dynamics during the seeking process—has received comparatively less attention. Such systems, which are naturally hybrid, also arise across different applications where either the plant is a hybrid system or the controller must be hybrid to address fundamental limitations of traditional smooth control techniques. These limitations can be related to achieving desired transient or steady-state performance or handling complexities such as dynamic communication networks, resource-constrained actuators, occluded operational spaces, or dynamic adversarial environments. ES systems with discrete states, such as logic modes, also arise when general “if-then” rules are incorporated into the decision-making algorithms, which is now a standard practice in the design and implementation of controllers and optimization algorithms for autonomous and [60] and cyber-physical systems [61]. Despite the limited available theoretical tools for their analysis and design, ES algorithms with logic states and switching rules have been explored for particular applications since the early 1970s [62], when a switching hysteresis-based mechanism was designed to stabilize a peak-holding adaptive controller in electrical machines with neglected dynamics. Modern approaches of ES that incorporate discrete-time behaviors via switches or resets have also been studied for the efficient control of photovoltaic power systems [63] and HVAC systems in industry [23]. However, a comprehensive theory for the study of hybrid ES systems has lagged behind their practical applications, despite its potential to enable the design of novel feedback architectures and techniques capable of addressing a broader class of problems than those handled by traditional ES methods.

As discussed later in the paper, ES systems with hybrid dynamics typically exhibit stability properties with respect to general *sets* rather than isolated equilibria. We therefore refer to these controllers as *hybrid set-seeking systems*, which are generally characterized by non-smooth dynamics modeled through differential and difference inclusions rather than standard differential or difference equations. Building on this perspective, the primary aim of this paper is to provide an accessible introduction to non-smooth and hybrid set-seeking systems formulated as hybrid inclusions. We begin with well-established smooth ES algorithms extensively studied in the literature [44], [64]–[67], which can be viewed as hybrid set-seeking schemes with negligible discrete-time dynamics. We then extend this perspective by incorporating hybrid dynamics through averaging tools, enabling the solution of complex model-free optimization and decision-making problems in static maps. Next, we show how singular perturbation methods for hybrid systems can address seeking problems in plants governed by dynamical systems rather than static maps. Taken together, these developments yield perturbation-based tools for multi-time-scale hybrid inclusions, providing a unified framework for analyzing and designing hybrid seeking algorithms that overcome the lim-

itations of traditional smooth ES methods. The effectiveness of this framework is demonstrated through diverse applications and numerical examples, showcasing the flexibility and robustness of the proposed tools.

Perturbation Theory and Seeking Systems

The key mathematical property that enables the design and analysis of most ES algorithms modeled as oscillatory, locally Lipschitz ODEs of the form

$$\dot{x} = f(x, \omega t), \quad x \in \mathbb{R}^n, \quad t \in \mathbb{R}_{\geq 0}, \quad (1)$$

is that, for a sufficiently large oscillation frequency ω , the solutions of (1) can be approximated on finite intervals by those of the so-called *average dynamics*:

$$\dot{\bar{x}} = f_{\text{ave}}(\bar{x}) := \frac{1}{T_\omega} \int_0^{T_\omega} f(\bar{x}, \omega t) dt, \quad \bar{x} \in \mathbb{R}^n, \quad (2)$$

where $T_\omega = 2\pi/\omega$ is the oscillation period of $f(x, \cdot)$. For example, to minimize an unknown smooth scalar static map $J : \mathbb{R} \rightarrow \mathbb{R}$ representing the plant, the simplest ES continuous-time algorithm based on periodic probing, studied in [44], [65], [66] can be modeled by the following equations:

$$u = \hat{u} + \varepsilon_a \sin(\omega t), \quad (3a)$$

$$\dot{\hat{u}} = -\frac{2}{\varepsilon_a} J(u) \sin(\omega t), \quad (3b)$$

where $\varepsilon_a > 0$ and $\omega > 0$ are tunable parameters. A Taylor expansion of J around \hat{u} for small values of ε_a , and a direct computation of (2) using the identities $\int_0^{T_\omega} \sin(\omega t) dt = 0$ and $\frac{1}{T_\omega} \int_0^{T_\omega} \sin(\omega t)^2 dt = \frac{1}{2}$ show that the average dynamics of (3) corresponds to the following ε_a -perturbed system, with state $\bar{u} \in \mathbb{R}$:

$$\dot{\bar{u}} = f_{\text{ave}}(\bar{u}) = -\frac{\partial J(\bar{u})}{\partial \bar{u}} + O(\varepsilon_a), \quad (4)$$

where $O(\varepsilon_a)$ indicates bounded perturbations (on compact sets) of order ε_a . In turn, as $\varepsilon_a \rightarrow 0^+$, the behavior of system (4) can be approximated by a standard gradient flow of J , with state $\tilde{u} \in \mathbb{R}$ and dynamics

$$\dot{\tilde{u}} = -\frac{\partial J(\tilde{u})}{\partial \tilde{u}}. \quad (5)$$

Under suitable regularity (e.g., locally Lipschitz) properties in system (5), we can use standard robustness results for differential equations (see “Closeness of solutions for Perturbed Systems”) to assert that the solutions of (4) and (5) are (T, ε) -close when ε_a is sufficiently small [57], [68]. Namely, for each compact set of initial conditions, each $T > 0$, and each $\varepsilon > 0$ there exists $\varepsilon_a^* > 0$ such that for all $\varepsilon_a \in (0, \varepsilon_a^*)$ the solutions of (4) and (5) satisfy the bound

$$\sup_{t \in [0, T]} |\bar{u}(t) - \tilde{u}(t)| \leq \frac{\varepsilon}{2}. \quad (6)$$

Similarly, by leveraging results on averaging theory for differential equations [59] (see “Averaging Theory: From ODEs to Hybrid Systems”), it can be shown that, for a fixed and sufficiently small $\varepsilon_a > 0$, the solutions of (3) and (4) are also (T, ε) -close when ω is sufficiently large, i.e., for each compact set of initial conditions, each $T > 0$, and each $\varepsilon > 0$ there exists

a sufficiently large frequency $\omega^* > 0$ such that for all $\omega > \omega^*$ the solutions of (3) and (4) satisfy the bound

$$\sup_{t \in [0, T]} |\hat{u}(t) - \bar{u}(t)| \leq \frac{\epsilon}{2}. \quad (7)$$

By combining the bounds (6) and (7), we can conclude that the trajectories of the ES dynamics (3) and those of the gradient flow (5) are also (T, ϵ) -close in compact sets. This property immediately allows us to obtain qualitative attributes for the behavior of the solutions of the model-free ES dynamics (3) based on the behavior of the solutions of the model-based gradient flow (5), provided the parameters (ω, ϵ_a) are appropriately tuned. Among such attributes, we can infer stability properties for system (3) based on the stability properties of (5), provided that such stability properties are "robust" to small perturbations, an attribute that, under the Lipschitz continuity of (5), can be readily established using, for example, Lyapunov functions. This perturbation-based methodology for the study of smooth ES lies at the heart of the design and stability analysis of most algorithms, including those whose average dynamics (2) are not simple perturbed gradient flows, but instead follow alternative well-posed optimization dynamics, such as primal-dual dynamics [69], projected gradient flows [70], Riemannian gradient flows [71], Newton flows [72], pseudo-gradient flows for games [51], decentralized optimization dynamics [73], etc, see [65] for a unifying framework.

Fortunately, the perturbation methodology described above extends to systems with hybrid dynamics under appropriate, mild regularity conditions and with an appropriate measure of closeness. For the latter, we note that, unlike smooth ODEs, solutions to hybrid systems are typically discontinuous, making the use of the uniform distance, as in (6)-(7), to measure the closeness between solutions of nominal and perturbed systems problematic. For instance, if \hat{u} is a solution of a hybrid system that has a discontinuity at time t' , and \bar{u} is a solution of a ϵ_a -perturbed version of the same system that has a discontinuity at time $t' + \epsilon_a$, then no matter how small ϵ_a is, \hat{u} and \bar{u} will never be (T, ϵ) -close at time t' , regardless of the choice of ϵ_a . Thus, a different measure of closeness is required to link the qualitative behaviors of the perturbed and unperturbed systems. Although this issue is well-known in the hybrid systems literature [74, Example 3], we will illustrate this phenomenon in a stylized hybrid set-seeking system that exhibits "jumps" in the states, resulting in Zeno-like behavior reminiscent of a bouncing ball without air resistance.

Generalized Solutions for Hybrid Seeking Systems

To extend the perturbation-based methodology to seeking systems with hybrid dynamics, we must generalize both the mathematical models we consider and their corresponding notions of solutions. Specifically, in studying hybrid seeking systems, we will parameterize solutions using a continuous-time index $t \in \mathbb{R}_{\geq 0}$ and a discrete-time index $j \in \mathbb{Z}_{\geq 0}$. The primary benefit of this parameterization is that it allows solutions to be defined in

hybrid time domains. For such solutions, the concept of (T, ϵ) -closeness can be naturally extended by measuring the distance between the *graphs* of the nominal and perturbed solutions, that is, by using set-convergence (between graphs) as opposed to the standard uniform convergence. This can be achieved, provided the hybrid dynamics exhibit certain mild regularity properties. We will illustrate these regularity properties through various examples of hybrid seeking systems with different types of hybrid time domains. By defining solutions in such domains and employing graphical convergence to analyze the limiting behavior of perturbed solutions, we can seamlessly extend the perturbation-based methodology traditionally used in extremum-seeking control [45], [65], [66] to general hybrid set-seeking systems.

Seeking Systems modeled as Hybrid Inclusions

Most ES dynamics studied via averaging are modeled by ODEs of the form (1). However, it is also useful to generalize these models for the study of hybrid seeking systems. For instance, hybrid systems often exhibit discontinuities, or "jumps," in the state, governed by a set-valued update rule of the form $x^+ \in G(x)$, where x^+ denotes the state value immediately after the jump. This type of update rule, known as a "difference inclusion", allows x^+ to take any value within the set $G(x)$, which may contain infinitely many points for a given x . These models are powerful because they can capture more general and flexible behaviors and decision-making rules compared to standard difference equations of the form $x^+ = g(x)$. Similarly, hybrid ES algorithms may also involve continuous-time dynamics described by differential inclusions of the form $\dot{x} \in F(x)$, which can arise from discontinuous vector fields requiring appropriate regularizations (e.g., Krasovskii, Filippov, etc) for analysis, or from optimization and decision-making algorithms that are inherently set-valued [75].

By incorporating set-valued updates in the continuous-time and/or discrete-time dynamics, hybrid inclusions can also provide a robust mathematical framework for modeling and analyzing seeking algorithms that are influenced by external discontinuous coordinating signals that govern system behavior. Such signals can arise in a variety of contexts, including switching dynamics [76], time-varying optimization problems [77], event-triggered systems [9], and systems with resetting timers [78], to name just a few examples. As such, most of the models in our study of hybrid set-seeking algorithms will be represented using hybrid inclusions.

The remainder of this paper is divided into three main sections. In Part 1, we present the preliminaries on hybrid systems and introduce the mathematical language necessary to study hybrid set-seeking systems. Part 2 focuses on hybrid seeking algorithms for plants characterized by static maps, while Part 3 extends these results to systems with dynamic plants. The main developments are complemented by several supporting discussions. "Continuous-Time Set-Valued Dynamical Systems" and "Discrete-Time Set-Valued Dynamical Systems" offer brief

introductions to dynamical systems modeled as differential and difference inclusions, respectively. "Averaging Theory: From ODEs to Hybrid Inclusions" provides a mathematical overview of averaging theory applicable to hybrid set-seeking systems, and "Singularly Perturbed Hybrid Dynamical Systems" introduces the mathematical tools needed for studying hybrid systems in singular perturbation form. The notation used throughout this article is defined in Table 1.

Summary

This article focuses on the analysis and synthesis of extremum-seeking systems that incorporate *hybrid dynamics* in the loop, encompassing both continuous-time and discrete-time behaviors. Such extremum-seeking systems arise from the need to use advanced control and optimization algorithms to overcome the limitations of standard smooth feedback techniques and to meet stringent transient and steady-state demands in high-performance applications. They also emerge in settings where traditional controllers must be implemented on plants that naturally exhibit hybrid behaviors, such as in cyber-physical and autonomous systems, which rely on digital devices for computation, actuation, and sensing.

To explore hybrid extremum-seeking dynamics using control-theoretic tools, we begin by reviewing the key technical concepts that enable the development of perturbation theory for hybrid inclusions. These concepts provide the foundations for both averaging and singular perturbation theory in these systems. We then demonstrate how these tools can be applied to the analysis and synthesis of various hybrid extremum-seeking algorithms for plants modeled as static maps. In particular, we present several examples of set-valued and switching extremum-seeking algorithms under various switching scenarios: arbitrarily fast, under dwell-time and average dwell-time constraints, and under average activation time constraints. Additionally, we explore state-based switching extremum seeking in the context of obstacle avoidance problems, as well as Gradient-Newton switching extremum-seeking schemes. Other topics include extremum seeking with momentum and resets, with intermittent updates, slowly-varying parameters, and using safety mechanisms to incorporate constraints. In all these applications, we show how the perturbation-based approach, traditionally used for studying smooth extremum seeking control, can naturally be extended to hybrid systems, provided they satisfy suitable mild regularity conditions and their solutions are modeled in a hybrid time domain. Finally, in part 3 we address dynamic plants and discuss how the proposed hybrid extremum-seeking controllers can be integrated with such plants to solve model-free feedback optimization and decision-making problems. Building on established results for extremum seeking and using various illustrative examples, this article aims to provide an introductory and tutorial-

style presentation of hybrid extremum-seeking systems, making it accessible to readers from different backgrounds, including those with no prior experience in hybrid systems.

PART 1: PRELIMINARIES IN HYBRID SYSTEMS

Hybrid dynamical systems (HDS), or simply "hybrid systems", are dynamical systems that combine continuous-time and discrete-time phenomena. Therefore, a natural mathematical representation of such systems would involve both differential equations and discrete-time recursions. In this article, we follow the formalism presented in [8] to study general hybrid systems; see also [74] for a tutorial dedicated exclusively to such systems. In its simplest form, a hybrid system with state $x \in \mathbb{R}^n$, can be represented by the following expressions:

$$x \in C, \quad \dot{x} = f(x), \quad (8a)$$

$$x \in D, \quad x^+ = g(x), \quad (8b)$$

where (8a) describes the continuous-time dynamics, and (8b) describes the discrete-time dynamics. The notation in (8a) indicates that the state x is allowed to evolve according to the continuous-time dynamics $\dot{x} = f(x)$ whenever the condition $x \in C$ holds, where the set $C \subset \mathbb{R}^n$ is called the *flow set*. Similarly, the notation in (8b) indicates that x is allowed to evolve

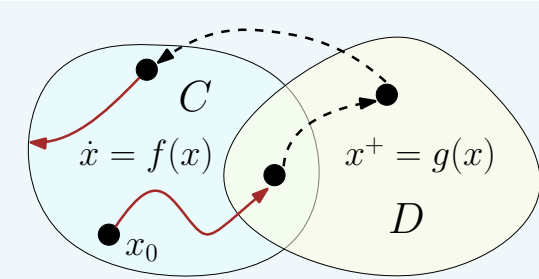


FIGURE 1 Abstract representation of a solution of a hybrid system (8) from the initial point x_0 .

according to the discrete-time dynamics $x^+ = g(x)$ whenever the condition $x \in D$ holds, where the set $D \subset \mathbb{R}^n$ is called the *jump set*, and where x^+ denotes the value of x after an "instantaneous" change –or jump– in the state. For consistency, we call the functions $f : \mathbb{R}^n \rightarrow \mathbb{R}^n$ and $g : \mathbb{R}^n \rightarrow \mathbb{R}^n$ the *flow map* and the *jump map*, respectively. In this way, the hybrid system (8) can be represented by the tuple $\mathcal{H} = \{f, C, g, D\}$, which we call the *data* of the system. Note that when $D = \emptyset$, the system (8) recovers a constrained continuous-time dynamical system. Similarly, when $C = \emptyset$, the system (8) recovers a constrained discrete-time dynamical system. Figure 1 shows an abstract representation of a possible "solution" to (8), starting from x_0 , and experiencing an initial interval of flow, followed by two consecutive jumps and a final interval of flow that eventually hits the boundary of C , forcing the solution to stop. We will

TABLE 1 Notation used in the paper.

Symbol	Definition
\mathbb{R}	Set of real numbers
\mathbb{R}^n	The n -dimensional Euclidean space
$\mathbb{Z}_{\geq 0}$	Set of non-negative integers
\dot{x}	Time derivative of the state of a system
x^+	State of a system after a jump
\emptyset	The empty set
$\bar{\mathcal{A}}$	The closure of the set \mathcal{A}
$\text{co}(\mathcal{A})$	The convex hull of the set \mathcal{A}
$\text{bd}(\mathcal{A})$	The boundary of the set \mathcal{A}
x^\top	The transpose of the vector x
$(x^\top, y^\top)^\top$	Equivalent notation for $[x^\top, y^\top]^\top$
$ x $	Euclidean norm of the vector x
\mathbb{B}	The closed unit ball, of appropriate dimension, in the Euclidean norm
S^1	The set $\{x = (x_1, x_2) \in \mathbb{R}^2 : x_1^2 + x_2^2 = 1\}$
S^n	The n th-Cartesian product $S^1 \times \dots \times S^1$.
$f : \mathbb{R}^n \rightarrow \mathbb{R}^m$	A function from \mathbb{R}^n to \mathbb{R}^m
$F : \mathbb{R}^n \rightrightarrows \mathbb{R}^m$	A set-valued mapping from \mathbb{R}^n to \mathbb{R}^m
\mathbf{R}_o	The matrix $\mathbf{R}_o = \begin{bmatrix} 0 & 1 \\ -1 & 0 \end{bmatrix}$
\mathcal{K}_∞	Class of functions $\alpha : \mathbb{R}_{\geq 0} \rightarrow \mathbb{R}_{\geq 0}$ that are zero at zero, continuous, strictly increasing, and unbounded.
\mathcal{KL}	Class of functions $\beta : \mathbb{R}_{\geq 0} \times \mathbb{R}_{\geq 0} \rightarrow \mathbb{R}_{\geq 0}$ that are nondecreasing in their first argument, nonincreasing in their second argument, satisfy $\lim_{r \rightarrow 0^+} \beta(r, s) = 0$ for each $s \in \mathbb{R}_{\geq 0}$, and $\lim_{s \rightarrow \infty} \beta(r, s) = 0$ for each $r \in \mathbb{R}_{\geq 0}$.

rigorously formalize this notion of "solution" and illustrate its application to study hybrid set-seeking systems.

Example 1 (Systems with Periodic Resets)

To illustrate how the data in (8) can be used to model a common class of systems encountered in practice in control, such as systems with periodic resets, let $x = (x_1, x_2) \in \mathbb{R}^2$, and consider the following hybrid dynamics:

$$x \in C := [0, T] \times \mathbb{R}, \quad \dot{x} = \begin{pmatrix} \dot{x}_1 \\ \dot{x}_2 \end{pmatrix} = f(x) := \begin{pmatrix} 1 \\ -\gamma x_2 \end{pmatrix},$$

$$x \in D := \{T\} \times \mathbb{R}, \quad x^+ = \begin{pmatrix} x_1^+ \\ x_2^+ \end{pmatrix} = g(x) := \begin{pmatrix} 0 \\ \frac{1}{2}x_2 \end{pmatrix},$$

where $T, \gamma > 0$ are tunable parameters. In this system, the state x_1 can be seen as a timer that grows linearly during flows and is reset to zero every time the condition $x_1 = T$ is satisfied. Whenever such resets occur, the state x_2 is also reset to one half of its previous value. Since resets of x_1 force x to satisfy conditions $x \in C$ and $x \notin D$, every jump in the system is followed by a period of flow of duration T , during which the continuous-time dynamics of x_2 make it decrease exponentially at a rate dictated by γ . Figure 2 shows the trajectories of x_1 and x_2 generated by this simple hybrid system, using $T = 10$, $\gamma = \frac{1}{10}$, and from the initial conditions $(0, 10)$. The dashed lines indicate the jumps in the values of the states x triggered by the discrete-time dynamics $x^+ = g(x)$. Note that for this system,

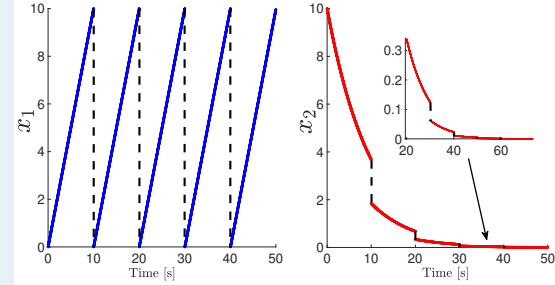


FIGURE 2 Trajectory generated by the hybrid system of Example 1, with initial condition $x_0 = (0, 10)$. Left: Trajectory of x_1 . Right: Trajectory of x_2 .

the intersection of the flow set and the jump set is not empty. In fact, we have $D \cap C = \{T\}$. However, for initial conditions satisfying $x_1 = T$, the continuous-time dynamics $\dot{x}_1 = 1$ cannot flow and extend x_1 without leaving the set C , for example, no solutions can evolve via flows from this initialization. On the other hand, from this same initial condition, the state x_1 can be extended in time via jumps by immediately resetting x_1 and x_2 . This type of behavior will be formalized later when we discuss the notion of solutions to hybrid systems of the form (8). In the meantime, we note that, while the state x_2 converges to zero in Figure 2, the state x_1 continues to oscillate restricted to the set $[0, T]$. Therefore, for this hybrid system it is reasonable to study the stability properties with respect to the compact set $\mathcal{A} = [0, T] \times \{0\}$. This simple example serves to illustrate the fact that, unlike differential equations of the form (3), stability properties in hybrid seeking systems will be studied with respect to general sets, as opposed to equilibrium points. \square

Dynamic timers, such as those in Example 1, are common in hybrid systems to model time-triggered jumps, which can arise in sampled-data systems, switching algorithms, event-triggered control, and reset-based controllers, to name just a few examples. Incorporating exogenous timers into hybrid systems is also useful for studying time-varying dynamics, which are particularly relevant in ES systems, such as (3). In this case, the overall dynamics can be written as a hybrid system with states $(x, \tau) \in \mathbb{R}^n \times \mathbb{R}$, and the dynamics given by

$$(x, \tau) \in C \times \mathbb{R}_{\geq 0}, \quad \dot{x} = f(x, \tau), \quad \dot{\tau} = \omega, \quad (9a)$$

$$(x, \tau) \in D \times \mathbb{R}_{\geq 0}, \quad x^+ = g(x), \quad \tau^+ = \tau, \quad (9b)$$

where $\omega > 0$ dictates the rate of evolution of τ . Note that (9) can be written as (8) using the extended state $y = (x, \tau)$.

The following example illustrates a class of time-varying hybrid systems with oscillating flow maps that are of interest in this article, which also exhibit a well-known behavior that can emerge in hybrid systems: Zeno phenomena.

Example 2 ("Bouncing" Seeking Systems)

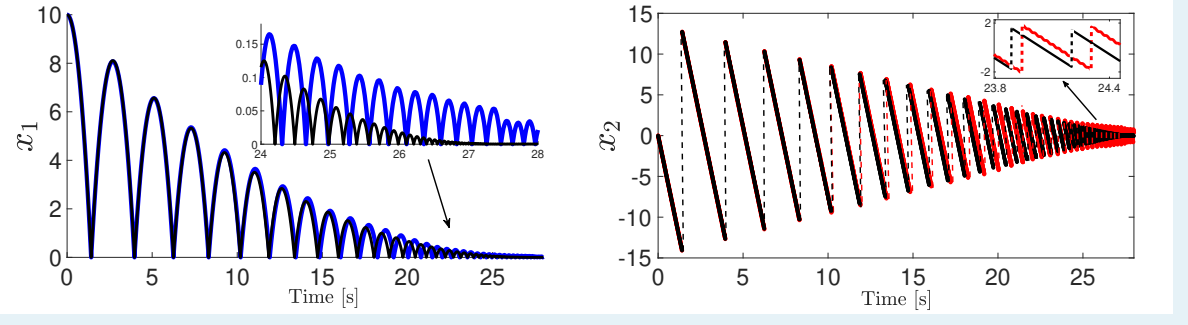


FIGURE 3 Trajectories of the "bouncing" seeking system with time-varying function $\gamma(\tau)$ using $\omega = 100$ (shown in color blue), and with constant $\gamma = \bar{\gamma} = 10$ (shown in color black). Left: Trajectories of the position x_1 . Right: Trajectories of the velocity x_2 , which experience jumps, illustrated with dashed lines.

Bouncing balls are classic examples of hybrid systems. Their dynamics are governed by Newtonian physics while the ball is in the air and experience instantaneous jumps upon hitting the ground. These models are most accurate when the ball is rigid and the deformations caused by impacts are negligible. Inspired by classic bouncing ball systems [8, Ex. 1.1], we can consider a hybrid system of the form (9), with state $x = (x_1, x_2) \in \mathbb{R}^2$, where x_1 models the vertical position of a point-mass ball bouncing vertically on a horizontal surface and x_2 models the vertical velocity of the ball. Following the notation in (9), the data of this system is given by

$$C := \{(x_1, x_2) \in \mathbb{R}^2 : x_1 \geq 0\}, \quad (16a)$$

$$\begin{pmatrix} \dot{x}_1 \\ \dot{x}_2 \end{pmatrix} = f(x, \tau) := \begin{pmatrix} x_2 \\ -\gamma(\tau), \end{pmatrix}, \quad \dot{\tau} = \omega, \quad (16b)$$

$$D = \{(x_1, x_2) \in \mathbb{R}^2 : x_1 = 0, x_2 \leq 0\}, \quad (16c)$$

$$\begin{pmatrix} x_1^+ \\ x_2^+ \end{pmatrix} = g(x) := \begin{pmatrix} 0 \\ -\lambda x_2 \end{pmatrix}, \quad \tau^+ = \tau, \quad (16d)$$

where the time-varying function $\gamma(\cdot)$ is given by

$$\gamma(\tau) = 2\bar{\gamma} \sin(\tau)^2, \quad (17)$$

and where $\bar{\gamma}$ denotes the nominal gravitational acceleration constant and $\lambda \in (0, 1)$ is a restitution coefficient. According to (16a), whenever the altitude is non-negative, the ball flows through the air via (16b) under oscillatory acceleration $-\gamma(\tau)$. On the other hand, according to (16c)-(16d), when the ball touches the ground (i.e., $x_1 = 0$) and its velocity is non-positive, the mapping g resets the sign of the velocity and also decreases its magnitude using the restitution coefficient λ . Note that the position of the ball does not change during jumps. Figure 3 illustrates the behavior of the solutions generated by this "bouncing" seeking system when $\omega = 100$ (colored trajectories), and also when $\gamma(\tau) = \bar{\gamma}$ is constant (black trajectories). It can be observed that the highly oscillatory hybrid dynamics that use $\omega = 100$ provide a suitable approximation of the behavior of the hybrid system that uses a constant acceleration γ . This approximation is particularly accurate at the beginning of the

simulation but, as shown on the inset, it eventually deteriorates, as seen by the bouncing times starting to deviate, as the number of jumps grows unbounded. Note that the hybrid system with constant acceleration $\dot{x}_2 = -\bar{\gamma}$ exhibits Zeno behavior as time approaches approximately 28s, as the amount of time between jumps decreases to zero. Similar phenomena typically emerge in certain hybrid control systems such as in event-triggered controllers [79]. This behavior is also "approximately" inherited by the hybrid system (16) with oscillatory acceleration $\gamma(\tau)$. To study hybrid set-seeking systems, we will formalize this "approximation" property using averaging theory for hybrid systems. \square

Switching systems constitute a class of hybrid dynamical systems that arise frequently in applications. When such systems are modeled within a hybrid systems framework, their qualitative behavior is typically analyzed with respect to prescribed *families* of switching signals [76], [80]. In this case, set-valued dynamics can provide a convenient mathematical tool to model different types of switching signals. We illustrate this idea in the following example.

Example 3 (Source-Seeking and Surveillance)

Consider a point-mass vehicle in the plane, with state $x \in \mathbb{R}^2$ modeling its position, and simple dynamics given by a single integrator

$$\dot{x} = \alpha, \quad (18)$$

where α is the input to be designed. We study a typical application of ES in the context of source-seeking [81]–[83], where the vehicle (18) seeks to stabilize its position at the location where a potential signal, only available via measurements, attains its maximum intensity. However, unlike standard source-seeking problems with a single static potential field, we consider the presence of multiple intermittent potential fields, which are "active" only during bounded periods of time and never simultaneously. In this case, the goal of the vehicle is to achieve *persistent source-seeking and surveillance* assuming the

Continuous-Time Set-Valued Dynamical Systems

Set-valued continuous-time dynamics modeled as *differential inclusions* typically arise in hybrid seeking systems due to discontinuous feedback-based optimization or decision-making algorithms, plants with uncertain parameters, or auxiliary states used to generate families of switching signals. Here, we review some basic information on differential inclusions [8, Ch.4], [68], [S1].

DIFFERENTIAL INCLUSIONS

Consider a constrained differential inclusion of the form

$$x \in C, \quad \dot{x} \in F(x), \quad (\text{S10})$$

where $C \subset \mathbb{R}^n$ and $F : \mathbb{R}^n \rightrightarrows \mathbb{R}^n$. System (S10) is said to satisfy the *Basic Conditions* if C is a closed set, and F is outer-semicontinuous and locally bounded relative to C , with $F(x)$ being non-empty and convex for each $x \in C$. Given $T > 0$, an absolutely continuous function $x : [0, T] \rightarrow \mathbb{R}^n$ is said to be a solution of (S10) if: a) $x(0) \in C$, and b) for almost all $t \in [0, T]$:

$$\frac{dx(t)}{dt} \in F(x(t)) \quad \text{and} \quad x(t) \in C. \quad (\text{S11})$$

When (S10) satisfies the Basic Conditions, the existence of solutions can be studied under the so-called viability conditions [8, Lemma 5.26]. To state such conditions, recall that the *tangent cone* to a set $S \subset \mathbb{R}^n$ at a point $x \in \mathbb{R}^n$, denoted $T_S(x)$, is given by all vectors $s \in \mathbb{R}^n$ for which there exist $x_i \in S$, $\tau_i > 0$ with $x_i \rightarrow x$ and $\tau_i \rightarrow 0^+$, such that $s = \lim_{i \rightarrow \infty} \frac{x_i - x}{\tau_i}$. In particular, under the Basic Conditions, we have that: (a)

1) (Necessity) If $x : [0, T] \rightarrow \mathbb{R}^n$, for some $T > 0$, is a solution of (S10), then

$$F(x(0)) \cap T_C(x(0)) \neq \emptyset. \quad (\text{S12})$$

2) (Sufficiency) Given $x_0 \in C$, if there exists a neighborhood U of x_0 such that for all $x \in U \cap C$,

$$F(x) \cap T_C(x) \neq \emptyset, \quad (\text{S13})$$

then there exists $T > 0$ and a solution $x : [0, T] \rightarrow \mathbb{R}^n$ to (S10) with $x(0) = x_0$.

Note that, in general, given an initial condition $x(0) = x_0 \in \mathbb{R}^n$, solutions to (S10) from x_0 might not be unique.

KRASOVSKII SOLUTIONS OF ODES

Differential inclusions (S10) often arise when studying discontinuous differential equations for which solutions might not exist from some initial conditions. In particular, given a set $C \subset \mathbb{R}^n$, a function $f : \mathbb{R}^n \rightarrow \mathbb{R}^n$, and an absolutely continuous function $x : [0, T] \rightarrow \mathbb{R}^n$, the function x is said to be a Krasovskii solution of the constrained system $x \in C$, $\dot{x} = f(x)$ if

$$x(t) \in \bar{C}, \quad \text{and} \quad \dot{x}(t) \in F_K(x(t)) := \overline{\text{co}}_{\epsilon > 0} f((x(t) + \epsilon \mathbb{B}) \cap C), \quad (\text{S14})$$

for almost all $t \in [0, T]$. When f is continuous, the mappings F_K and f coincide. The construction (S14) is also valid whenever f is set-valued but does not necessarily satisfy the Basic Conditions. Indeed, by construction (see [8, Example 6.6]), if f is locally bounded relative to \bar{C} , then the differential inclusion (S14) satisfies the Basic Conditions.

ROBUSTNESS: CONTINUOUS-TIME HERMES SOLUTIONS

For differential equations with a continuous right-hand side, small additive perturbations to the states do not significantly affect the system's behavior. In contrast, small perturbations can drastically impact the behavior of systems with a discontinuous right-hand side. The effect of arbitrarily small perturbations on such systems can be analyzed using the concept of Hermes solutions [S2]. The function $x : [0, T] \rightarrow \mathbb{R}^n$ is said to be a Hermes solution of the constrained system $x \in C$, $\dot{x} = f(x)$ if there exists a sequence of absolutely continuous functions $x_i : [0, T] \rightarrow \mathbb{R}^n$ and a sequence of measurable functions $e_i : [0, T] \rightarrow \mathbb{R}^n$ such that

$$\begin{aligned} x_i(t) + e_i(t) &\in C, \quad \text{for all } t \in (0, T), \\ \dot{x}_i(t) &= f(x_i(t) + e_i(t)), \quad \text{for almost all } t \in [0, T], \end{aligned}$$

the sequence $\{x_i\}_{i=1}^{\infty}$ converges uniformly to x on $[0, T]$, and the sequence $\{e_i\}_{i=1}^{\infty}$ converges uniformly to the zero function on $[0, T]$. In words, Hermes solutions capture the limiting effect of arbitrarily small additive state perturbations acting on the system $x \in C$, $\dot{x} = f(x)$. The connection between Hermes solutions and Krasovskii solutions is established in the following lemma, corresponding to [8, Thm. 4.3].

Lemma 1 (Continuous-Time Krasovskii Solutions)

Suppose that f is locally bounded and let $x : [0, T] \rightarrow \mathbb{R}^n$ be an absolutely continuous function. Then x is a Hermes solution of $\dot{x} = f(x)$ if and only if it is a Krasovskii solution of the same system.

Put simply, Lemma 1 suggests that to accurately characterize the behavior of the solutions of the system $\dot{x} = f(x)$ under arbitrarily small additive perturbations of the state, we should consider its Krasovskii solutions. A different concept of solutions explored in the literature of discontinuous differential equations is that of Filippov solutions [S1]. An absolutely continuous function $x : [0, T] \rightarrow \mathbb{R}^n$ is said to be a Filippov solution of $\dot{x} = f(x)$ if it satisfies

$$\dot{x}(t) \in F_F(x(t)) := \overline{\text{co}}_{\epsilon > 0, \mu(S)=0} f((x(t) + \epsilon \mathbb{B}) \setminus S), \quad (\text{S15})$$

where μ is the Lebesgue measure. While the constructions (S14) and (S15) are similar, the construction in (S15) ignores the behavior of f on sets S with zero measure. Hence, Filippov solutions are Krasovskii solutions, but the converse is generally not true. Thus, in light of Lemma 1, Filippov solutions are problematic as they do not completely capture the behavior of the original dynamics under small additive state perturbations. For further discussions on the difference between Filippov and Krasovskii solutions and for a proof of Lemma 1 for the special case where $C = \mathbb{R}^n$, we refer the reader to [S3].

REFERENCES

- [S1] A. F. Filippov, "Differential Equations with Discontinuous Right-hand Sides", Ed. Kluwer, 1988.
- [S2] H. Hermes, "Discontinuous vector fields and feedback control", in *Differential Equations and Dynamical Systems*, 1967.
- [S3] O. Hájek, "Discontinuous Differential Equations, I", in *Journal of differential equations*, Vol. 32, 1979, pp. 149-170.

The primary aim of this paper is to provide an accessible introduction to non-smooth and hybrid set-seeking systems formulated as hybrid inclusions

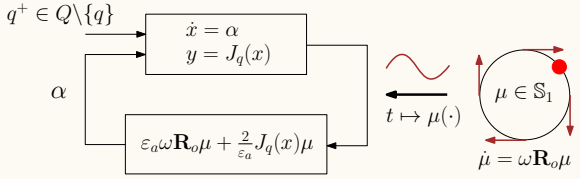


FIGURE 4 Scheme of source-seeking dynamics for point-mass vehicle models under intermittent switching potentials with distinct optimal points x_q^* .

intermittence of the sources is low, i.e., they remain individually active for "sufficiently" long periods of time. This problem can be modeled using the formalism of hybrid set-seeking systems. In particular, let $\mathcal{Q} := \{0, 1, \dots, q_{\max}\}$ denote a finite set of logic modes, where $q_{\max} \in \mathbb{Z}_{\geq 1}$. For each $q \in \mathcal{Q}$, we let $J_q : \mathbb{R}^2 \rightarrow \mathbb{R}$ denote a potential field that attains its maximum at the point x_q^* . For simplicity, we assume that each function $-J_q(\cdot)$ is strongly convex and has a globally Lipschitz gradient ∇J_q . For each fixed potential field $J_q(\cdot)$, the vehicle can achieve source-seeking by implementing the following standard seeking feedback law [84]:

$$\alpha = \epsilon_a \omega \mathbf{R}_o \mu + \frac{2}{\epsilon_a} J_q(x) \mu, \quad (19)$$

where $\epsilon_a, \omega > 0$ are tunable parameters and μ is a state that models a dithering signal with dynamics given by the following constrained differential equation:

$$\mu \in \mathbb{S}^1, \quad \dot{\mu} = \omega \mathbf{R}_o \mu. \quad (20)$$

The linear oscillator (20) provides an alternative time-invariant approach to generate sinusoidal functions, such as those used in (3), for the purpose of exploration. In particular, by direct computation, any solution of (20) has the form

$$\mu(t) = \begin{bmatrix} \cos(\omega t) & \sin(\omega t) \\ -\sin(\omega t) & \cos(\omega t) \end{bmatrix} \begin{bmatrix} \mu_1(0) \\ \mu_2(0) \end{bmatrix}, \quad (21)$$

where $\mu_1(0)^2 + \mu_2(0)^2 = 1$. In this way, the feedback law (19) emulates the source-seeking algorithm studied in [84] in the context of single-source seeking problems, but using a time-invariant model of the dynamics (with μ restricted to evolve in \mathbb{S}^1), see Fig. 4 for a graphical representation of the system.

To incorporate the switching behavior of the logic state q that indexes the potential fields J_q , we can consider the following set-valued hybrid dynamics with states $(q, \tau) \in \mathcal{Q} \times \mathbb{R}_{\geq 0}$, which

are parameterized by the constants $N_0 \geq 1$ and $\eta_d > 0$:

$$(q, \tau) \in \mathcal{Q} \times [0, N_0], \quad \dot{q} = 0, \quad \dot{\tau} \in [0, \eta_d], \quad (22a)$$

$$(q, \tau) \in \mathcal{Q} \times [1, N_0], \quad q^+ \in \mathcal{Q} \setminus \{q\}, \quad \tau^+ = \tau - 1. \quad (22b)$$

Similar to Example 1, in this system the state τ acts as a timer that regulates how frequently q can jump to other values in the set \mathcal{Q} . However, in this case, the continuous-time dynamics of τ in (22a) are set-valued and allow the derivative $\dot{\tau}$ to be any (measurable) selection from the set $[0, \eta_d]$, which includes keeping τ constant via $\dot{\tau} = 0$, increasing τ at the maximum rate $\eta_d > 0$ until $\tau = N_0$, or any other absolutely continuous function τ (not necessarily constant) having a derivative lower bounded by 0 and upper bounded η_d . This flexibility allows the model (22) to capture a large class of switching signals q acting on the feedback law (19), including signals that never switch (corresponding to $\dot{\tau} = 0$ for all time). In fact, for the case where $N_0 = 1$, all switching signals generated by (22) satisfy the *dwell-time* condition [85]. When $N_0 \in \mathbb{Z}_{\geq 2}$, all switching signals generated by (22) satisfy an *average dwell-time* condition [80] (see also "Switching Set-Seeking Systems with Average Dwell-time"). Both classes of switching signals are common in the modeling and stability analysis of switching systems, and by using (22) interconnected with (18)-(20) (with $x^+ = x$), we obtain a hybrid system suitable for the study of the source-seeking feedback law (19) under average dwell-time switches of J_q . Figure 5 shows an example of this switching signal for the case when $\eta_d = 1/100$, $N_0 = 1$, and $q_{\max} = 1$, such that $\mathcal{Q} = \{0, 1\}$. When η_d is sufficiently small, the resulting slowly-switching set-seeking system generates the stable behavior shown in Figure 6. In the left plot, we show the trajectories of (18) under the feedback law (19) with $\omega = 1000$, $\epsilon_a = 0.01$, and from different initial conditions shown with red dots. The trajectories converge to a neighborhood of the set $\Omega(K)$, shown in green.

This set, called the "Omega-limit set from K ", described later in equation (77), turns out to be (semi-globally practically) asymptotically stable for the overall hybrid set-seeking system (18)-(22) as $\eta_d \rightarrow 0^+$, $\epsilon_a \rightarrow 0^+$, and $1/\omega \rightarrow 0^+$. While in certain cases the set $\Omega(K)$ can be computed explicitly [86], its mere existence is typically guaranteed in slowly switching systems with individually asymptotically stable modes, under mild assumptions [8, Sec. 7.4]. \square

The preceding example underscores the advantages of considering hybrid set-seeking systems with *set-valued* dynamics. Consequently, for the remainder of this paper, we will focus on

hybrid systems that generalize (8), and are represented by the following *hybrid inclusions*:

$$x \in C, \quad \dot{x} \in F(x), \quad (23a)$$

$$x \in D, \quad x^+ \in G(x), \quad (23b)$$

where the flow map $F : \mathbb{R}^n \rightrightarrows \mathbb{R}^n$ and the jump map $G : \mathbb{R}^n \rightrightarrows \mathbb{R}^n$ are in general set valued. Note that for particular cases in which such maps are single-valued, we can still use the formalism (23) by defining

$$F(x) := \begin{cases} \{f(x)\}, & x \in C \\ \emptyset, & x \notin C \end{cases} \quad (24a)$$

$$G(x) := \begin{cases} \{g(x)\}, & x \in D \\ \emptyset, & x \notin D. \end{cases} \quad (24b)$$

The data of (23) is also denoted $\mathcal{H} := \{C, F, D, G\}$, and, similarly to (9), for the case where (23) depends on exogenous time-varying signals, we can consider models of the form

$$(x, \tau) \in C \times \mathbb{R}_{\geq 0}, \quad \dot{x} \in F(x, \tau), \quad \dot{\tau} = \omega, \quad (25a)$$

$$(x, \tau) \in D \times \mathbb{R}_{\geq 0}, \quad x^+ \in G(x), \quad \tau^+ = \tau, \quad (25b)$$

where $\omega > 0$ dictates the rate of evolution of the auxiliary timer state τ . Note that (25) can be written as (23) using the overall state $y = (x, \tau)$. Also, note that for hybrid systems with periodic flows, it is also possible to consider models with bounded timers by incorporating periodic resets in τ , similar to Example 1.

The Hybrid Basic Conditions

A crucial factor in establishing the stability properties of hybrid set-seeking systems is ensuring robustness to perturbations in the states and dynamics. To guarantee this property, we will impose the appropriate regularity conditions on the data of the hybrid system (23). For differential equations, such conditions are reduced to the continuity of the vector field. However, to study dynamic inclusions we will consider set-valued maps that are outer-semicontinuous (OSC) and locally bounded (LB). A set-valued mapping $M : \mathbb{R}^p \rightrightarrows \mathbb{R}^n$ is OSC at $z \in \mathbb{R}^p$ if for each convergent sequence $\{z_i, s_i\} \rightarrow (z, s) \in \mathbb{R}^p \times \mathbb{R}^n$ satisfying $s_i \in M(z_i)$ for all $i \in \mathbb{Z}_{\geq 0}$, we have $s \in M(z)$. A mapping M

is locally bounded (LB) at z if there exists an open neighborhood $N_z \subset \mathbb{R}^p$ of z such that $M(N_z)$ is bounded. The mapping M is OSC and LB relative to a set $K \subset \mathbb{R}^p$ if the mapping from \mathbb{R}^p to \mathbb{R}^n defined by $M(z)$ for $z \in K$ and \emptyset for $z \notin K$, is OSC and LB at each $z \in K$. Using OSC and LB, as well as standard convexity and closeness notions for sets [87], we consider hybrid systems (23) that satisfy the following *Hybrid Basic Conditions*:

(a)

- 1) The sets C and D are closed.
- 2) The set-valued mapping F is OSC and LB relative to C , and for each $x \in C$ we have that $F(x)$ is non-empty and convex.
- 3) The set-valued mapping G is OSC and LB relative to D , and for each $x \in D$ we have that $G(x)$ is non-empty.

Outer-semicontinuity of a set-valued mapping $M : \mathbb{R}^p \rightarrow \mathbb{R}^n$ relative to a set $K \subset \mathbb{R}^p$ is equivalent to asking for closedness of the graph of M with respect to K , i.e., the set $\text{gph}(M) := \{(z \in \mathbb{R}^p, s \in \mathbb{R}^n) : z \in K, s \in M(z)\}$ is relatively closed in $K \times \mathbb{R}^n$ [8, Lemma 5.10]. Throughout this paper, we will work only with hybrid systems that satisfy the Hybrid Basic Conditions. In the context of ES, the controllers will always be designed to satisfy these conditions.

Hybrid Time Domains, Hybrid Arcs, and Solutions

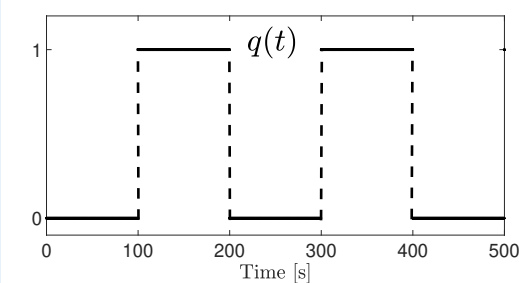
For continuous-time systems of the form (8a) or (23a), solutions $x : \text{dom}(x) \rightarrow \mathbb{R}^n$ are given by absolutely continuous functions with respect to time $t \in \text{dom}(x) \subset \mathbb{R}_{\geq 0}$ (see "Continuous-Time Set-Valued Dynamical Systems"). Similarly, for discrete-time systems of the form (8b) or (23b), solutions $x : \text{dom}(x) \rightarrow \mathbb{R}^n$ are defined as sequences parameterized by a discrete-time index $j \in \text{dom}(x) \subset \mathbb{Z}_{\geq 0}$ (see "Discrete-Time Set-Valued Dynamical Systems"). Therefore, to define solutions for hybrid systems of the form (8) or (23), we consider a "hybrid" parameterization of the solutions that depends on both a continuous-time index $t \in \mathbb{R}_{\geq 0}$, which increases continuously during flows, and a discrete-time index $j \in \mathbb{Z}_{\geq 0}$, which increases by one during jumps. In this way, solutions to (8) or (23) are defined in *hybrid time domains*. A set $E \subset \mathbb{R}_{\geq 0} \times \mathbb{Z}_{\geq 0}$ is called a *compact hybrid time domain* if $E = \bigcup_{j=0}^{J-1} ([t_j, t_{j+1}], j)$ for some finite sequence of times $0 = t_0 \leq t_1 \dots \leq t_J$. A set $E \subset \mathbb{R}_{\geq 0} \times \mathbb{Z}_{\geq 0}$ is a *hybrid time domain* if it is the union of a non-decreasing sequence of compact hybrid time domains, namely, E is the union of compact hybrid time domains E_j with the property that $E_0 \subset E_1 \subset E_2 \subset \dots \subset E_j \dots$, etc.

Figure 7 shows five different types of hybrid time domains, including those corresponding to Zeno behavior, average dwell time between jumps, purely discrete solutions, and purely continuous solutions.

Using the notion of hybrid time domain, the following definition formalizes what we call *solutions* to hybrid systems of the form (23).

Definition 1 (Hybrid Arcs and Solutions)

FIGURE 5 Evolution in time of a switching signal q taking values in the set $\{0, 1\}$, indicating which potential field is active in the source-seeking problem.



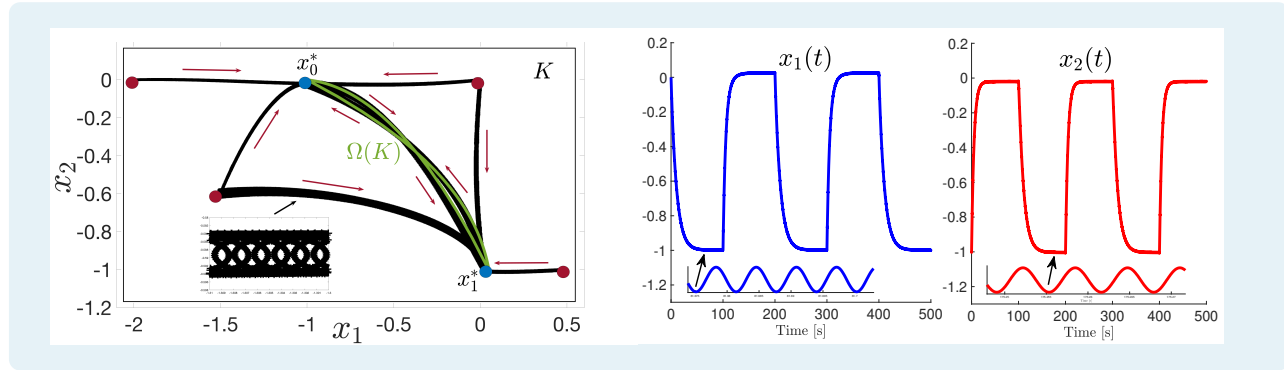


FIGURE 6 Left: Trajectories of system (18) (shown in color black) under the feedback law (19), evolving on the plane, and converging to a neighborhood of the set $\Omega(K)$, shown in color green. Right: Evolution in time of the position of the vehicle, which oscillates between the two optimal points x_0^* and x_1^* , which are contained in $\Omega(K)$.

A function $x : \text{dom}(x) \mapsto \mathbb{R}^n$ is a hybrid arc if $\text{dom}(x)$ is a hybrid time domain and $t \mapsto x(t, j)$ is a locally absolutely continuous function for each j such that the interval $I_j := \{t : (t, j) \in \text{dom}(x)\}$ has non-empty interior. A hybrid arc x is a *solution* to (23) if $x(0, 0) \in C \cup D$, and the following two conditions hold:

(a)

1) For each $j \in \mathbb{Z}_{\geq 0}$:

$$x(t, j) \in C, \text{ for almost all } t \in I_j$$

$$\dot{x}(t, j) \in F(x(t, j)), \text{ for almost all } t \in I_j;$$

2) For each $(t, j) \in \text{dom}(x)$ such that $(t, j+1) \in \text{dom}(x)$:

$$x(t, j) \in D, \text{ and } x(t, j+1) \in G(x(t, j)). \quad (34)$$

A solution x to system (23) is said to be *forward pre-complete* if its domain is compact or unbounded. It is said to be *forward complete* if its domain is unbounded, and it is said to be *maximal* if there does not exist another solution ψ to (23) such that $\text{dom}(x)$ is a proper subset of $\text{dom}(\psi)$, and $x(t, j) = \psi(t, j)$ for all $(t, j) \in \text{dom}(x)$. In general, given an initial condition $x(0, 0) \in C \cup D$, the solutions to system (23) might not be unique. This will be the case if, for example, the intersection $C \cap D$ is not empty and from a point in this intersection it is possible to flow, or if the flow or jump maps in (23a)-(23b) admit non-unique solutions due to set-valuedness, or lack of Lipschitz continuity in the flow map.

Example 5 (Periodic Hybrid System (Continued))

Recall the hybrid system discussed in Example 1, which implements periodic jumps in the state x_2 triggered by a periodic resetting timer x_1 with resetting period T . Figure 8 shows the hybrid arcs corresponding to the trajectories x_1 and x_2 shown in Figure 2, from the initial conditions $x_1(0, 0) = 0$ and $x_2(0, 0) = 10$. As observed, the values of the states x_1 and x_2 can be fully identified via the hybrid time indices for all $(t, j) \in \text{dom}(x)$. \square

Example 6 (Bouncing Seeking System (Continued))

Recall the “bouncing” seeking system discussed in Example 2. Figure 9 shows the hybrid arcs corresponding to the trajectories x_1 shown in the left plot of Figure 3. The trajectory in color black is generated by the hybrid dynamics (16) using constant acceleration, i.e., $\dot{x}_2 = -\bar{\gamma}$. On the other hand, the blue trajectory implements highly-oscillatory acceleration, i.e., $\dot{x}_2 = -2 \sin(\omega\tau)^2 \bar{\gamma}$. Both trajectories were generated from the same initial conditions as in Example 2. As observed, both hybrid arcs remain “close” to each other during the simulation. Specifically, the *graphs* of the hybrid arcs are similar. This hints to some closeness property, akin to the one discussed when studying system (3) and its average dynamics (4) using inequality (7). In fact, by working with hybrid arcs, hybrid time domains, and a suitable metric for these objects, it is possible to naturally extend the notion of (T, ϵ) -closeness of solutions to hybrid seeking systems, thus opening the door to the development and study of novel algorithms and applications with hybrid dynamics in the loop. \square

Graphical Convergence and (T, ϵ) -Closeness in Hybrid Systems

As discussed in the analysis of the smooth ES dynamics (3), using the average dynamics (4) and the nominal dynamics (5), the closeness-of-solutions property is crucial for the study of ES controllers based on periodic dithering. Specifically, inequalities (6) and (7) showed that the solutions of the seeking dynamics (3) behave similarly to those of a gradient flow, with this “similarity” being quantified, in compact sets and time domains, using the uniform distance between solutions. However, this approach does not extend directly to hybrid systems. The following example, which continues the discussion from Example 2, illustrates some of the challenges that arise when using the standard uniform distance to gauge the closeness between solutions of nominal and perturbed hybrid systems. These challenges can be addressed by working with solutions defined on hybrid time domains,

as opposed to solutions defined on $\mathbb{R}_{\geq 0}$, and by studying the closeness of solutions using the distance between the graphs of the hybrid arcs.

Example 7 (Bouncing Seeking System (continued))

Consider the “bouncing” seeking system with hybrid dynamics (16), which experiences a high-frequency oscillating acceleration given by $-\gamma(\tau)$. Using the fact that the average of $\sin(\tau)^2$ over one period of oscillations is equal to $\frac{1}{2}$, the average dynamics of (16b) can be explicitly computed (see “Averaging Theory: From ODEs to Hybrid Systems”) to be

$$C := \{\bar{x} \in \mathbb{R}^2 : \bar{x}_1 \geq 0\}, \quad \dot{\bar{x}} = \bar{f}(\bar{x}) := \begin{pmatrix} \bar{x}_2 \\ -\bar{\gamma} \end{pmatrix}, \quad (35a)$$

$$D = \{\bar{x} \in \mathbb{R}^2 : \bar{x}_1 = 0, \bar{x}_2 \leq 0\}, \quad \bar{x}^+ = g(\bar{x}) := \begin{pmatrix} 0 \\ -\lambda \bar{x} \end{pmatrix}, \quad (35b)$$

where $\bar{x} = (\bar{x}_1, \bar{x}_2) \in \mathbb{R}^2$ is the state of the average hybrid system and $\bar{\gamma}$ is the same gravitational constant of (17). We can argue, at least visually based on Figure 3, that there exist $T, \varepsilon > 0$ such that the solutions of the oscillating hybrid dynamics (16) and the non-oscillating hybrid dynamics (35) in general do not satisfy bounds of the form (6) or (7), no matter how large we select ω in (16b). For example, this behavior is evident in the right plot of Figure 3, where after approximately 15 seconds a significant mismatch emerges between the jump times of the red and black trajectories. Specifically, following a jump in the black trajectory, the red trajectory fails to closely track it due to the discontinuity, regardless of how large ω is chosen. This occurs because the red trajectory has not yet undergone its corresponding jump at that moment, preventing the satisfaction of inequalities of the form (6) or (7) at that time. \square

To overcome the issues described in the previous example, and to study the closeness of solutions of hybrid systems of the form (23), we consider an equivalent notion that compares the *distance*

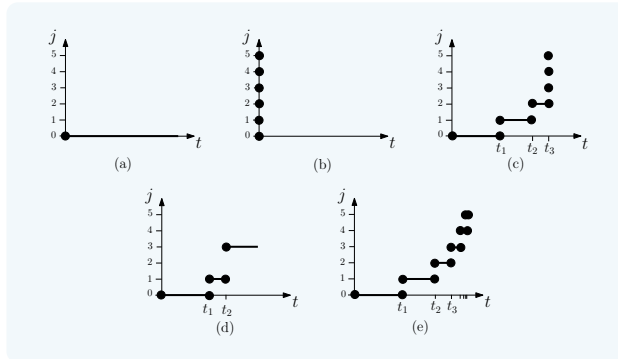


FIGURE 7 Five different hybrid time domains illustrating different types of solutions in a hybrid system: (a) Purely continuous solution; (b) Purely discrete solution; (c) Eventually discrete solution; (d) Solution with average-dwell time; (e) Solution with Zeno behavior.

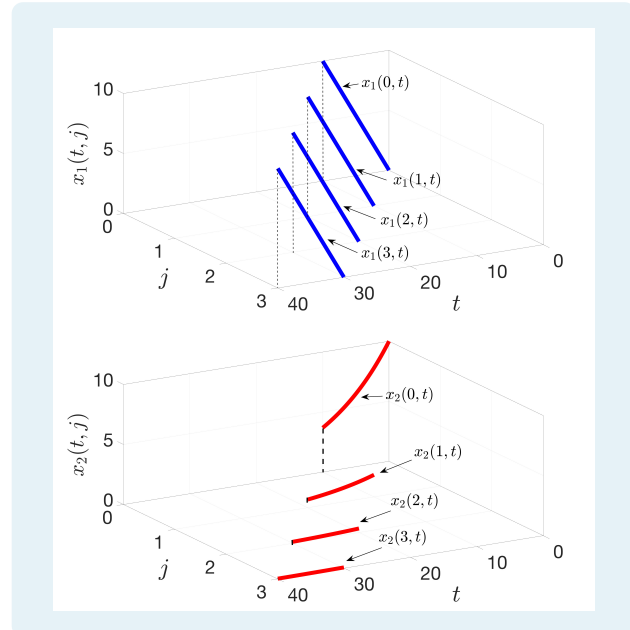


FIGURE 8 Hybrid arcs of a solution of the system studied in Example 1, illustrated as a function of time t in Figure 2.

between solutions defined under the same jump index j for which both solutions are defined [8, Def. 5.23], i.e., we use the distance between *their graphs*. Specifically, given constants $\tau \geq 0$ and $\varepsilon > 0$, two hybrid arcs x and \tilde{x} are said to be (τ, ε) -close if the following conditions are satisfied:

- 1) For each $(t, j) \in \text{dom}(x)$ with $t + j \leq \tau$, there exists $s \in \mathbb{R}_{\geq 0}$ such that $(s, j) \in \text{dom}(\tilde{x})$, $|t - s| \leq \varepsilon$, and

$$|x(t, j) - \tilde{x}(s, j)| < \varepsilon. \quad (36)$$

- 2) For each $(t, j) \in \text{dom}(\tilde{x})$ with $t + j \leq \tau$, there exists $s \in \mathbb{R}_{\geq 0}$ such that $(s, j) \in \text{dom}(x)$, $|t - s| \leq \varepsilon$, and

$$|\tilde{x}(t, j) - x(s, j)| < \varepsilon. \quad (37)$$

Figure 10 presents an illustration of this property, which essentially asks that the *graphs* of x and \tilde{x} are “close” to each other when truncated in (hybrid) time. This property can also be leveraged to study a type “graphical” convergence between hybrid arcs, akin to the standard uniform convergence properties studied for solutions of ODEs. In particular, given a sequence of hybrid arcs $\{x_i\}_{i=1}^{\infty}$ with $x_i : \text{dom}(x_i) \rightarrow \mathbb{R}^n$, and a hybrid arc x with $x : \text{dom}(x) \rightarrow \mathbb{R}^n$, the property that for each $\tau \geq 0$ and each $\varepsilon > 0$ there exists $i^* \in \mathbb{Z}_{\geq 1}$ such that for all $i > i^*$ the hybrid arcs x_i and x are (τ, ε) -close implies the property that the sequence $\{x_i\}_{i=1}^{\infty}$ converges graphically to x , i.e., the sequence of sets $\{\text{gph } x_i\}_{i=1}^{\infty}$ converges (in the sense of set convergence, see [8, Def. 5.1]) to the set $\{\text{gph } x\}$. The converse implication is also true whenever the sequence $\{x_i\}_{i=1}^{\infty}$ is locally eventually

Discrete-Time Set-Valued Dynamical Systems

Discrete-time dynamical systems modeled as *difference inclusions* are common in optimization, estimation, and control algorithms. They are also relevant for the study of robustness properties in discrete-time systems with a discontinuous right-hand side. Here, we review some fundamentals on difference inclusions.

DIFFERENCE INCLUSIONS

Consider the constrained difference inclusion of the form

$$x \in D, \quad x^+ \in G(x), \quad (\text{S26})$$

where $D \subset \mathbb{R}^n$, and $G : \mathbb{R}^n \rightrightarrows \mathbb{R}^n$ is a set-valued mapping. System (S26) is said to satisfy the *Basic Conditions* if D is a closed set, G is outer-semicontinuous and locally bounded relative to D , and $G(x)$ is not empty for each $x \in D$. Given $J \in \mathbb{Z}_{\geq 1}$, a sequence $x : \{0, 1, \dots, J\} \rightarrow \mathbb{R}^n$ is said to be a solution of (S26) if it satisfies

$$x(j) \in D, \quad \text{and} \quad x(j+1) \in G(x(j)), \quad (\text{S27})$$

for all $j \in \{0, 1, \dots, J-1\}$. For system (S26), the existence of solutions is always guaranteed provided $D \neq \emptyset$. In general, given a solution $x : \text{dom}(x) \rightarrow \mathbb{R}^n$, it will not be the unique solution from $x(0)$ if $G(x(j))$ is not single valued for some j in $\text{dom}(x)$ such that $x(j) \in D$.

KRASOVSKII SOLUTIONS TO DISCRETE-TIME SYSTEMS

Difference inclusions of the form (S26) are relevant for the study of robustness properties in discontinuous discrete-time systems. In particular, given a set $D \subset \mathbb{R}^n$ and a function $g : \mathbb{R}^n \rightarrow \mathbb{R}^n$, a sequence $x : \{0, 1, \dots, J\} \rightarrow \mathbb{R}^n$ is said to be a Krasovskii solution of the constrained difference equation

$$x \in D, \quad x^+ = g(x), \quad (\text{S28})$$

if it satisfies:

$$x(j) \in \overline{D}, \quad \text{and} \quad x(j+1) \in G_K(x) := \overline{g((x + \epsilon \mathbb{B}) \cap D)}, \quad (\text{S29})$$

for all $j \in \{0, 1, \dots, J\}$ [8, Def. 4.13]. When D is closed, the sets \overline{D} and D coincide. Similarly, when g is continuous, the mappings G_K and g coincide. However, when g is discontinuous, the map G_K is set valued at the points of discontinuity. In particular, G_K describes the outer-semicontinuous hull of g , namely the unique set-valued mapping G_K satisfying $\text{graph}(G_K) = \overline{\text{graph}(g)}$. The construction in (S29) also holds when g is a set-valued mapping. In this case, by construction (see [8, Ex. 6.6]), if g is locally bounded relative to \overline{D} , then the difference inclusion (S29) also satisfies the Basic Conditions.

Example 4 (Regularization of Sign Function)

Consider the discrete-time system given by

$$x^+ = x - \alpha \cdot \text{sign}(x), \quad x \in \mathbb{R}^n, \quad (\text{S30})$$

for $\alpha > 0$, were the sign function is defined as

$$\text{sign}(x) = \begin{cases} 1 & \text{if } x > 0 \\ 0 & \text{if } x = 0 \\ -1 & \text{if } x < 0 \end{cases} \quad (\text{S31})$$

To obtain G_K , in this case it suffices to close the graph of $\text{sign}(x)$. We obtain the set-valued mapping:

$$\overline{\text{sign}}(x) = \begin{cases} 1 & \text{if } x > 0 \\ \{-1, 0, 1\} & \text{if } x = 0 \\ -1 & \text{if } x < 0 \end{cases} \quad (\text{S32})$$

and the difference inclusion:

$$x^+ \in G_K(x) := x - \alpha \cdot \overline{\text{sign}}(x), \quad x \in \mathbb{R}^n. \quad (\text{S33})$$

ROBUSTNESS: DISCRETE-TIME HERMES SOLUTIONS

As in the continuous-time case, the limiting effect of small additive state disturbances on difference equations can be captured using the notion of Hermes solutions. A function $x : \{0, 1, \dots, J\} \rightarrow \mathbb{R}^n$ is said to be a Hermes solution of the constrained difference equation (S28) if there exists a sequence of functions $x_i : \{0, 1, \dots, J-1\} \rightarrow \mathbb{R}^n$ and $e_i : \{0, 1, \dots, J-1\} \rightarrow \mathbb{R}^n$ such that for all $j \in \{0, 1, \dots, J-1\}$:

$$x_i(j) + e_i(j) \in D, \quad x_i(j+1) = g(x_i(j) + e_i(j)),$$

and the sequence $\{x_i\}_{i=1}^{\infty}$ converges uniformly to x on $j \in \{0, 1, \dots, J\}$, and, moreover, the sequence $e_i : \{0, 1, \dots, J\} \rightarrow \mathbb{R}^n$ converges uniformly to the zero function on $\{0, 1, \dots, J\}$ [8, Def. 4.12]. As in the continuous-time case, there is a close connection between discrete-time Hermes and Krasovskii solutions, which is stated in the next lemma, corresponding to [8, Thm. 4.17].

Lemma 2 (Discrete Time Krasovskii Solutions)

Consider the function $x : \{0, 1, \dots, J\} \rightarrow \mathbb{R}^n$, for some $J \in \mathbb{Z}_{\geq 1}$, and suppose that g is locally bounded. Then x is a Hermes solution of the constrained difference equation (S28) if and only if it is a Krasovskii solution of the same system.

The result of Lemma 2 indicates that in order to study the robustness properties of difference equations with a discontinuous right-hand side, we should focus on studying their Krasovskii solutions. For further details on the study of difference inclusions, we refer the reader to references [S1] and [S2]. Discrete-time extremum seeking algorithms based on difference equations and inclusions have been studied in [88] and [89] using finite-difference approximation methods to estimate the gradients of cost functions. In the context of hybrid set-seeking systems via averaging, difference inclusions can be used to model synchronization mechanisms in multi-agent systems [90], switching systems under dwell-time or average dwell-time constraints [91], etc.

REFERENCES

- [S1] C. M. Kellett, A. R. Teel, "On the Robustness of \mathcal{KL} -Stability for Difference Inclusions: Smooth Discrete-Time Lyapunov Functions", *SIAM Journal on Control and Optimization*, Vol. 44, pp. 777-800, 2005.
- [S2] C. M. Kellett, A. R. Teel, "Smooth Lyapunov functions and robustness of stability for difference inclusions", *Systems & Control Letters*, Vol 52, No. 5, pp. 395-405, 2004.

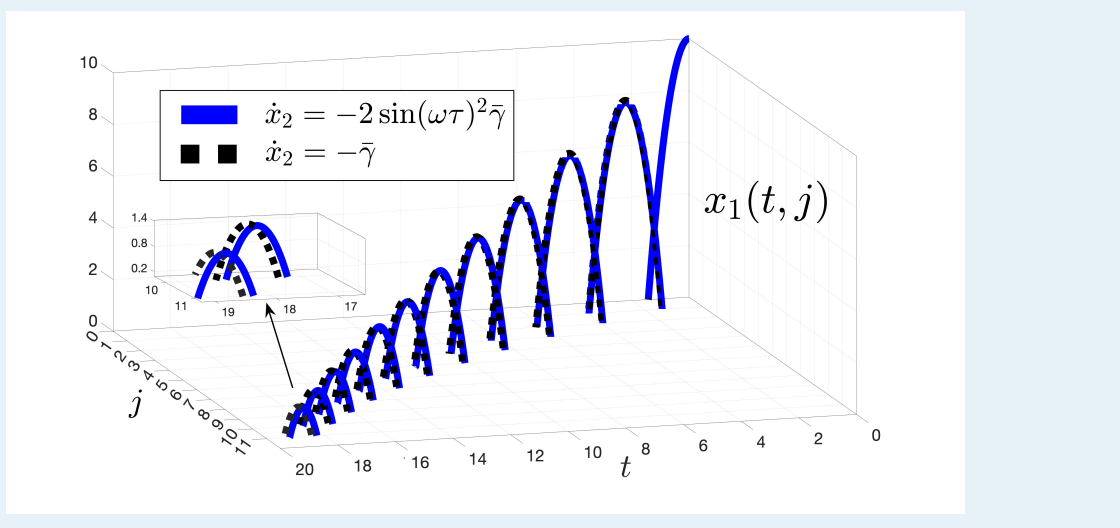


FIGURE 9 Component x_1 of the hybrid arcs associated with the solutions of hybrid system (16), as studied in Example 2, shown as a function of time t in Figure 3. The blue trajectory is generated using the highly-oscillatory acceleration $\gamma(\tau)$, with $\omega = 100$. The dotted black trajectory is generated using the constant acceleration $\bar{\gamma}$, which is just the average of $\gamma(\tau)$.

The use of hybrid time domains and graphical convergence to study solutions in hybrid systems is the key enabling mathematical tool for the development of a comprehensive theory in hybrid set-seeking control.

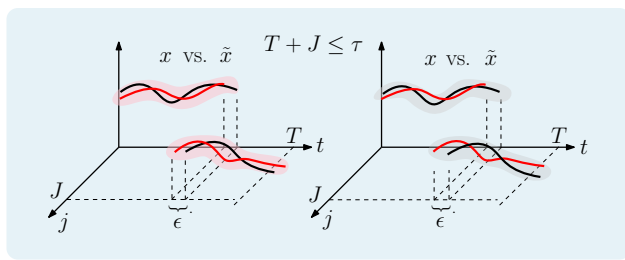


FIGURE 10 Graphical illustration of the property of (τ, ϵ) -closeness in two hybrid arcs x and \bar{x} .

bounded¹ [8, Thm. 5.25].

By working with hybrid time domains, we can now see (at least at this point, visually based on Figure 9) that the hybrid arcs describing the two solutions considered in Example 2 are (τ, ϵ) -close when ω is sufficiently large. However, to formalize this property for a broad class of hybrid systems of interest, including those with additive perturbations on the states and

dynamics (as in the perturbed gradient flow (4)), we need to introduce an “inflated” version of hybrid systems of the form (23), which will be particularly useful in the context of averaging (see “Averaging Theory: From ODEs to Hybrid Systems”) and singular perturbation theory (see “Singularly Perturbed Hybrid Dynamical Systems”).

Inflated Hybrid Systems

Given a hybrid system \mathcal{H} of the form (23) with state $x \in \mathbb{R}^n$, a continuous function $\sigma : \mathbb{R}^n \rightarrow \mathbb{R}^n$, and $\rho > 0$, consider the following “inflated” hybrid system \mathcal{H}_ρ with state $x \in \mathbb{R}^n$, and data constructed from the data of (23) as follows:

$$C_\rho := \{x \in \mathbb{R}^n : (x + \rho\sigma(x)\mathbb{B}) \cap C \neq \emptyset\}, \quad (38a)$$

$$F_\rho(x) := \overline{\text{co}} F((x + \rho\sigma(x)\mathbb{B}) \cap C) + \rho\sigma(x)\mathbb{B}, \quad \forall x \in C_\rho, \quad (38b)$$

$$D_\rho := \{x \in \mathbb{R}^n : (x + \rho\sigma(x)\mathbb{B}) \cap D \neq \emptyset\}, \quad (38c)$$

$$G_\rho(x) := \left\{ v \in \mathbb{R}^n : v \in g + \rho\sigma(g)\mathbb{B}, \quad g \in G((x + \rho\sigma(x)\mathbb{B}) \cap D) \right\}, \quad \forall x \in D_\rho. \quad (38d)$$

This inflated hybrid system can capture different types of perturbations acting on the flow and jump sets of the nominal hybrid dynamics, as well as in the nominal flow and jump

¹A sequence of hybrid arcs is said to be locally eventually bounded if for any $m > 0$, there exists $i_0^* \in \mathbb{Z}_{\geq 1}$ and a compact set K such that for all $i > i_0^*$ and all $(t, j) \in \text{dom}(x_i)$ with $t + j \leq m$, we have that $x_i(t, j) \in K$.

maps. For example, the inflated flow map F_ρ and the jump map G_ρ can capture additive disturbances acting on the states and dynamics of the flow and jump maps of system (23). Similarly, the inflated flow set C_ρ and jump set D_ρ can model measurement noise or other small additive disturbances acting on the states of the nominal system (23). As shown in the following example, the inflated system (38b) can also be used for the study of continuous-time seeking systems, including system (3).

Example 8 (Inflations in Smooth Seeking Systems)

Consider the standard ES smooth dynamics (3), which can be written as (9) using an auxiliary state τ , and dynamics:

$$\dot{\hat{u}} = f_\varepsilon(\hat{u}, \tau) := -\frac{2}{\varepsilon_a} J(\hat{u} + \varepsilon_a \sin(\tau)) \sin(\tau), \quad \dot{\tau} = \omega, \quad (39)$$

where $\omega = \frac{2\pi}{\varepsilon_\omega}$, $\varepsilon = (\varepsilon_a, \varepsilon_\omega) \in \mathbb{R}_{>0}$ are tunable parameters, and where the flow set is given by the condition $(\hat{u}, \tau) \in C := \mathbb{R} \times \mathbb{R}_{\geq 0}$. For small values of ε_a , a Taylor expansion of J leads to

$$f_\varepsilon(\hat{u}, \tau) = -\left(\frac{2}{\varepsilon_a} J(\hat{u}) \sin(\tau) + 2 \frac{\partial J(\hat{u})}{\partial \hat{u}} \sin(\tau)^2 + O(\varepsilon_a)\right),$$

where, for a given compact set $K \subset \mathbb{R}$, the notation $O(\varepsilon_a)$ indicates high-order terms $o_h(\tau, \hat{u})$ that satisfy, for some $k > 0$, the inequality $|o_h(\tau, \hat{u})| \leq k\varepsilon_a$ for all $\tau \in \mathbb{R}_{\geq 0}$ and all $\hat{u} \in K$. Since $\int_0^{\frac{2\pi}{\omega}} \sin(\tau) d\tau = 0$ and $\int_0^{\frac{2\pi}{\omega}} \sin(\tau)^2 d\tau = \frac{1}{2}$, it follows that the average map f_{ave} of f_ε , given by (2), is precisely system (4), which satisfies

$$\begin{aligned} f_{\text{ave}}(\bar{u}) &= -\frac{\partial J(\hat{u})}{\partial \hat{u}} + O(\varepsilon_a) \in \overline{\text{co}} \left(\frac{\partial J(\bar{u} + k\varepsilon_a \mathbb{B})}{\partial \bar{u}} \right) + k\varepsilon_a \mathbb{B} \\ &= F_{k\varepsilon_a}(\bar{u}), \end{aligned}$$

for all $\bar{u} \in K$, where $F_{k\varepsilon_a}$ is precisely the set-valued map defined in (38b) with $F = -\frac{\partial J}{\partial \hat{u}}$, $C = \mathbb{R}$, a constant function $\sigma = k$, and $\rho = \varepsilon_a$. The above inclusion implies that, on compact sets K , the set of solutions of system $\dot{\bar{u}} = f_{\text{ave}}(\bar{u})$ is contained in the set of solutions of the differential inclusion $\dot{\bar{u}} \in F_{k\varepsilon_a}(\bar{u})$. Hence, by verifying appropriate properties for *all solutions* of this differential inclusion (which is just an inflation of the model-based gradient flow), we can guarantee that these properties also hold for all solutions of $\dot{\bar{u}} = f_{\text{ave}}(\bar{u})$

□

By using the construction of the inflated hybrid system (38), the following key technical property, corresponding to [8, Prop. 6.34], opens the door to a perturbation-based methodology to study hybrid set-seeking systems, thus generalizing the approach used to study the smooth ES algorithm (3). We recall that throughout this paper we assume that the hybrid system \mathcal{H} given by (23) always satisfies the Hybrid Basic Conditions by design.

Lemma 3 (Key Technical Lemma)

Suppose that $x_0 \in \mathbb{R}^n$ is such that each maximal solution of \mathcal{H} from x_0 is complete or bounded. Then, for all $\tau \geq 0$ and $\varepsilon > 0$ there exists $\rho > 0$ such that for each solution x_ρ to the perturbed HDS (38), with $|x_\rho(0, 0) - x_0| \leq \rho$, there exists a solution x to

the nominal hybrid system \mathcal{H} , given by (23), with $x(0, 0) = x_0$, such that x and x_ρ are (τ, ε) -close. □

Lemma 3 also applies to differential equations simply by taking $D = \emptyset$, $C = \mathbb{R}^n$, and F being a continuous function. For instance, for the smooth ES system considered in Example 8, we can use Lemma 3 to directly conclude that, on compact sets, for each solution \bar{u}_{ε_a} of the differential inclusion $\dot{\bar{u}}_{\varepsilon_a} \in F_{k\varepsilon_a}(\bar{u}_{\varepsilon_a})$, there exists a solution \bar{u} of the model-based gradient flow $\dot{\bar{u}} = -\frac{\partial J(\bar{u})}{\partial \bar{u}}$ such that \bar{u}_{ε_a} and \bar{u} are (τ, ε) -close. Since, as shown before, on compact sets we have $f_{\text{ave}} \in F_{k\varepsilon_a}$, it follows that the (τ, ε) -closeness property also holds for the solutions of the average dynamics of (39) and the solutions of the target gradient flow. This analytical methodology extends beyond gradient flows and smooth dynamics to general hybrid set-seeking systems, enabling the establishment of closeness-of-solutions properties via perturbation theory for hybrid systems. In this context, the use of hybrid time domains and graphical convergence in analyzing hybrid system solutions provides a foundational mathematical framework for developing a comprehensive theory of hybrid set-seeking control.

Stability Notions for Hybrid Set-Seeking Systems

Since hybrid systems usually incorporate logic modes, timers, clocks, and other auxiliary states that do not settle into a point but rather evolve on bounded sets, we study the uniform stability properties of hybrid set-seeking systems with respect to general compact sets.

Definition 2 (Uniform Global Asymptotic Stability)

A compact set $\mathcal{A} \subset \mathbb{R}^n$ is said to be *uniformly globally asymptotically stable* (UGAS) for system (23) (or (25)) if there exists a class- \mathcal{KL} function β such that any maximal solution of \mathcal{H} satisfies the bound

$$|x(t, j)|_{\mathcal{A}} \leq \beta(|x(0, 0)|_{\mathcal{A}}, t + j), \quad \forall (t, j) \in \text{dom}(x). \quad (40)$$

If there exist positive constants $c_1, c_2 > 0$ such that $\beta(r, s) = c_1 r e^{-c_2 s}$, then \mathcal{A} is said to be *uniformly globally exponentially stable* (UGES). □

When $\mathcal{A} = \{0\}$, the definition 2 recovers the standard asymptotic stability notions studied for differential equations [57, Ch. 4] and smooth ES systems [44], [64]. The use of \mathcal{KL} bounds in (40) provides uniformity in terms of rates of convergence and overshoots. Note that Definition 2 requires that *all* solutions to the HDS (23) satisfy the bound (40) at all times in the domain of the solution. However, it does not require that all solutions be complete. For hybrid systems, the completeness of solutions is usually established independently.

Example 9 (Dynamics with Vanishing Coefficients)

Under suitable assumptions, gradient flows and other optimization dynamics typically satisfy the UGAS property in Definition 2, relative to the set of minimizers of a cost function J . However,

this assumption does not hold for all gradient systems, even if J is strongly convex. For instance, systems with vanishing coefficients of the form

$$\dot{x} = -\alpha(\tau)\nabla J(x), \quad \text{or} \quad \ddot{x} + \alpha(\tau)\dot{x} + \nabla J(x) = 0, \quad (41)$$

for which $\lim_{\tau \rightarrow \infty} \alpha(\tau) = 0$, typically exhibit non-uniform convergence properties with respect to $\tau(0)$, thus precluding bounds of the form (40) [92]. However, under appropriate hybrid regularizations of τ , e.g., time-triggered [69], [93] or event-triggered restarting [94], the resulting hybrid dynamics can satisfy (40) for some $\beta \in \mathcal{KL}$, see also "Set-Seeking Dynamics with Momentum and Resets". \square

Since ES systems rely on perturbation theory, the following stability property is commonly used in the analysis of seeking algorithms.

Definition 3 (Semi-Global Practical Stability)

Consider a HDS \mathcal{H}_ε , where $\varepsilon > 0$ is a tunable parameter. System \mathcal{H}_ε is said to render a compact set \mathcal{A} semi-globally practically asymptotically stable (SGPAS) if there exists a class- \mathcal{KL} function β such that for each $\Delta > \nu > 0$ there exists $\varepsilon^* > 0$ such that for all $\varepsilon \in (0, \varepsilon^*)$ and all initial conditions $|x(0, 0)| \leq \Delta$, any maximal solution of \mathcal{H}_ε satisfies the bound

$$|x(t, j)|_{\mathcal{A}} \leq \beta(|x(0, 0)|_{\mathcal{A}}, t + j) + \nu, \quad \forall (t, j) \in \text{dom}(x). \quad (42)$$

If there exist positive constants $c_1, c_2 > 0$ such that $\beta(r, s) = c_1 r e^{-c_2 s}$, then \mathcal{A} is said to be *semi-globally practically exponentially stable* (SGPES). \square

The SGPAS property can be extended to hybrid systems that depend on multiple parameters $\varepsilon = (\varepsilon_1, \varepsilon_2, \dots, \varepsilon_m)$. In this case, we use the notation SGPAS as $(\varepsilon_1, \varepsilon_2, \dots, \varepsilon_m) \rightarrow 0^+$ to denote that (42) holds with the parameters ε_i sufficiently small and being selected sequentially, starting from ε_1 and ending with ε_m . While the sequential tuning of certain parameters in ES can be relaxed in some cases [66], to simplify our presentation we do not study such relaxations in this paper. Instead, we observe that for most seeking dynamics based on averaging—though not all (see [95]–[97])—whether modeled as differential equations or hybrid systems, the property of SGPAS is typically the strongest guarantee one can expect. For smooth seeking systems such as in (3), the small parameters in ε are related to the dither amplitude ε_a , the inverse of the dither frequency ω , and, when additional dynamics such as filters are used, the corresponding inverse of the filter gain. For hybrid seeking systems, we will allow ε to also include parameters that are intrinsic to the hybrid dynamics, e.g., η_d in the "Source-Seeking and Surveillance" application discussed in Example 3.

PART 2: HYBRID SET-SEEKING SYSTEMS FOR STATIC MAPS

Equipped with the modeling and analysis tools introduced in Part I, we now consider a broad class of hybrid set-seeking

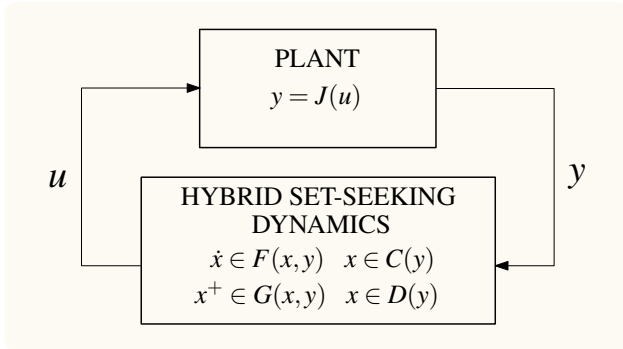


FIGURE 11 High-level conceptual feedback scheme of hybrid set-seeking systems for static maps.

systems for solving model-free decision-making problems. The primary objective in extremum seeking is to regulate the plant input u using only measurements of the output y , to drive u toward the solution of an *application-dependent* optimization or decision-making problem of the form:

$$\text{optimize } J(u), \quad \text{s.t. } u \in \hat{\mathbb{U}}, \quad (47)$$

where the set $\hat{\mathbb{U}} \subset \mathbb{R}^n$ captures the constraints on the input and $J(\cdot)$ corresponds to the cost function, which is assumed to be sufficiently smooth. We assume that the set of solutions to the problem (47) is not empty and we denote it by $\mathcal{O} \subset \mathbb{R}^n$, which is also assumed to be compact. The fact that \mathcal{O} might not be a singleton further motivates the terminology "set-seeking" as opposed to the more traditional names "extremum-seeking" or "equilibrium-seeking".

Remark 1

The decision-making problem (47) can also be formulated to study multi-agent networked systems (MAS) with individual outputs y_i and cost functions J_i , for all $i \in \{1, \dots, N\}$, where N is the number of subsystems. This case is relevant for distributed optimization problems, as well as for Nash equilibrium seeking problems in game theoretic scenarios; see, for instance [51], [104], [105], [106], [107] for different examples of seeking dynamics studied in these settings.

For the remainder of this section, we assume that the plant to be optimized is characterized by a static map J , as illustrated in the scheme of Figure 11. In this scheme, we use suggestive notation in which the data of the hybrid controller $\mathcal{H} = \{C, F, D, G\}$ is allowed to depend on y , the output signal of the plant. This notation indicates that the particular structure of the *data* of \mathcal{H} is designed specifically for each application of interest. However, the general structure of hybrid set-seeking controllers remains largely consistent across applications. To investigate hybrid set-seeking systems with dynamic inclusions in the loop, we begin by extending the smooth seeking dynamics (3) to the setting of hybrid systems. Specifically, similar to Example 3, and to avoid dealing with time-varying differential inclusions whose

Averaging Theory: From ODEs to Hybrid Systems

Dynamical systems with time-varying oscillating vector fields are traditionally studied using averaging theory. Classic references on averaging theory for differential equations include [98], [56], [99] and [57]. For hybrid dynamical systems, averaging tools have also been studied in [100], [101], [69], [102], and [103]. Below, we review some results on averaging theory for hybrid systems, adapted from [99], [102], and [69].

Hybrid Systems with Oscillating Flow Maps

Consider a hybrid dynamical system of the form (9), with states $z = (x, p) \in \mathbb{R}^n \times \mathbb{R}^m$ and $\tau \in \mathbb{R}_{\geq 0}$, and dynamics

$$(x, p, \tau) \in C := C_x \times C_p \times \mathbb{R}_{\geq 0}, \quad \begin{cases} \dot{x} = f(x, p, \tau) \\ \dot{p} \in F_p(p) \\ \dot{\tau} = \frac{1}{\varepsilon} \end{cases} \quad (\text{S43a})$$

$$(x, p, \tau) \in D := D_x \times D_p \times \mathbb{R}_{\geq 0}, \quad \begin{cases} x^+ = g(x, p) \\ p^+ \in G_p(p) \\ \tau^+ = \tau \end{cases} \quad (\text{S43b})$$

where $\varepsilon > 0$ is a small parameter, $C_x, D_x \subset \mathbb{R}^n$, $C_p, D_p \subset \mathbb{R}^m$. The state p can model logic states, timers, oscillators, as well as other auxiliary states. We assume that system (S43) satisfies the Hybrid Basic Conditions. In (S43a), the small parameter ε introduces a time-scale separation between the dynamics of τ and those of (x, p) . When the vector field f is periodic with respect to τ , the rapid fluctuations in τ result in fast oscillatory behaviors in \dot{x} , which can be averaged out to approximate the dynamics of x using a non-oscillating vector field. The following definition formalizes this notion of average, which for system (S43) involves only the function f .

Definition 4 (The Average Map)

The function f is said to have an *average map* $\bar{f}(\cdot)$ if for each compact set $K_0 \subset \mathbb{R}^n \times \mathbb{R}^m$ there exists a continuous, non-increasing function γ satisfying $\lim_{\mathcal{T} \rightarrow \infty} \gamma(\mathcal{T}) = 0$, such that for all $(x, p, \tau, T) \in K_0 \times \mathbb{R}_{\geq 0} \times \mathbb{R}_{\geq 0}$:

$$\left| \frac{1}{T} \int_{\tau}^{\tau+T} (f(x, p, s) - \bar{f}(x, p)) ds \right| \leq \gamma(T). \quad (\text{S44})$$

The function $\gamma(\cdot)$ is called the *convergence function*.

When f is periodic, as it is usually the case in ES, for each compact set K_0 there exists $c_0 > 0$ such that we can take $\gamma(\mathcal{T}) = \frac{c_0}{1+\mathcal{T}}$, and it suffices to verify the integral (S44) in the interval $[0, \mathcal{T}]$, where \mathcal{T} is the period of the oscillations. In the rest of this section, we make the additional standing assumptions that f is periodic with respect to τ and that \bar{f} is continuous. However, we note that periodicity of f can be relaxed by working with generalized averages in (S44).

By using the average map \bar{f} , we can study (S43) by inspecting a "simpler" non-oscillating system, with states (\bar{x}, \bar{p}) , and the following *average hybrid dynamics*:

$$(\bar{x}, \bar{p}) \in C := C_x \times C_p, \quad \begin{cases} \dot{\bar{x}} = \bar{f}(\bar{x}, \bar{p}) \\ \dot{\bar{p}} \in F_p(\bar{p}) \end{cases} \quad (\text{S45a})$$

$$(x, p) \in D := D_x \times D_p, \quad \begin{cases} \bar{x}^+ = g(\bar{x}, \bar{p}) \\ \bar{p}^+ \in G_p(\bar{p}) \end{cases} \quad (\text{S45b})$$

Given that hybrid systems usually lack the uniqueness of solutions property, and might also exhibit solutions with discontinuities, standard results on closeness of solutions established in the literature of averaging for differential equations do not trivially extend to hybrid systems. Instead, we can establish that for every solution (x, p, τ) of the original hybrid system (S43) there exists some solution (\bar{x}, \bar{p}) of the average hybrid dynamics (S45) that is (T, ε) -close. In particular, the following theorem follows from the results in [99], [100], [102]:

Theorem 1 (Closeness of Solutions via Averaging)

Consider the hybrid systems (S43) and (S45). Suppose that system (S45) has no finite escape times. Then, for each compact set of initial conditions $K_0 \subset \mathbb{R}^n$, $T \in \mathbb{R}_{>0}$ and $\varepsilon \in \mathbb{R}_{\geq 0}$, there exists $\varepsilon^* > 0$ such that for all $\varepsilon \in (0, \varepsilon^*)$ and for all solutions (x, p, τ) to (S43) from K_0 there exists a solution (\bar{x}, \bar{p}) to (S45) such that (\bar{x}, \bar{p}) and (x, p) are (T, ε) -close.

The result of Theorem 1 is a closeness of solutions property for hybrid systems that parallels similar properties used for the study of smooth extremum seeking systems. By using this property, as well as suitable uniform stability properties in the average hybrid dynamics, the following theorem can be established.

Theorem 2 (SGPAS via Averaging in HDS)

Consider the hybrid systems (S43) and (S45). Suppose that there exists a compact set $\mathcal{A} \subset \mathbb{R}^{n+m}$ that is UGAS for system (S45). Then, system (S46) renders the set $\mathcal{A} \times \mathbb{R}_{\geq 0}$ SGPAS as $\varepsilon \rightarrow 0^+$.

The stability result from Theorem 2 can be applied to analyze hybrid set-seeking dynamics of the form (S43). This result remains valid even when the stability of the averaged dynamics (S45) is only semi-globally practically asymptotically stable (SGPAS) with respect to a tunable parameter δ [69, Thm. 7]. This is commonly the case in extremum-seeking control, where δ can represent the residual terms that appear in the average dynamics, and which are of the same order as the amplitude of the dither signals. In the context of hybrid set-seeking dynamics, δ may encompass additional parameters, offering greater flexibility in the design of the algorithms.

Averaging using Time-Invariant Models

Theorems 1 and 2 can be extended to other types of models, including hybrid systems of the form

$$(x, p, \tau) \in C := C_x \times C_p \times \mathbb{R}_{\geq 0}, \quad \begin{cases} \dot{x} \in F_x(x, p) \\ \dot{p} = f_p(p, x, \tau) \\ \dot{\tau} = \frac{1}{\varepsilon}, \end{cases} \quad (\text{S46a})$$

$$(x, p, \tau) \in D := D_x \times D_p \times \mathbb{R}_{\geq 0}, \quad \begin{cases} x^+ \in G_x(x, p) \\ p^+ \in G_p(x, p) \\ \tau^+ = \tau \end{cases} \quad (\text{S46b})$$

where all the mappings and sets are selected to satisfy the Hybrid Basic Conditions. Here, the dynamics of x are set-valued, but the average map can still be computed as in (S44) using f_p instead of f .

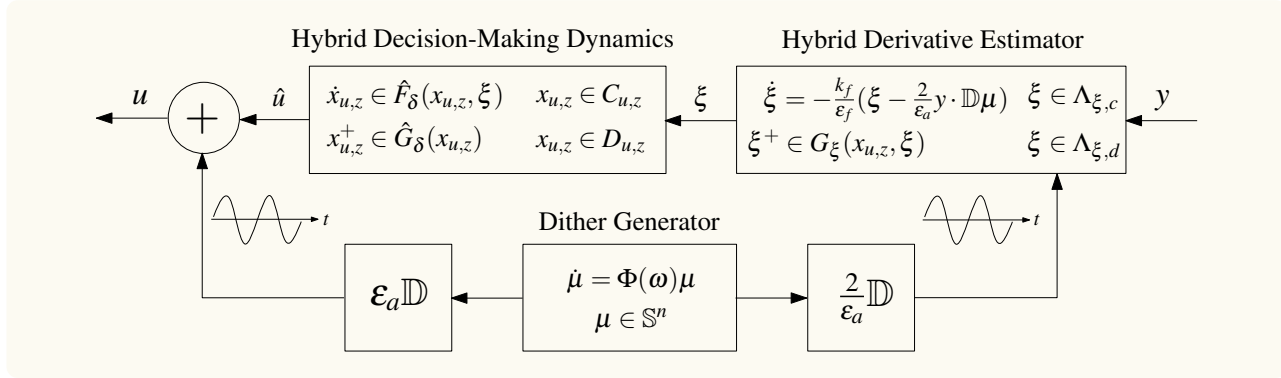


FIGURE 12 Main components of hybrid set-seeking systems with periodic probing.

averaged maps may be difficult to compute explicitly, we consider a class of time-invariant hybrid seeking systems consisting of a *dynamic derivative estimator* and *dither generator*, with states $(\xi, \mu) \in \mathbb{R}^n \times \mathbb{R}^{2n}$, and a *hybrid decision-making algorithm* with internal state $x_{u,z} := (\hat{u}, \hat{z}) \in \mathbb{R}^n \times \mathbb{R}^r$. Figure 12 shows a block diagram representation of the set-seeking controllers. Our objective is to design the system's core components so that, using only output measurements, the plant input $u \in \mathbb{R}^n$ is driven to a small neighborhood of the solution set of (47). The design must also ensure that the resulting closed-loop system satisfies the Hybrid Basic Conditions.

Autonomous Derivative Estimators

The dynamic derivative estimators make use of n linear oscillators of the form (20), with overall state $\mu := (\mu_1, \dots, \mu_n) \in S^n \subset \mathbb{R}^{2n}$, satisfying $\mu_i = (\mu_{i,1}, \mu_{i,2})^\top \in S^1$, for all $i \in \{1, \dots, n\}$, and dynamics

$$\dot{\mu} = \Phi(\omega)\mu, \quad \mu \in S^n, \quad (48)$$

where the ω -parameterized block matrix $\Phi_\omega : \mathbb{R}^{2n} \rightarrow \mathbb{R}^{2n}$ is given by

$$\Phi_\omega := \begin{bmatrix} \omega_1 \mathbf{R}_o & \mathbf{0} & \dots & \mathbf{0} \\ \mathbf{0} & \omega_2 \mathbf{R}_o & \dots & \mathbf{0} \\ \vdots & \vdots & \ddots & \vdots \\ \mathbf{0} & \mathbf{0} & \dots & \omega_n \mathbf{R}_o \end{bmatrix}, \quad (49)$$

with $\omega = (\omega_1, \dots, \omega_n)$. The entries of ω are selected as $\omega_i = \frac{\kappa_i}{\varepsilon_\omega}$, where $\varepsilon_\omega > 0$ is a tunable constant, and the κ_i 's are rational numbers that satisfy $\kappa_i \neq \kappa_j$ for $i \neq j$ and $(i, j) \in \{1, \dots, n\}$.

The role of system (48) is to generate a vector of n periodic probing signals with different frequency for the purpose of real-time *exploration*. This is achieved by extracting the odd entries of the vector μ , given by $\mu_{i,1}(t) = \cos(\omega_i t)\mu_{2i-1}(0) + \sin(\omega_i t)\mu_{2i}(0)$, for each $i \in \{1, \dots, n\}$, via multiplication with the matrix $\mathbb{D} := [e_1, \mathbf{0}, e_2, \mathbf{0}, \dots, e_i, \dots, \mathbf{0}, e_n, \mathbf{0}]$, where $\mathbf{0} \in \mathbb{R}^n$ corresponds to a column vector of zeros, and $e_i \in \mathbb{R}^n$ corresponds to the unitary vector with the i^{th} entry equal to 1. Since, by the definition of its flow set in (48), the oscillator is restricted to evolve in S^n , we have $\mu_{2i-1}(0)^2 + \mu_{2i}(0)^2 = 1$.

Moreover, the set S^n is forward invariant and, since the system (48) has no solutions defined outside S^n , the set is also trivially UGAS for the dynamics (48). We note that although other types of dither signals and oscillators can be considered—including hybrid ones [108]—we focus here, for simplicity, on standard sinusoidal probing signals generated by linear oscillators.

The performance of the derivative estimators in ES systems can usually be enhanced by incorporating filters into the dynamics. For hybrid set-seeking, we can consider a simple low-pass filter with state $\xi \in \mathbb{R}^n$ and continuous-time dynamics

$$\dot{\xi} = -\frac{k_f}{\varepsilon_f} \cdot \left(\xi - \frac{2}{\varepsilon_a} y \cdot \mathbb{D}\mu \right), \quad (50)$$

where $k_f, \varepsilon_f > 0$ are tunable parameters and which is allowed to evolve in a compact set $\Lambda_\xi := \lambda_\xi \mathbb{B} \subset \mathbb{R}^n$, with $\lambda_\xi \in \mathbb{R}_{>0}$ selected sufficiently large to encompass all the complete solutions of interest. As shown later in Theorem 4 and in "Hybrid Set-Seeking Dynamics with Momentum and Resets", it is also possible to incorporate filters with hybrid dynamics to, for example, improve transient performance. However, we can simply take $\xi^+ = \xi$ when no discrete-time updates are incorporated into the filters. The compactness assumption on Λ_ξ can also be relaxed under additional structure on the dynamics.

Hybrid Decision-Making Dynamics

As mentioned in the introduction, the smooth ES algorithm (3) is designed to approximate—on average—the behavior of the model-based "target" gradient flow (5). In the context of hybrid set-seeking systems, we aim to consider more general hybrid target systems for optimization and decision making. Therefore, instead of (3), we consider a class of hybrid seeking dynamics with state $x_{u,z} := (\hat{u}, \hat{z}) \in \mathbb{R}^n \times \mathbb{R}^r$, $r \in \mathbb{Z}_{\geq 0}$, where \hat{u} is the main state and output of the system, and where $z \in \mathbb{R}^r$ is an auxiliary state that can model timers, logic modes, memory states, momentum, etc.

The state $x_{u,z}$ evolves according to the following *hybrid*

decision-making dynamics:

$$\dot{x}_{u,z} \in \hat{F}_\delta(x_{u,z}, \xi), \quad x_{u,z} \in C_{u,z}, \quad (51a)$$

$$x_{u,z}^+ \in \hat{G}_\delta(x_{u,z}), \quad x_{u,z} \in D_{u,z}, \quad (51b)$$

where the set-valued mappings $\hat{F}_\delta : \mathbb{R}^{n+r} \times \mathbb{R}^n \rightrightarrows \mathbb{R}^{n+r}$ and $\hat{G}_\delta : \mathbb{R}^{n+r} \rightrightarrows \mathbb{R}^{n+r}$ are allowed to depend on a small tunable parameter $\delta > 0$ that provides flexibility for the design of the controller. It follows that the data of system (51) is given by $\hat{\mathcal{H}}_\delta := \{C_{u,z}, \hat{F}_\delta, D_{u,z}, \hat{G}_\delta\}$, it receives as input the state ξ , generated by the filter (50), and it generates as output the state \hat{u} , which acts on the plant via the following control law:

$$u = \hat{u} + \varepsilon_a \mathbb{D}\mu. \quad (52)$$

The nominal hybrid decision-making dynamics (51) are designed so that the following assumption holds:

Assumption 1 (Hybrid Decision-Making Dynamics)

The following properties hold: (a)

- 1) There exists $\delta^* \in \mathbb{R}_{>0}$ such that for all $\delta \in (0, \delta^*]$: 1.
 - a) the sets $C_{u,z}$ and $D_{u,z}$ are closed, and satisfy $P_u(C_{u,z}) \subset \mathbb{U}$, $P_u(D_{u,z}) \subset \mathbb{U}$, where P_u denotes the projection on the u -component of the set.
 - b) $\hat{F}_\delta(\cdot, \cdot)$ is OSC, LB, and convex-valued relative to $C_{u,z} \times \mathbb{R}^n$, and $\hat{G}_\delta(\cdot)$ is OSC and LB relative to $D_{u,z}$.
- 2) There exists a compact set $\Psi \subset \mathbb{R}^r$ such that the set $\mathcal{A} := \mathcal{O} \times \Psi$ is SGPAS as $\delta \rightarrow 0^+$ for the *target hybrid decision-making system* corresponding to (51) with $\xi := \nabla J(\hat{u})$, where the set \mathcal{O} is the set of solutions to (47).

While condition (a) provides regularity to the data of system $\hat{\mathcal{H}}_\delta$, item (b) indicates that $\hat{\mathcal{H}}_\delta$ should be designed to guarantee that the set of solutions to problem (47) is stabilized *under the assumption that the gradient ∇J is known by the hybrid decision-making dynamics*. Figure 13 shows a block diagram representation of the target hybrid decision-making system considered in item (b) of Assumption 1. However, we stress that, in practice, the hybrid controller will use only real-time measurements of J , and the exact mathematical forms of J and ∇J are assumed to be unknown. However, qualitative properties of J , e.g., quadratic-like structures, convexity, invexity, etc, are typically used to study stability in ES algorithms.

If $\hat{\mathcal{H}}_\delta$ does not depend on any parameter δ , then item (b) in Assumption 1 simply asks that the set \mathcal{A} is UGAS. If, additionally, system (51) does not depend on any auxiliary state $\hat{z} \in \mathbb{R}^r$, then the set Ψ can be neglected, and we can take $C_{u,z} = C_u \subset \mathbb{R}^n$ and $D_{u,z} = D_u \subset \mathbb{R}^n$. We will use the convention $r = 0$ to specify this case. Finally, note that if, in addition, we have that $D_u = \emptyset$, $C_u = \mathbb{R}^n$, and \hat{F}_δ is a Lipschitz continuous function, then the above properties reduce to the standard assumptions considered in the literature of smooth extremum seeking [65], [72], [109]. Local (practical) stability results can also be established when only local qualitative properties of ∇J or J are known.

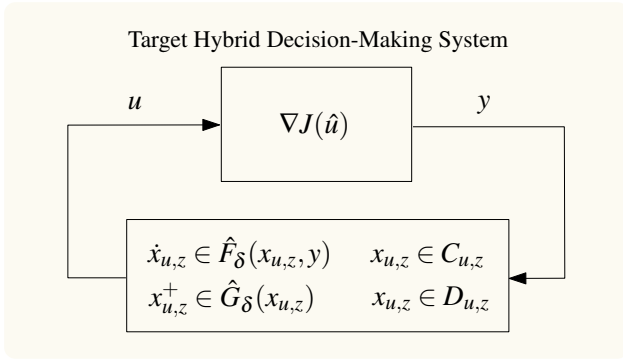


FIGURE 13 Conceptual feedback scheme of the target hybrid decision-making system considered in Assumption 1.

Hybrid-Set Seeking: Closed-Loop System

The overall hybrid set-seeking dynamics are obtained by interconnecting the static plant $y = J(u)$, the oscillator (48), the filter (50), and the hybrid decision-making dynamics (51) using the feedback law (52). The resulting hybrid system has an overall state $x := (x_{u,z}, \xi, \mu) \in \mathbb{R}^{r+4n}$, and data given by $\mathcal{H} := \{C, F, D, G\}$, with

$$C := C_{u,z} \times \Lambda_\xi \times \mathbb{S}^n \quad (53a)$$

$$\dot{x} \in F(x) := \begin{pmatrix} \hat{F}_\delta(x_{u,z}, \xi) \\ -\frac{k_f}{\varepsilon_f} \left(\xi - \frac{2}{\varepsilon_a} y \cdot \mathbb{D}\mu \right) \\ \Phi(\omega)\mu \end{pmatrix} \quad (53b)$$

$$D := D_{u,z} \times \Lambda_\xi \times \mathbb{S}^n \quad (53c)$$

$$x^+ \in G(x) := \begin{pmatrix} \hat{G}_\delta(x_{u,z}) \\ \xi \\ \mu \end{pmatrix}. \quad (53d)$$

The stability properties of (53) are captured by the following theorem, which follows by computing the average dynamics of (53) with respect to μ , and then applying singular perturbation arguments to study the average hybrid dynamics as a perturbed multi-time scale system with the state ξ evolving on a faster time scale, see Theorem 6 and Remark 1 in “Singularly Perturbed Hybrid Dynamical Systems”.

Theorem 3

Suppose that Assumption 1 holds. Then, the hybrid set-seeking system (53) with $y = J(u)$ and the feedback control law (52) renders the set $\mathcal{A} \times \Lambda_\xi \times \mathbb{S}^n$ SGPAS as $(\delta, \varepsilon_f, \varepsilon_a, \varepsilon_\omega) \rightarrow 0^+$. \square

The stability result of Theorem 3 states that the trajectories of (53) satisfy bounds of the form (40) with respect to the set $\mathcal{A} \times \Lambda_\xi \times \mathbb{S}^n$. In particular, since Λ_ξ and \mathbb{S}^n are compact, the state $x_{u,z}$ in (53) satisfies

$$|x_{u,z}(t, j)|_{\mathcal{A}} \leq \beta(|x_{u,z}(0, 0)|_{\mathcal{A}}, t + j) + \nu, \quad (54)$$

for all $(t, j) \in \text{dom}(x_{u,z})$. Note that Theorem 3 does not make assertions about completeness of solutions, since these properties

need to be established for each particular application under an appropriate design of the data of the hybrid system.

Remark 2

The SGPAS result of Theorem 3 also establishes a tuning order for the parameters $(\delta, \varepsilon_f, \varepsilon_a, \varepsilon_\omega)$. The first parameter to be selected "sufficiently" small is δ , such that item (b) in Assumption 1 holds. Subsequently, the parameters ε_f , ε_a , and ε_ω should be selected to be sufficiently small, in that order. \square

Corollary 1

Suppose that Assumption 1 holds and the sets $C_{u,z}$ and $D_{u,z}$ are bounded. Then, the hybrid dynamics (53) with $y = J(u)$ and control law (52) renders the set $\mathcal{A} \times \Lambda_\xi \times \mathbb{S}^n$ Globally Practically Asymptotically Stable as $(\delta, \varepsilon_f, \varepsilon_a, \varepsilon_\omega) \rightarrow 0^+$. \square

Achieving *global* stability results when the flow and jump sets are bounded is particularly relevant for ES problems defined on smooth compact manifolds. In such spaces, standard ES algorithms with target decision-making dynamics characterized by smooth ODEs can achieve only local, or at best, almost global, asymptotic stability. This follows because such spaces are not contractible, a property that is needed for global stability in smooth dynamical systems [110]. However, hybrid set-seeking systems can overcome these limitations and achieve global bounds of the form (54), see [111], [112].

Remark 3

When $D_{u,z} := \emptyset$, system (53) does not experience jumps and the set-seeking dynamics reduce to the continuous-time system

$$C := C_{u,z} \times \Lambda_\xi \times \mathbb{S}^n, \quad (55a)$$

$$\dot{x} \in F(x) := \begin{pmatrix} \hat{F}_\delta(x_{u,z}, \xi) \\ -\frac{k_f}{\varepsilon_f} \left(\xi - \frac{2}{\varepsilon_a} y \cdot \mathbb{D}\mu \right) \\ \Phi(\omega)\mu \end{pmatrix}. \quad (55b)$$

Set-valued ES systems of the form (55) can emerge in applications where the optimizing vector field is discontinuous. In such cases, \hat{F}_δ will correspond to the Krasovskii regularization of the vector field (see "Krasovskii Solutions of ODEs" in "Continuous-Time Set-Valued Dynamical Systems"). If, on the other hand, \hat{F}_δ is a Lipschitz continuous function, and $C_{u,z} = \mathbb{R}^n$, then (55) recovers the standard framework for the study of gradient-based smooth ES dynamics [45], [66], [65]. \square

One of the advantages of modeling seeking systems with autonomous dither generators of the form (48) is that the resulting closed-loop system (53) satisfies the Hybrid Basic Conditions and has suitable stability properties with respect to a compact set (see Theorem 3). As a consequence, one can study the inflated hybrid system (38) obtained from the data of the hybrid seeking dynamics (53) to establish the following robustness result via [8, Thm. 7.21].

Corollary 2

Suppose that Assumption 1 holds. For each compact set of initial conditions $K_0 \subset \mathbb{R}^{n+r}$ let Theorem 3 generate sufficiently small parameters $(\delta, \varepsilon_f, \varepsilon_a, \varepsilon_\omega)$ such that property (54) holds. Then, the *inflated* hybrid set-seeking system (38) with control law (52) renders the set $\mathcal{A} \times \Lambda_\xi \times \mathbb{S}^n$ SGPAS as $\rho \rightarrow 0^+$ (relative to K_0). \square

Since, as discussed in Part 1 of this article, the inflated system (38) can capture a variety of additive disturbances and perturbations acting on the states and dynamics of the algorithms, the result of Corollary 2 essentially implies that the hybrid set-seeking algorithms (53) will retain their (semi-global practical) stability properties under a broad class of small additive disturbances on the states and dynamics.

Remark 4

To account for situations where the plant output is influenced by external events, such as sporadic feedback measurements or external malicious signals, the filter in (53b) can be modified to adopt the more general structure

$$\dot{\xi} = -\frac{k_f}{\varepsilon_f} \left(\xi - \frac{2}{\varepsilon_a} \gamma(x_{u,z}) y D\mu \right), \quad (56)$$

where $\gamma(\cdot)$ is a continuous function. In this case, item (b) of Assumption 1 should hold with $\xi = \gamma(x_{u,z}) \nabla J(\hat{u})$. \square

Hybrid-Set Seeking Dynamics with Hybrid Filters

By removing any explicit dependence of \hat{F}_δ on the oscillatory signal μ , the non-hybrid low-pass filter considered in (53) facilitates the computation of the average hybrid dynamics for a broad class of set-valued decision-making dynamics (51). However, this comes at the price of having an additional time scale in the system induced by selecting $\varepsilon_f > 0$ sufficiently small, and by restricting ξ to evolve in a compact set for the purpose of stability analysis. Nevertheless, it is possible to relax these assumptions by replacing the flow and jump sets of (53) by the more general sets

$$C := C_{u,z} \times \Lambda_{\xi,c} \times \mathbb{S}^n, \quad D := D_{u,z} \times \Lambda_{\xi,d} \times \mathbb{S}^n, \quad (57a)$$

where $\Lambda_{\xi,c}, \Lambda_{\xi,d} \subset \mathbb{R}^n$ are closed sets, and by considering the following flow and jump maps:

$$\dot{x} \in F(x) := \begin{pmatrix} \hat{F}_\delta(x_{u,z}, \xi) \\ -k_f \left(\xi - \frac{2}{\varepsilon_a} y \cdot \mathbb{D}\mu \right) \\ \Phi(\omega)\mu \end{pmatrix} \quad (57b)$$

$$x^+ \in G(x) := \begin{pmatrix} \hat{G}_\delta(x_{u,z}, \xi) \\ G_\xi(x_{u,z}, \xi) \\ \mu \end{pmatrix}, \quad (57c)$$

where the set-valued maps \hat{G}_δ and G_ξ are both assumed to be OSC and LB relative to $D_{u,z} \times \Lambda_{\xi,d}$. In this case, we consider the following assumption:

Assumption 2

Items (a) of Assumption 1 holds, and for the target hybrid decision-making dynamics

$$\begin{pmatrix} \dot{x}_{u,z} \\ \dot{\xi} \end{pmatrix} \in \begin{pmatrix} \hat{F}_\delta(x_{u,z}, \xi) \\ -k_f(\xi - \kappa \nabla J(\hat{u})) \end{pmatrix}, (x_{u,z}, \xi) \in C_{u,z} \times \Lambda_{\xi,c} \quad (58a)$$

$$\begin{pmatrix} x_{u,z}^+ \\ \xi^+ \end{pmatrix} \in \begin{pmatrix} \hat{G}_\delta(x_{u,z}, \xi) \\ G_\xi(x_{u,z}, \xi) \end{pmatrix}, (x_{u,z}, \xi) \in D_{u,z} \times \Lambda_{\xi,d}, \quad (58b)$$

where $k_f > 0$, there exist $\kappa \in \mathbb{R}$ and compact sets $\Psi_z \subset \mathbb{R}^r$ and $\Psi_f \subset \mathbb{R}^n$ such that the set $\mathcal{A} := \mathcal{O} \times \Psi_z \times \Psi_f$ is SGPAS as $\delta \rightarrow 0^+$.

With Assumption 2 at hand, we can establish the following theorem.

Theorem 4

Suppose that Assumption 2 holds. Then, the hybrid set-seeking system (57) with $y = J(u)$ and control law (52) renders the set $\mathcal{A} \times S^n$ SGPAS as $(\delta, \varepsilon_a, \varepsilon_\omega) \rightarrow 0^+$. \square

Seeking systems with hybrid filters are useful for incorporating resets or restarting mechanisms to reduce overshoot, improve transient performance [69], [94], [113], or regularize accelerated gradient flows with dynamic damping, which can speed up convergence when the cost function exhibits low curvature [69], [114], [115]. In such systems, the continuous-time dynamics of ξ can be appropriately modified without significantly altering the structure of (58).

Hybrid Set-Seeking Dynamics with Growing Timers

We now consider the simpler hybrid set-seeking systems that dispense with the filters and for which the time variation in the dither signal is generated by an exogenous timer that grows unbounded, as in system (3) and (25), see also “Averaging Theory: From ODEs to Hybrid Systems”. In this case, we can consider hybrid set-seeking systems with control law (52) and dynamics

$$(x_{u,z}, \tau) \in C_{u,z} \times \mathbb{R}_{\geq 0}, \quad \begin{cases} \dot{x}_{u,z} = \hat{F}_\delta(x_{u,z}, y \cdot \mu_{\varepsilon_a}(\tau)) \\ \dot{\tau} = \frac{1}{\varepsilon_\omega} \end{cases} \quad (59a)$$

$$(x_{u,z}, \tau) \in D_{u,z} \times \mathbb{R}_{\geq 0}, \quad \begin{cases} x_{u,z}^+ = \hat{G}_\delta(x_{u,z}) \\ \tau^+ = \tau \end{cases}, \quad (59b)$$

where $\mu_{\varepsilon_a}(\tau) := \frac{2}{\varepsilon_a}(\sin(2\pi\kappa_1\tau), \sin(2\pi\kappa_2\tau), \dots, \sin(2\pi\kappa_n\tau))$, and the parameters $\kappa_i > 0$ are rational and satisfy $\kappa_i \neq \kappa_j$ for all $i \neq j \in \{1, 2, \dots, n\}$. Note that the “bouncing” seeking system studied in Example 2 has the form of (59). When $D_{u,z} = \emptyset$, $C_{u,z} = \mathbb{R}^n$, and $\hat{F}_\delta = -y\mu_{\varepsilon_a}(\tau)$ we recover the most basic continuous-time ES scheme studied in the literature [45], [66].

The stability properties of the hybrid set-system (59) are studied under the following assumption, which leverages the

notion of *average map* introduced in “Averaging Theory: From ODEs to Hybrid Systems”.

Assumption 3

There exists $\delta^* \in \mathbb{R}_{>0}$ such that for all $\delta \in (0, \delta^*]$ the following properties hold: (a)

1) Item (a)-1. of Assumption 1 is satisfied, and the functions \hat{F}_δ and \hat{G}_δ are continuous.

2) There exists a compact set $\Psi \subset \mathbb{R}^r$ such that the set $\mathcal{A} := \mathcal{O} \times \Psi$ is SGPAS as $\delta \rightarrow 0^+$ for the target hybrid decision-making dynamics

$$\dot{x}_{u,z} = \hat{F}_\delta(x_{u,z}, \nabla J(\hat{u})), \quad x_{u,z} \in C_{u,z} \quad (60a)$$

$$x_{u,z}^+ = \hat{G}_\delta(x_{u,z}), \quad x_{u,z} \in D_{u,z}. \quad (60b)$$

3) For each compact set $K \subset \mathbb{R}^n$ there exists $\varepsilon_a^* > 0$ such that for all $\varepsilon_a \in (0, \varepsilon_a^*)$ the average map of \hat{F}_δ , denoted \bar{F}_δ , satisfies $\bar{F}_\delta(\bar{x}_{u,z}) \in F_a(\bar{x}_{u,z})$ for all $\bar{x}_{u,z} \in K$, where F_a is the inflated set-valued map constructed as in (38b) from the data $F(x_{u,z}) := \hat{F}_\delta(x_{u,z}, \nabla J(\hat{u}))$.

The conditions of Assumption 3 essentially ask that the flow map in (59) is designed such that, as $\varepsilon_\omega \rightarrow 0^+$, and on average, the hybrid dynamics behave as an ε_a -perturbed hybrid system for which the unperturbed nominal dynamics (60) are able to solve the decision-making problem (47).

A direct application of averaging tools—see Theorems 1-2 in *Averaging Theory: From ODEs to Hybrid Systems*—along with robustness results for hybrid systems satisfying the Hybrid Basic Conditions (see [8, Thm. 7.21]), leads to the following theorem concerning the closed set $\mathcal{A} \times \mathbb{R}_{\geq 0}$:

Theorem 5

Suppose that Assumption 3 holds. Then, the hybrid set-seeking system (59) with $y = J(u)$ and control law

$$u = \hat{u} + \frac{\varepsilon_a^2}{2} \mu_{\varepsilon_a}(\tau),$$

renders the set $\mathcal{A} \times \mathbb{R}_{\geq 0}$ SGPAS as $(\delta, \varepsilon_a, \varepsilon_\omega) \rightarrow 0^+$. \square

Hybrid Set-Seeking Systems with Estimates of Higher Derivatives

A variety of decision-making dynamics benefit from incorporating higher-order derivatives of the cost function to improve transient performance. For example, Newton methods utilize the second derivative of J to eliminate convergence dependence on the cost function’s curvature. In smooth ES systems, it has been shown [64], [65], [72] that higher-order derivatives can also be embedded into the controller through suitable design and manipulation of the dither signals μ and the output function y . Naturally, similar extensions are possible in the context of hybrid set-seeking systems by appropriately modifying the flow maps in (53b) or (59a). While we do not explore these manipulations in detail, we refer the reader to [64], [65], [72], [116], [117], as well as to an example in the next section, where

an ES algorithm switches between Newton and gradient-based dynamics to enhance performance.

EXAMPLES AND APPLICATIONS OF HYBRID SET-SEEKING SYSTEMS

The study of adaptive seeking systems with logic modes, event-based rules, and set-valued dynamics opens new avenues for research at the intersection of real-time, model-free control, and computer science, with applications in cyber-physical systems. In particular, equipped with the previous theoretical tools, in this section, we now study different types of hybrid set-seeking algorithms, including systems that can be modeled as logic-based switching ES, state-based switched ES, and reset-based ES. By working with well-posed hybrid systems, we show how different "if-then" rules can be systematically incorporated into set-seeking algorithms, while providing stability and robustness guarantees that parallel those existing for continuous-time systems.

Constrained Seeking via Set-Valued Dynamics

By considering (53) with $x_{uz} = \hat{u}$, $r = 0$, $\xi = \nabla J$, and sets $C_{u,z} = \hat{\mathbb{U}}$, $D_{u,z} = \emptyset$, $C_z = D_z = \Psi = \hat{G}_\delta = \emptyset$, we can apply Theorem 3 to establish stability properties for a broad class of novel continuous-time set-valued set-seeking systems, where the target decision-making dynamics evolve according to

$$\dot{\hat{u}} \in f(\hat{u}, \nabla J(\hat{u})), \quad \hat{u} \in \hat{\mathbb{U}}. \quad (61)$$

In particular, set-valued algorithms of the form (61) are common in decision-making problems with constraints due to the use of inner parametric optimization loops [118]–[120], projections [121], or state-dependent switching rules [122].

The example below considers a set-valued seeking algorithm inspired by population dynamics [118], and also illustrates the discussion on Remark 1.

Example 10 (Nash-Seeking in Population Games)

Consider a multi-agent system with three agents having payoffs of the form

$$J_1 = u_1(-u_3 + u_2), \quad J_2 = u_2(-u_3 + u_1), \quad J_3 = u_3(-u_2 + u_1), \quad (62)$$

and actions $u = (u_1, u_2, u_3) \in \mathbb{R}^3$ restricted to evolve in the simplex set $\hat{\mathbb{U}} := \{u \in \mathbb{R}_{\geq 0}^3 : u_1 + u_2 + u_3 = 1\}$, which is compact and convex. The agents seek to optimize their own payoff J_i by controlling their own action u_i , subject to the coupled constraint imposed by the set $\hat{\mathbb{U}}$, resulting in a generalized Nash equilibrium (NE) seeking problem. Since the vector of partial gradients $\nabla J = (\nabla_1 J_1, \nabla_2 J_2, \nabla_3 J_3)$ has entries given by $\nabla_1 J_1 = -u_3 + u_2$, $\nabla_2 J_2 = -u_3 + u_1$, and $\nabla_3 J_3 = -u_2 + u_1$, the Nash-seeking problem can also be studied as a Rock-Paper-Scissors population game with three strategies [118]. The unique NE of this game is given by $u^* = (\frac{1}{3}, \frac{1}{3}, \frac{1}{3})$. To converge to u^* using only measurements

of J_i , players can implement (53) with dynamics

$$\dot{\hat{u}} \in -k\hat{u} + k \left\{ w \in \hat{\mathbb{U}} : w^\top \xi = \max_{\hat{u} \in \hat{\mathbb{U}}} \hat{u}^\top \xi \right\}, \quad \hat{u} \in \hat{\mathbb{U}}, \quad (63)$$

where $k > 0$. By construction, the set-valued dynamics (63) satisfy item (a) of Assumption 1. Moreover, item (b) of Assumption 1 can be verified by studying the target system $\dot{\hat{u}} \in -\hat{u} + \{w \in \hat{\mathbb{U}} : w^\top \nabla J = \max_{\hat{u} \in \hat{\mathbb{U}}} \hat{u}^\top \nabla J\}$, $\hat{u} \in \hat{\mathbb{U}}$, which renders UGAS the NE u^* . Indeed, this stability property holds for a broader class of population games that satisfy $(u_a - u_b)^\top (\nabla J(u_a) - \nabla J(u_b)) \leq 0$ for all $u_a, u_b \in \hat{\mathbb{U}}$ [118, Thm. 7.2.7], which allows us to verify Assumption 1 without the explicit knowledge of the costs J_i . Figure 14 shows three different trajectories generated by the set-seeking dynamics (53) using (63), evolving on the set $\hat{\mathbb{U}}$, and converging to a neighborhood of the NE u^* . Note that the slow-frequency oscillations shown in the inset upper plot are not induced by the probing signals μ , but instead by the discontinuous nature of the dynamics (63). On the other hand, the oscillatory behavior on the state ξ , induced by the probing signals, is clearly shown on the lower plot. For this simulation, the parameters were selected as $\varepsilon_a = 0.01$, $k = 0.005$, $k_f/\varepsilon_a = 10$, and $\omega = (18.5, 20, 25.3) \times 10^4$.

Set-valued dynamical systems are also common in the analysis of projected gradient-based algorithms. The following example illustrates this application in a seeking algorithm that satisfies Assumption 2, where the filter and the decision-making dynamics are designed to operate on the same time scale.

Example 11 (Set-Seeking with Projected Dynamics)

Consider a model-free optimization problem of the form (47), where J is strictly convex and $\hat{\mathbb{U}}$ is a closed and convex set with non-empty interior, describing safety constraints that need to be satisfied for all time. To tackle this problem, we can consider the set-seeking system (53) with $D = \emptyset$ and

$$\dot{\hat{u}} = k\mathcal{P}_{T_{\hat{\mathbb{U}}}(\hat{u})}(-\xi), \quad \hat{u} \in \hat{\mathbb{U}}, \quad (64)$$

where $k > 0$ and $\mathcal{P}_{T_{\hat{\mathbb{U}}}(\cdot)}(\cdot)$ projects the vector $-\xi$ onto the tangent cone of $\hat{\mathbb{U}}$ at \hat{u} . In general, this projection leads to discontinuous vector fields, necessitating tools from nonsmooth analysis (see "Continuous-Time Set-Valued Dynamical Systems"); namely, the use of Krasovskii regularizations (S14). Indeed, under mild regularity assumptions on J and $\hat{\mathbb{U}}$, see [70], the Krasovskii solutions to (53) and (64) coincide with their standard (Caratheodory) solutions. Therefore, the resulting target average system (58), given by

$$\dot{\hat{u}} = \mathcal{P}_{T_{\hat{\mathbb{U}}}(\hat{u})}(-\xi), \quad \dot{\xi} = -k_f(\xi - \nabla J(\hat{u})), \quad \hat{u} \in \hat{\mathbb{U}}, \quad (65)$$

renders the set $\mathcal{A} = \{u^*\} \times \{\nabla J(u^*)\} \in \hat{\mathbb{U}} \times \mathbb{R}^n$ UGAS for k_f sufficiently small and $\kappa = 1$, see [70, Lemma 10]. It follows that Assumption 2 is satisfied with $\Lambda_{\xi,c} = \Lambda_{\xi,d} = \mathbb{R}^n$, and $k_f, \kappa > 0$ sufficiently small [70, Lemma 10]. Therefore, by Theorem 4, the model-free set-seeking dynamics (53) assure convergence to a neighborhood of the optimal solution u^* in $\hat{\mathbb{U}}$.

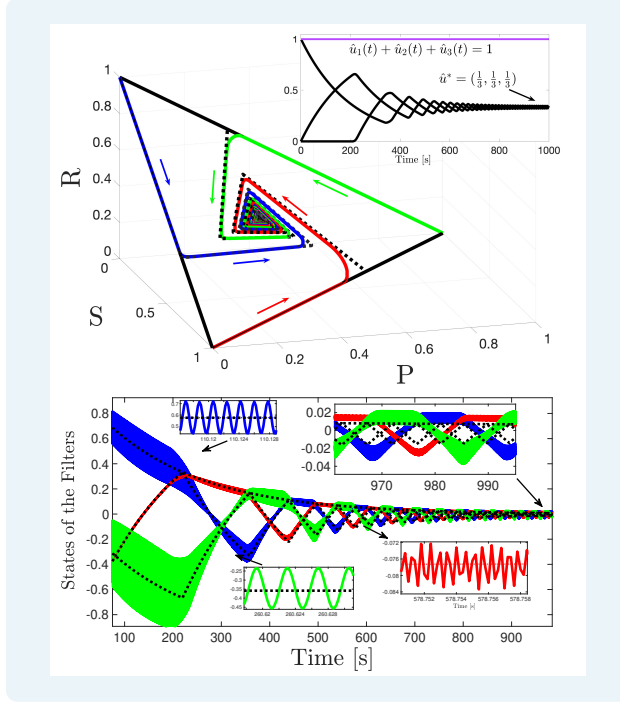


FIGURE 14 Trajectories of the set-seeking system studied in Example 10. **Top:** Three simulations with different initial conditions $\hat{u}(0)$, evolving on the simplex $\hat{\mathbb{U}}$ and converging to a neighborhood of u^* . **Bottom:** Time evolution of the filter states for one particular initialization of the algorithm.

Figure 15 shows a trajectory generated by (53) using the dynamics (64), approximately tracking the time-varying minimizer of a slowly-varying cost function of the form $J(u) = (u_1 - q_1)^2 + (u_2 - q_2)^2$, where $t \mapsto q(t) := (q_1(t), q_2(t))$ is a slowly varying parameter, and where the feasible set $\hat{\mathbb{U}}$ corresponds to a 45°-rotated box centered at the origin. As observed, the trajectories \hat{u} generated by the set-seeking dynamics remain in $\hat{\mathbb{U}}$ for all time. The simulation used the parameters $\varepsilon_a = 0.01$, $\omega = (100, 150)$, $k_f = 1$, $k = 0.2$. The state q was generated by a linear oscillator of the form (20) with frequency equal to 0.001. We note that seeking systems with projected dynamics can also be studied using Lipschitz vector fields [70, Sec. IV.A], as well as smooth Riemannian projections for decision-making problems defined on manifolds [106], [112].

Example 12 (Seeking with Unknown Constraints)

In Examples 10 and 11, the constraints that describe the decision-making problem (47) were known *a priori* by the practitioner. However, in certain applications, the precise mathematical form of the function that describes the constraints is also unknown. In particular, consider the constrained ES problem (47) where J is strictly convex, and

$$\hat{\mathbb{U}} = \{u \in \mathbb{R}^n : c(u) \leq 0\}, \quad (66)$$

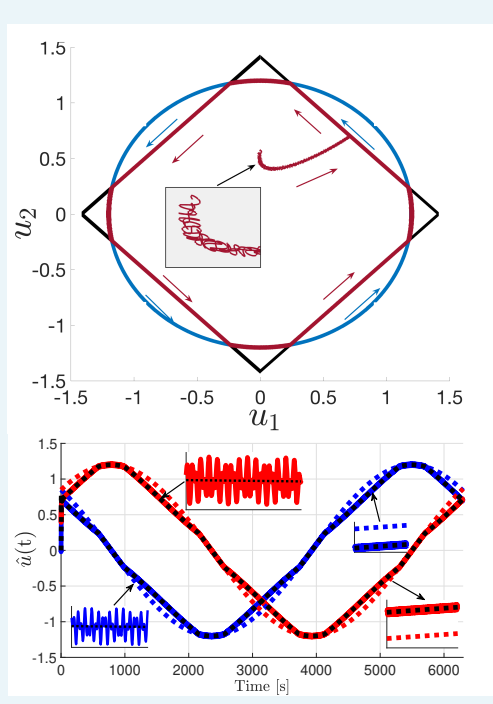


FIGURE 15 Trajectories of the set-seeking system studied in Example 11. **Top:** Evolution of the trajectories \hat{u} (red) within the feasible set $\hat{\mathbb{U}}$, corresponding to the rotated square. The blue trajectory represents the slowly varying minimizer of the cost function J in \mathbb{R}^n . As shown, the red trajectories closely follow the blue trajectory inside the feasible set. **Bottom:** Trajectories of \hat{u}_1 (blue) and \hat{u}_2 (red), the optimal solution u^* (black dotted), and the time-varying maximizers in \mathbb{R}^2 (dotted red and blue). As shown in inset, the trajectory \hat{u} closely tracks the constrained optimal solution u^* .

where $c : \mathbb{R}^n \rightarrow \mathbb{R}$ is an unknown smooth convex function that is accessible only via evaluations, and such that $\hat{\mathbb{U}}$ has non-empty interior. To tackle the seeking problem with unknown constraints we can consider the dynamics (53) with $D = \emptyset$ and the set-valued rule

$$\dot{\hat{u}} \in k \cdot \begin{cases} \{-\xi_J\} & \text{if } c(\hat{u}) < 0 \\ K(\xi_J, \xi_c) & \text{if } c(\hat{u}) = 0 \\ \{-\xi_c\} & \text{if } c(\hat{u}) > 0, \end{cases} \quad (67)$$

where $k > 0$, $K(\xi_J, \xi_c) := \{z \in \mathbb{R}^n : z = \lambda \xi_J + (1 - \lambda) \xi_c, \lambda \in [0, 1]\}$, and where the states ξ_J and ξ_c are generated by low-pass filters of the form (50), with inputs $y = J(u)$ and $y = c(u)$, respectively. It follows that item (a) of Assumption 1 holds [122], and the target decision-making system (51) associated with (67) is given by:

$$\dot{\hat{u}} \in k \cdot \begin{cases} \{-\nabla J(\hat{u})\} & \text{if } c(\hat{u}) < 0 \\ K(\hat{u}) & \text{if } c(\hat{u}) = 0 \\ \{-\nabla c(\hat{u})\} & \text{if } c(\hat{u}) > 0 \end{cases} \quad (68)$$

where $K(\hat{u}) := \{z \in \mathbb{R}^n : z = \lambda \nabla J(\hat{u}) + (1 - \lambda) \nabla c(\hat{u}), \lambda \in [0, 1]\}$, which also satisfies item (b) of Assumption 1 [122]. Therefore, by Theorem 3, the trajectories of (53) with dynamics

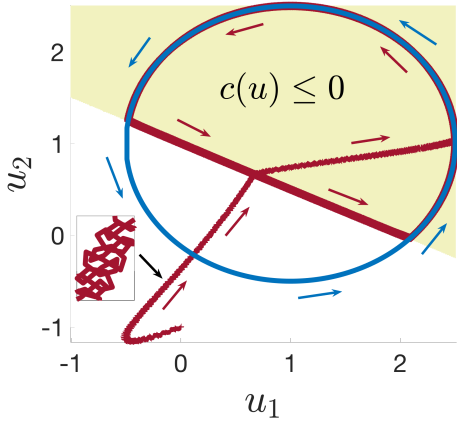


FIGURE 16 Trajectories \hat{u} of the seeking dynamics in Example 12. After converging to the feasible set, the trajectories track the slowly varying optimizer u^* .

(67) converge to a neighborhood of u^* , the optimizer of J in $\hat{\mathbb{U}}$. Figure 16 depicts a trajectory of the seeking dynamics generated by (67). The trajectory is initialized outside the feasible set (shaded region) and tracks the minimizer of a slowly varying cost function $J(u)$. In this case, $c(u) = a^\top u + b$, where $a = [-1 \ 2]$, $b = 2$, and J is the same as in Example 11. The parameters used in the simulation were $\varepsilon_a = 0.01$, $\omega = (100, 250)$, $k_f = 1$, and $k = 0.1$. As shown, the trajectory exhibits two phases. Initially, it converges to the feasible set while disregarding feedback from the cost function. Once inside the feasible set, the seeking dynamics drive it to a neighborhood of the optimal solution u^* . As is typical, the discontinuous nature of (67) induces chattering along the boundary of the feasible set $\hat{\mathbb{U}}$. In the next sections, we show how to avoid this chattering by introducing time regularization via resetting timers, or spatial regularization via switching conditions that induce hysteresis.

Seeking with Arbitrarily Fast Switching Dynamics

Let $\mathcal{Q} := \{1, \dots, q_{\max}\}$, where $q_{\max} \in \mathbb{Z}_{\geq 1}$ and consider a collection of set-valued mappings $f_q : \mathbb{R}^n \times \mathbb{R}^n \rightrightarrows \mathbb{R}^n$, with main state $\hat{u} \in \mathbb{R}^n$, auxiliary state $q \in \mathcal{Q}$, and target decision-making dynamics (51) with $\xi = \nabla J$, given by

$$\dot{\hat{u}} \in f_q(\hat{u}, \nabla J(\hat{u})), \quad \dot{q} = 0, \quad (\hat{u}, q) \in \hat{\mathbb{U}} \times \mathcal{Q} \quad (69a)$$

$$\hat{u}^+ = \hat{u}, \quad q^+ \in \mathcal{Q}, \quad (\hat{u}, q) \in \hat{\mathbb{U}} \times \mathcal{Q} \setminus \{q\}. \quad (69b)$$

The update rule (69a) describes a gradient-based differential inclusion parameterized by a constant q . On the other hand, the dynamics (69b) model the switches of q to a different mode in the set \mathcal{Q} , while keeping the main state \hat{u} constant. Figure 17 provides a common graphical representation of logic-based systems that switch between different modes. Such types of representation are connected to the well-known hybrid automata,

which can also be written as a HDS (23), see [8, Ex. 1.10]. In this sense, the tools presented in this article can also be used for the synthesis and analysis of seeking systems based on hybrid automata. Nonsmooth systems of the form (69a) can also be considered for the study of ES algorithms with finite-time or fixed-time (practical) convergence properties [123], [124].

Let the data of (69) satisfy the conditions of Assumption 1-(a), so that it can be used as a suitable target hybrid decision-making system. The following proposition, adapted from [91], [125], establishes that item (b) in Assumption 1 also holds under arbitrarily fast switching of q , provided that there exists a common Lyapunov function that certifies the stability of (69a) with respect to the set \mathcal{O} across all modes $q \in \mathcal{Q}$.

Proposition 1 (Seeking under Fast Switching)

Suppose that for each $q \in \mathcal{Q}$ the mapping f_q in (69a) is OSC, LB, and convex-valued. Suppose also that there exists $\alpha_1, \alpha_2 \in \mathcal{K}_\infty$, a continuous positive definite function $W : \mathbb{R}_{\geq 0} \rightarrow \mathbb{R}_{\geq 0}$, and a continuously differentiable function $V : \text{dom}(V) \rightarrow \mathbb{R}_{\geq 0}$, with $\hat{\mathbb{U}} \subset \text{dom}(V)$ such that for all $\hat{u} \in \hat{\mathbb{U}}$, all $\tilde{f} \in f_q$, and all $q \in \mathcal{Q}$:

$$\alpha_1(|\hat{u}|_{\mathcal{O}}) \leq V(\hat{u}) \leq \alpha_2(|\hat{u}|_{\mathcal{O}}) \quad (70a)$$

$$\langle \nabla V(\hat{u}), \tilde{f} \rangle \leq -W(|\hat{u}|_{\mathcal{O}}). \quad (70b)$$

Then, the differential inclusion

$$\dot{\hat{u}} \in \hat{F}(\hat{u}, \nabla J(\hat{u})) := \overline{\text{co}}_{q \in \mathcal{Q}} f_q(\hat{u}, \nabla J(\hat{u})), \quad \hat{u} \in \hat{\mathbb{U}}, \quad (71)$$

has the structure of (51) with the state $x_{uz} = \hat{u}$, $r = 0$, $\xi = \nabla J$, and sets $C_{u,z} = \hat{\mathbb{U}}$, $D_{u,z} = \emptyset$, $C_z = D_z = \Psi = \hat{G}_\delta = \emptyset$. Moreover, system (71) satisfies Assumption 1, and for each non-purely discrete solution (\hat{u}, q) of the switching system (69), \hat{u} is also a solution of (71). \square

The main takeaway from Proposition 1 is that seeking algorithms can be designed and analyzed to switch arbitrarily fast between a finite number of modes, provided that their continuous-

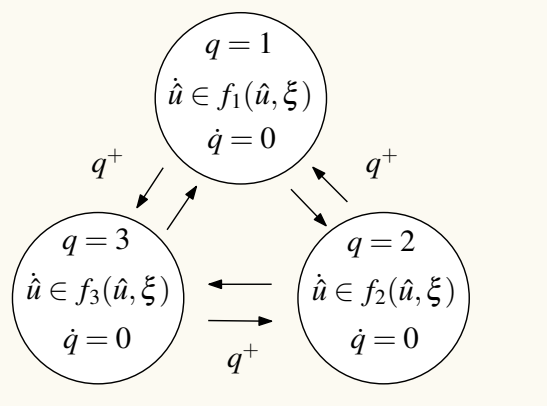


FIGURE 17 Logic-based ES allows to switch between different algorithms or “operating modes”.

time target decision-making dynamics share a common Lyapunov function. In this case, all (non-discrete) solutions of the switching decision-making dynamics (69) can be generated by the differential inclusion (71). Note that common Lyapunov functions satisfying the conditions of Proposition 1 emerge frequently in optimization algorithms, since the cost function J usually serves as a common Lyapunov function for different optimization dynamics. For example, this is the case in the standard gradient ascent and Newton methods, as well as related dynamics such as the Newton variable structure algorithm or the continuous Jacobian matrix transpose algorithm, for quadratic cost functions (see [126, Ch. 2]). A common Lyapunov function also emerges frequently in algorithms for distributed optimization, and learning in multi-agent systems with undirected switching communication topologies [127], [128].

Example 13 (Switching Multi-Agent Seeking Systems)

Consider a multi-agent system where N agents seek to cooperatively solve the following consensus-optimization problem:

$$\min J(u) = \sum_{i=1}^N J_i(u_i), \quad u_i \in \mathbb{R}^{n_i}. \quad (72)$$

Agents can communicate only to neighbors, who are characterized by an undirected graph that is allowed to change topology arbitrarily fast, but which is connected at all times. Since (72) is a well-studied problem in the literature whenever the gradients ∇J_i are known to the agents, there is a plethora of potential target nominal dynamics (51) that could be considered for the design of an ES system [129]. To illustrate the use of Krasovskii solutions, we consider the dynamics

$$\dot{\hat{u}}_i \in \hat{F}_{\delta,i}(\hat{u}_i, \xi_i) = \frac{k}{\delta} \sum_{j \in \mathcal{N}_i(t)} \overline{\text{sign}}(\hat{u}_j - \hat{u}_i) - k\gamma\xi_i, \quad (73)$$

where $\overline{\text{sign}}$ is the set-valued map defined in (S14), i.e.,

$$\overline{\text{sign}}(z) = \begin{cases} \{1\} & \text{if } z > 0 \\ [-1, 1] & \text{if } z = 0 \\ \{-1\} & \text{if } z < 0 \end{cases}. \quad (74)$$

To generate ξ_i , each agent implements its own autonomous derivative estimator (48) using its own cost function J_i as input. In this way, agents share information with neighbors only via the dynamics (73). By indexing all possible graph topologies using a set of logic modes $\mathcal{Q} = \{1, 2, \dots, q_{\max}\}$, the resulting system has the form (69), where each fixed logic mode q represents a particular graph topology. Figure 18 presents a numerical example with 5 agents, showing the evolution in time of the states \hat{u}_i , which converge to the optimal solution. The cost functions used in the simulations are given by $J_i = \frac{1}{2}u_i^\top u_i - 100b_i^\top u_i$, where $b_1 = (1, 2, 3, 4, 5)^\top$, $b_2 = (5, 4, 3, 2, 1)^\top$, $b_3 = (2, 3, 4, 5, 1)^\top$, $b_4 = (3, 4, 5, 1, 2)^\top$, $b_5 = (4, 5, 1, 2, 3)^\top$, and the ES parameters are $\varepsilon_a = 0.8$, $k = 0.05$, $k_f = 0.1$, $\varepsilon_l = 0.1$, $\omega = 500(5/6, 3/8, 2/3, 4/5, 7/10)$, $\alpha = 15$, $\gamma = 0.1$. It can be verified that the target nominal system (73) with $\xi_i = \nabla J_i$ and sufficiently large δ admits a common Lyapunov function across all connected undirected graphs [129]. It follows that Proposition

1 holds and therefore, by Theorem 3, the set-seeking dynamics achieve practical convergence to the set of solutions of (72).

Seeking with Average Dwell-time Switching

When a common Lyapunov function does not exist for the target switching system (69), it is still possible to stabilize \mathcal{O} in a semi-global practical sense by restricting how fast the state q switches between modes. For example, this can be achieved by imposing a dwell-time or an average dwell-time constraint on the switching signal. As discussed in Example 3, systems with jumps that satisfy these types of constraints can be modeled by using a hybrid automaton with state $\tau_1 \in \mathbb{R}_{\geq 0}$ and dynamics

$$\dot{\tau}_1 \in [0, \eta_1], \quad \tau_1 \in [0, N_0] \quad (75a)$$

$$\tau_1^+ = \tau_1 - 1, \quad \tau_1 \in [1, N_0], \quad (75b)$$

where $\eta_1 \in \mathbb{R}_{>0}$ and $N_0 \in \mathbb{Z}_{\geq 1}$. In particular, every solution of (75) has a hybrid time domain E with the property that for each of its elements $(s, i), (t, j) \in E$ with $s + i \leq t + j$, the following inequality holds:

$$N(t, s) := j - i \leq \eta_1(t - s) + N_0, \quad (76)$$

where $N(t, s)$ denotes the number of jumps in the interval $[s, t]$, see [80]. Therefore, when considering the joint hybrid dynamics (69) and (75), the hybrid time domains of the resulting system also satisfies inequality (76), thus effectively imposing a bound on how frequently q can switch in (69). When $N_0 = 1$, inequality (76) reduces to the well-known *dwell-time* condition, see [85]. When $N_0 \in \mathbb{Z}_{>1}$, inequality (76) describes an *average dwell-time* condition. It turns out that any hybrid time domain satisfying (76) can be generated by the hybrid automaton (75), see [130, Proposition 1.1]. Therefore, these dynamics can be used to study switching set-seeking systems under dwell-time and average dwell-time constraints on the switching signal.

Proposition 2 (Seeking with Slow Switching)

Suppose that for each $q \in \mathcal{Q}$ the mapping f_q in (69a) is OSC, LB, and convex-valued. Moreover, suppose that for each $q \in \mathcal{Q}$ the \hat{u} -dynamics in system (69a) render UGAS the set \mathcal{O} . Then, the HDS generated by Equations (69) and (75) has the structure of (51) with $r = 2$, $\delta = \eta_1$, $\hat{z} := (q, \tau)^\top$, $C_{u,z} := \hat{\mathcal{U}} \times \mathcal{Q} \times [0, N_0]$, $D_{u,z} := \hat{\mathcal{U}} \times \mathcal{Q} \times [1, N_0]$, $\Psi := \mathcal{Q} \times [0, N_0]$, $\hat{F}_\delta := f_q \times \{0\} \times [0, \eta_1]$, and $\hat{G}_\delta := \{\hat{u}\} \times \mathcal{Q} \setminus \{q\} \times \{\tau_1 - 1\}$. Moreover, this HDS satisfies all the items in Assumption 1. \square

The result of Proposition 2, which follows from [8, Corollary 7.28], enables the study of switching seeking dynamics where each seeking mode is able to individually stabilize the set \mathcal{O} , and where the switching between modes is "sufficiently slow" on average. Such types of problems might emerge in multi-agent systems with switching directed communication graphs for which a common Lyapunov function do not exist, as well as in seeking problems with slow variations in the landscape of the cost function, or problems that require a persistent switching of

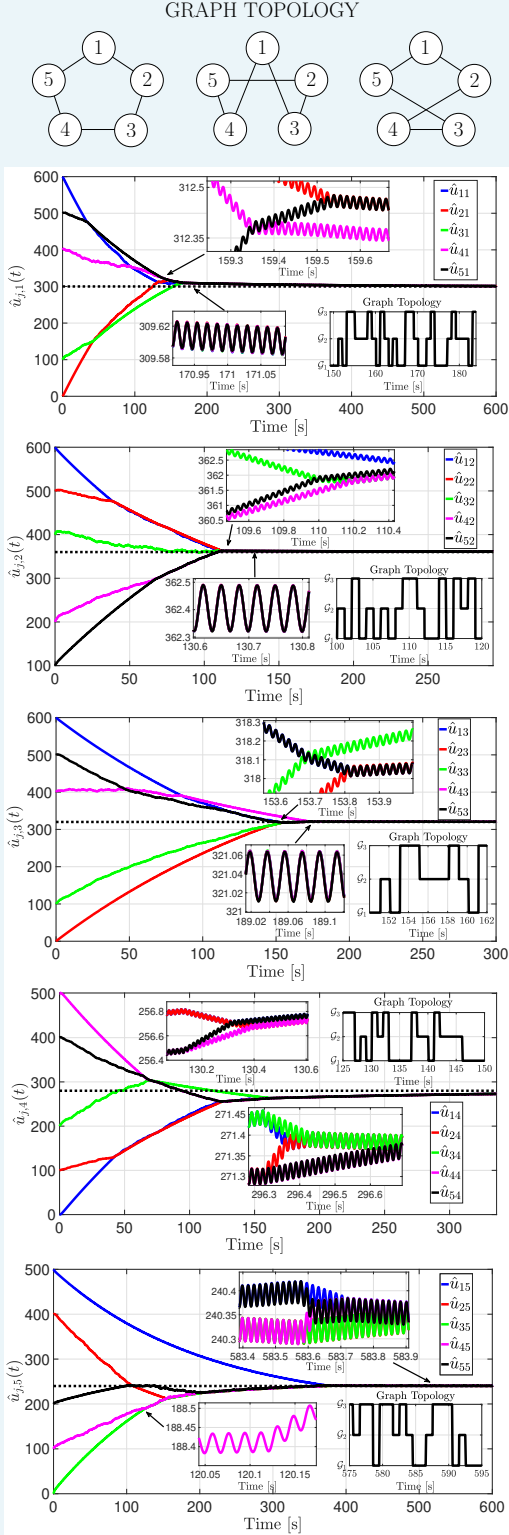


FIGURE 18 Trajectories of hybrid set-seeking algorithm (73) with communication graphs allowed to switch every 0.1 seconds.

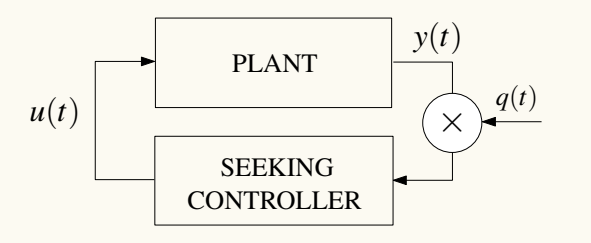


FIGURE 19 Scheme of ES controller under persistent multiplicative attacks ($q \in \{-1, 1\}$) on the output measurements.

the adaptation gains to achieve a desired performance.

The result of Proposition 2 can also be extended to ES systems with switching cost functions, even when the cost functions do not share the same minimizer $u_q^* \in \mathbb{R}^n$, as in Example 3. For instance, when $f_q(\cdot)$ is single-valued and continuous, for a sufficiently large compact set K of initial conditions, the (practical) stability of the resulting switching dynamics (69) and (75) can be studied with respect to the Omega-limit set from K , denote $\Omega(K)$, which is given by $\Omega(K) = \bigcup_{q \in \mathcal{Q}} \Omega_q$, where

$$\Omega_q = \overline{\bigcup_{j \in \mathbb{Z}_{\geq 0}} R_0 \left(\left(\{u_q^*\} + \frac{1}{j+1} \mathbb{B} \right) \times \{q\} \times [0, N_0] \right)}, \quad (77)$$

and where $R_0(K)$ denotes the reachable set from K . An illustration of this set is presented in Figure 6 for the source-seeking problem with persistent surveillance. For further details on switching systems with distinct equilibrium points, we refer the reader to [86].

Seeking with Switching Unstable Modes

In many applications, such as source-seeking missions, seeking algorithms are often implemented in highly adversarial and dynamic environments. In these settings, intermittent communication, sensing, or actuation failures are unavoidable due to external factors. Such intermittent failures can lead to unstable behaviors, which, however, can be corrected if the system is able to return to its nominal operating condition "sufficiently" often. This scenario can be analyzed using the framework of hybrid set-seeking systems by considering both stable and unstable modes in (69). Specifically, the compact set $\mathcal{Q} := \{1, \dots, q_{\max}\}$ can be partitioned as $\mathcal{Q} = \mathcal{Q}_u \cup \mathcal{Q}_s$, where the modes $q \in \mathcal{Q}_s$ represent stable dynamics and the modes $q \in \mathcal{Q}_u$ represent unstable dynamics. For this type of systems, stability can be guaranteed as long as the total activation time $T(s, t)$ of unstable modes during any time interval (s, t) satisfies the bound

$$T(s, t) := \int_s^t \mathbb{1}_{\mathcal{Q}_u}(q(r, j(r))) dr \leq T_0 + \eta_2(t - s), \quad (78)$$

where $\eta_2 \in [0, 1]$, $T_0 \in \mathbb{R}_{\geq 0}$, and $j(r)$ is the minimum j such that $(r, j) \in E$. Similarly to (75) and (76), the average activation-time constraint (78) can also be imposed on the switching signal q by using the following hybrid automaton with state $\tau_2 \in \mathbb{R}_{\geq 0}$

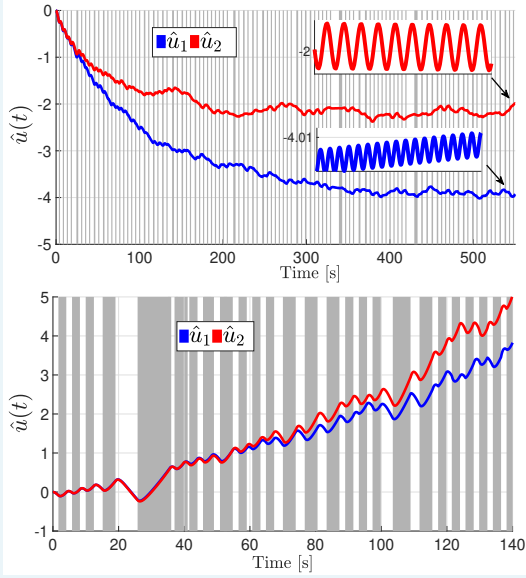


FIGURE 20 ES dynamics in \mathbb{R}^2 , under persistent attacks on the gradient estimation mechanism. The intensity of the attacks is modeled using (79). As shown in the upper plot, when η_2 is sufficiently small, the ES dynamics preserve stability. The lower plot shows the unstable behavior that emerges when η_2 is moderate.

and dynamics

$$\dot{\tau}_2 \in [0, \eta_2] - \mathbb{I}_{\mathcal{Q}_u}(q), \quad \tau_2 \in [0, T_0], \quad (79a)$$

$$\tau_2^+ = \tau_2, \quad \tau_2 \in [0, T_0], \quad (79b)$$

where $\mathbb{I}_{\mathcal{Q}_u}(\cdot)$ corresponds to the standard indicator function. In particular, every solution of the HDS given by (69) and (79) has a hybrid time domain E , such that for each of its elements $(s, i), (t, j) \in E$ with $s + i \leq t + j$ and signal $q : E \rightarrow \mathcal{Q}$ we have that the bound (78) holds. In fact, each hybrid time domain E with elements $(s, i), (t, j) \in E$ with $s + i \leq t + j$, satisfying (78) can be generated by the hybrid dynamics (69) and (79). Therefore, by combining dynamics (69), (75), and (79), we can design different types of hybrid algorithms (51) that satisfy Assumption 1 even when the decision-making algorithms operate under a persistent loss of communication, sensing, or actuation.

Proposition 3 (Seeking with Unstable Dynamics)

Suppose that for each $q \in \mathcal{Q}$ the mapping f_q in (69) is OSC, LB, and convex-valued, and that there exist $\chi \in \mathbb{R}_{\geq 1}$, $\alpha_{1,q}, \alpha_{2,q} \in \mathcal{K}_{\infty}$, $\lambda_s \in \mathbb{R}_{>0}$, $\lambda_u \in \mathbb{R}_{>0}$ and smooth functions $V_q : \hat{\mathbb{U}} \rightarrow \mathbb{R}_{\geq 0}$, such that the following inequalities hold:

$$\alpha_{1,q}(|\hat{u}|_{\mathcal{O}}) \leq V_q(\hat{u}) \leq \alpha_{2,q}(|\hat{u}|_{\mathcal{O}}), \quad \forall (q, \hat{u}) \in \mathcal{Q} \times \hat{\mathbb{U}}, \quad (80a)$$

$$\langle \nabla V_{q_s}, \tilde{f} \rangle \leq -\lambda_s V_{q_s}(\hat{u}), \quad \forall (q_s, \hat{u}, \tilde{f}) \in \mathcal{Q}_s \times \hat{\mathbb{U}} \times f_q, \quad (80b)$$

$$\langle \nabla V_{q_u}, \tilde{f} \rangle \leq \lambda_u V_{q_u}(\hat{u}), \quad \forall (q_u, \hat{u}, \tilde{f}) \in \mathcal{Q}_u \times \hat{\mathbb{U}} \times f_q. \quad (80c)$$

$$V_p(\hat{u}) \leq \chi V_q(\hat{u}), \quad \forall (q, p), \hat{u} \in \mathcal{Q} \times \hat{\mathbb{U}}. \quad (80d)$$

If the above parameters satisfy the following inequality:

$$\lambda_s > \eta_1 \log(\mu) + \eta_2(\lambda_s + \lambda_u), \quad (81)$$

then, the HDS composed by equations (69), (75), and (79), has the structure of (51) with $r = 3 \hat{z} := (q, \tau_1, \tau_2)$, $C_u = D_u = \hat{\mathbb{U}}$, $C_z = \mathcal{Q} \times [0, N_0] \times [0, T_0]$, $D_z = \mathcal{Q} \times [1, N_0] \times [0, T_0]$, and $\Psi := \mathcal{Q} \times [0, N_0] \times [0, T_0]$. Moreover, this HDS satisfies the items in Assumption 1, and the solutions' hybrid time domains satisfy the bounds (76) and (78). \square

The Lyapunov-based conditions (80) and the inequality (81) are common in the literature of switching systems with unstable modes. In this sense, Proposition 3 simply recasts such conditions using the hybrid automaton (75) and the hybrid monitor (79) such that, when interconnected with the target nominal dynamics (69), the resulting system has the form (51) and satisfies all the conditions needed for the analysis of switching set-seeking systems with unstable modes. We note that verification of the assumptions in Proposition 3 can be straightforward for some problems and algorithms, particularly when the cost J is quadratic, which leads to linear gradients ∇J . In fact, conditions (80a) and (80b) simply ask for UGAS of \mathcal{O} for each mode f_q , where $q \in \mathcal{Q}_s$. Similarly, condition (80c) simply asks that solutions of the differential inclusions associated to the unstable modes $q \in \mathcal{Q}_u$ have no finite escape times. Additionally, condition (80d) is easily satisfied if the Lyapunov functions are quadratic. In this case, conservative estimates of the parameters λ_s , λ_u , and μ , can be used to design the parameters η_1 and η_2 such that (81) holds.

To illustrate Proposition 3 as well as the discussion of Remark 4, we consider an ES algorithm with standard gradient dynamics $\dot{u} = -\xi$, operating in an environment where the sign of the measurements of y is corrupted in real time. Specifically, we consider a quadratic cost function $J(u) = 0.01u^T Qu + b^T u$, where $Q = [1, 1/2; 1/2, 3/2]$, $b = (0.1, 0.1)$, and we define $q \in \mathcal{Q} = \{-1, 1\}$, where $q = -1$ indicates that the output has been corrupted. See Figure 19 for a block-diagram representation. Figure 20 shows the time evolution of the resulting hybrid set-seeking dynamics with two different average activation times of the mode $q = -1$, using $\omega = (810, 420)$, $\varepsilon_a = 0.1$ and $\varepsilon_f = 1$. As observed, when the activation time is sufficiently short (i.e., η_2 is small), the seeking system successfully converges to the optimal point. In contrast, when η_2 is too large, the system becomes unstable. For related applications of ES in the context of deceptive attacks on gradient estimates, we refer the reader to [131]. Note that by redefining the set \mathcal{Q} as $\mathcal{Q} = \{0, 1\}$, the

previous model can also capture ES systems operating under sporadic feedback. In this case, source-seeking can still be achieved, provided that the condition (78) is satisfied. Multi-agent seeking problems involving persistent adversarial agents can also be analyzed using similar techniques; see [91, Sec. 6.3].

Seeking with Slowly Varying or Jumping Parameters

In many practical seeking problems, the parameters associated with the plant or the algorithm vary slowly over time. For instance, this occurs when the response map J is time varying or exhibits mild jumps on some of its parameters. Although slowly-varying seeking problems have been studied under the assumption that the target decision-making algorithm is input-to-state stable (ISS) with respect to the time derivatives of the varying signals in the cost [123], [132], [133], the ISS property may not necessarily hold for a broad class of decision-making algorithms (51). Nevertheless, such problems can still be addressed using the hybrid set-seeking systems framework studied in this paper. In particular, by letting q represent the time-varying parameter (or its derivative, depending on the application), redefining \mathcal{Q} in (69) as a compact but not necessarily finite set, and by allowing the flow dynamics in the hybrid system (69) to depend explicitly on q , i.e., $\dot{u} \in f(\hat{u}, \nabla J(\hat{u}), q)$, the slowly varying, weakly jumping behavior of q within \mathcal{Q} can be effectively modeled via the inclusions

$$\dot{q} \in \eta_3 \mathbb{B}, \quad \text{and} \quad q^+ \in q + \eta_3 \mathbb{B}, \quad \text{where} \quad \eta_3 \in \mathbb{R}_{>0}, \quad (82)$$

which replaces the q -dynamics in (69). In this scenario, we assume that for each $q \in \mathcal{Q}$, there exists an optimal compact set $\mathcal{O}_q \subset \hat{\mathbb{U}}$ that minimizes J , and we employ a simple average dwell-time automaton of the form (75) to rule out purely discrete-time solutions in the hybrid system. The following proposition is a direct consequence of [8, Corollary 7.27].

Proposition 4 (Seeking under Slowly-Varying Parameters)

Let $\mathcal{O}_q \subset \hat{\mathbb{U}}$ and suppose that for each $q \in \mathcal{Q}$ the mapping f_q in (69a) satisfies item (a) in Assumption 1 with the flow map given by $f(\hat{u}, \nabla J(\hat{u}), q)$ and the q -dynamics given by (69). Suppose also that for each $q \in \mathcal{Q}$ the dynamics $\dot{u} \in f(\hat{u}, \nabla J(\hat{u}), q)$ render the set \mathcal{O}_q UGAS. Then, this HDS combined with the dynamics (75) has the structure of (51) with $r = 2$, $\delta = \eta_3$, $\hat{z} := (q, \tau_1)$, $C_u = D_u = \hat{\mathbb{U}}$, $C_z = \mathcal{Q} \times [0, N_0]$, $D_z := \mathcal{Q} \times [1, N_0]$, $\mathcal{O} := \{(\hat{u}, q) : \hat{u} \in \mathcal{O}_q, q \in \mathcal{Q}\}$, and $\Psi := \mathcal{Q} \times [0, N_0]$. Moreover, this HDS satisfies all the items in Assumption 1. \square

An application of Proposition 4 was already illustrated in Example 11 and in Figure 15, where a slowly varying parameter q defines the cost function J . In particular, when $\dot{q} = 0$, the state q remains constant and the trajectories \hat{u} of the system converge to a neighborhood of the optimal point $u^*(q)$. Conversely, when $\dot{q} \in \eta_3 \mathbb{B}$, with \mathcal{Q} compact and $\eta_3 > 0$ sufficiently small, the tracking error $\tilde{u} = \hat{u} - u^*(q)$ converges to a neighborhood of zero.

Seeking in Noncontractible Spaces: Source-seeking with Obstacles

Smooth controllers, and dynamical systems in general, face fundamental limitations in stabilization problems when operating in complex spaces, particularly when obstacles are present. This is a consequence of the fact that obstacles usually preclude contractibility of the operational space, which is a necessary condition for *global* stabilization [110] under smooth feedback laws. For example, it has been shown that in obstacle avoidance problems, different types of controllers, including those based on navigation functions or CBFs can generate “deadlocks” [134] and undesirable spurious equilibria in the closed-loop system [135]. While it is well known that such undesirable points—often forming a set of measure zero—can be “pushed out” to the boundary of the feasible set [136], introducing even arbitrarily small perturbations from measurement noise or external disturbances in the closed-loop system can cause these problematic points in the state space to no longer be of measure zero, thereby precluding (almost) global convergence guarantees. However, these obstructions to *robust* global stabilization under obstacles, which also apply to optimization dynamics, can be overcome using hybrid set-seeking systems [83], [111], [112], [137]. For example, consider a vehicle operating on the plane according to the simple point-mass dynamics

$$\dot{p} = \alpha, \quad p \in \mathbb{R}^2, \quad (83)$$

where $p = (p_1, p_2)$ is the position and $\alpha \in \mathbb{R}^2$ is the control input. The main goal of the vehicle is to “discover” in real time the location $\mathcal{O} = \{u^*\} \in \mathbb{R}^2$ where a potential field J attains its maximum value, using only intensity measurements, while simultaneously avoiding an obstacle $\mathcal{N} \subset \mathbb{R}^2$ in the plane. As discussed in [110] and [137], this problem cannot be robustly solved using target decision-making algorithms (51) characterized by smooth feedback dynamics due to the topological obstructions introduced by the obstacle. Therefore, in order to achieve source-seeking and obstacle avoidance, we consider a hybrid source-seeking controller with feedback law given by

$$\alpha = \varepsilon_a \omega \mathbf{R}_0 \mu + \xi. \quad (84)$$

Assuming that we have access to measurements of J at the points p (to be used by the filter (50)) and $p - \varepsilon_a \mu$ (to be used in the flow and jump sets), which is possible via collocation of sensors, we consider the change of variable $\hat{u} = p - \varepsilon_a \mu$ to obtain the dynamics $\dot{\hat{u}} = \xi$, which puts the system into the form (55b) with $\hat{F} = \xi$ and $y = J(\hat{u} + \varepsilon_a \mu)$. To design the target hybrid decision-making dynamics (51), and inspired by [137], we let $q \in \mathcal{Q} = \{1, 2\}$ be a logic state that remains constant during flows and which is used to construct the following mode-dependent function:

$$\hat{f}_q(\hat{u}) = -J(\hat{u}) + B_q(\hat{u}), \quad (85)$$

where B_q is a mode-dependent barrier function to be designed. We restrict our attention to bounded obstacles $\mathcal{N} \subset \mathbb{R}^n$ for which there exists $p_0 = (p_{0,1}, p_{0,2}) \in \mathbb{R}^2$, $\rho \in \mathbb{R}_{>0}$ and $\delta \in \mathbb{R}_{>0}$ such that $\mathcal{N} \subset p_0 + \rho \mathbb{B}$ and $(p_0 + 2\rho\sqrt{2}\mathbb{B}) \cap (u^* +$

The study of adaptive seeking systems with logic modes and event-based rules opens new avenues for research at the intersection of real-time, model-free control and computer science, with applications in cyber-physical systems.

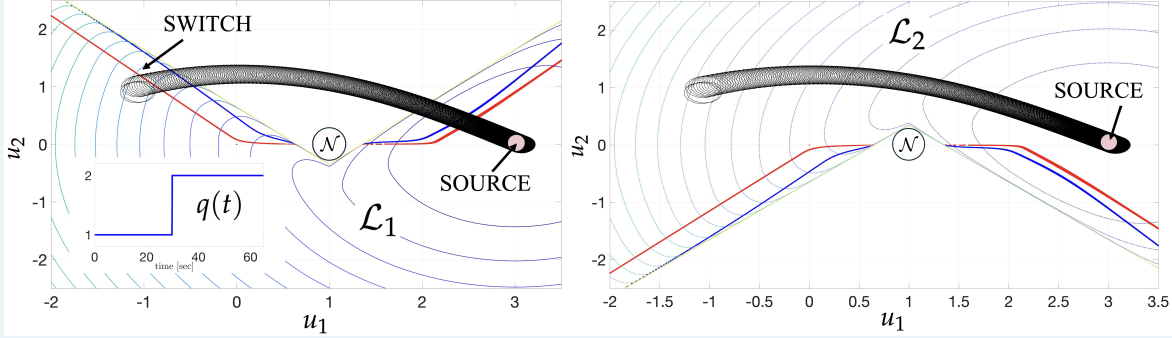


FIGURE 21 Trajectories of vehicle in \mathbb{R}^2 , controlled via a hybrid source-seeking algorithm for obstacle avoidance. The trajectories are shown over the virtual partitions \mathcal{L}_1 and \mathcal{L}_2 . The system is initialized in \mathcal{L}_1 with $q = 1$, but eventually switches to mode $q = 2$ to evolve in \mathcal{L}_2 , until it converges to a neighborhood of the source.

$\delta\mathbb{B}) = \emptyset$, that is, the obstacle \mathcal{N} is contained in a ball of radius ρ , centered at the point p_0 , and located sufficiently far away from the target p^* . To achieve obstacle avoidance, we divide the space into two different regions, each region indexed by a mode $q \in \{1, 2\}$, and having a corresponding mode-dependent signal $\hat{J}_q(\cdot)$, defined in (85). The main goal is to design the regions so that the vehicle can synergistically use the two potential fields $\hat{J}_q(\cdot)$ to safely navigate the space. To formalize this idea, consider the set

$$\mathcal{B}_{p_0, \rho} := \left\{ p : \|p - p_0\|_1 \leq 2\rho\sqrt{2} \right\}, \quad (86)$$

which satisfies $\{p_0\} + \rho\mathbb{B} \subset \mathcal{B}_{p_0, \rho} \subset \{p_0\} + 2\rho\sqrt{2}\mathbb{B}$. Additionally, consider the following subsets of \mathbb{R}^2 :

$$\begin{aligned} L_{1a} &:= \left\{ p : p_2 < -p_1 + p_{0,2} + p_{0,1} - 2\rho\sqrt{2} \right\}, \\ L_{1b} &:= \left\{ p : p_2 < p_1 + p_{0,2} + p_{0,1} - 2\rho\sqrt{2} \right\}, \\ L_{2a} &:= \left\{ p : p_2 > p_1 + p_{0,2} + p_{0,1} + 2\rho\sqrt{2} \right\}, \\ L_{2b} &:= \left\{ p : p_2 > -p_1 + p_{0,2} + p_{0,1} + 2\rho\sqrt{2} \right\}, \end{aligned}$$

and let $\mathcal{L}_1 := L_{1a} \cup L_{1b}$, $\mathcal{L}_2 := L_{2a} \cup L_{2b}$, $\mathcal{U} := \mathcal{L}_1 \cup \mathcal{L}_2$. Figure 21 illustrates the construction of the sets \mathcal{L}_1 and \mathcal{L}_2 , which satisfy $u^* \in \mathcal{L}_1 \cap \mathcal{L}_2$, and also $\mathcal{L}_1 \cap \mathcal{N} = \emptyset$, $\mathcal{L}_2 \cap \mathcal{N} = \emptyset$. In fact, $\mathcal{U} = \mathbb{R}^2 \setminus \mathcal{B}_{p_0, \rho}$. The mode-dependent barrier function B_q is designed such that the function $W(\hat{u}, q) := \hat{J}_q(\hat{u}) + J(\hat{u}^*)$ satisfies the following assumption:

Assumption 4 (Mode-Dependent Barrier Functions)

(a)

- 1) For each $q \in \mathcal{Q}$, the map $\hat{J}_q : \mathbb{R}^2 \rightarrow \mathbb{R}_{\geq 0} \cup \{\infty\}$ is continuously differentiable in \mathcal{L}_q , and as $\hat{u} \rightarrow \infty$ or $\hat{u} \rightarrow \text{bd}(\mathcal{L}_q)$ we have that $\hat{J}_q(\hat{u}) \rightarrow \infty$. Moreover, for every $\hat{u} \in \mathbb{R}^2 \setminus \mathcal{L}_q$, we define $J_q(\hat{u}) := \infty$.
- 2) There exist functions $\alpha_1, \alpha_2 \in \mathcal{K}_{\infty}$, and a proper indicator² $\tilde{\omega}$ of u^* on \mathcal{U} , such that

$$\alpha_1(\tilde{\omega}(\hat{u})) \leq \min_{s \in \mathcal{Q}} W(\hat{u}, s) \leq \alpha_2(\tilde{\omega}(\hat{u})), \quad \forall \hat{u} \in \mathcal{L}.$$

- 3) There exists a positive definite function ρ , such that for each $q \in \mathcal{Q}$:

$$|\nabla \hat{J}_q(\hat{u})|^2 \geq \rho(W(\hat{u}, q)),$$

for all $\hat{u} \in \mathcal{L}_q$. □

The above properties essentially guarantee that in each region \mathcal{L}_q , a gradient-based feedback law of the form $\dot{\hat{u}} = -\nabla \hat{J}_q(\hat{u})$ can steer the vehicle towards points where the virtual potential \hat{J}_q has smaller values, without leaving the region \mathcal{L}_q . Since it is not possible to satisfy property (c) in the entire space using only one barrier function, we ask that the condition holds only in each of the regions \mathcal{L}_q via a different potential \hat{J}_q .

²A function $\tilde{\omega} : \mathcal{U} \rightarrow \mathbb{R}_{\geq 0}$ is a proper indicator on the open set \mathcal{U} if it is continuous and $\tilde{\omega}(x_i) \rightarrow \infty$ when $i \rightarrow \infty$ if either $|x_i| \rightarrow \infty$ or the sequence $\{x_i\}_{i=1}^{\infty}$ approaches the boundary of \mathcal{U} .

By using the measurements of \hat{J}_q at the points \hat{u} , we can now introduce the flow and jump sets for the hybrid set-seeking system, with state (u, q) :

$$C_{u,q} := \{(\hat{u}, q) \in \bar{\mathcal{U}} \times \mathcal{Q} : \hat{J}_q(\hat{u}) \leq \chi \hat{J}_{3-q}(\hat{u})\}, \quad (87a)$$

$$D_{u,q} := \{(\hat{u}, q) \in \bar{\mathcal{U}} \times \mathcal{Q} : \hat{J}_q(\hat{u}) \geq (\chi - \lambda) \hat{J}_{3-q}(\hat{u})\}, \quad (87b)$$

where $\chi \in (1, \infty)$ and $\lambda \in (0, \chi - 1)$ are tunable parameters. The set $C_{u,q}$ describes the points in the space where the controller uses the potential field \hat{f}_q , while the set $D_{u,q}$ indicates the "switching zones" for the controller, where the controller toggles the logic state using $q^+ = 3 - q$. By construction, this switching behavior will take place whenever the value of the current function \hat{f}_q exceeds a threshold compared to the other function \hat{f}_{3-q} . In particular, the construction of the flow and jump sets imposes a *hysteresis* property on the switching controller, which precludes Zeno behavior. The red and blue lines in Figure 21 illustrate the boundaries of $D_{u,q}$ and $C_{u,q}$ respectively. The following proposition shows that the resulting nominal target hybrid controller has the form (51) and satisfies all the properties of Assumption 1 relative to $\bar{U} \times Q$.

Proposition 5 (Source-Seeking & Obstacle Avoidance)

Consider the hybrid set-seeking system (53), with sets $C_{u,q}$ and $D_{u,q}$ given by (87), function $\hat{F}_\delta = \xi$, and input $y = \hat{f}_q$. Suppose that Assumption 4 holds. Then, system (53) satisfies item (a) in Assumption 1 with $r = 1$, $\delta = 0$, $\hat{z} = q$, $\Psi = \mathcal{Q}$, $\mathcal{O} = \{u^*\}$. Moreover, item (b) holds with basin of attraction $\mathcal{U} \times \mathcal{Q}$. \square

To illustrate the stability properties of the resulting hybrid source-seeking system for obstacle avoidance, we show in Figure 21 the constructions of the partitions \mathcal{L}_1 and \mathcal{L}_2 , as well as the trajectory of the vehicle (83) under the control law (84), evolving over the two virtual partitions. As observed, the hybrid controller can (practically) stabilize the source of the signal J by switching the potential field after approximately 30s of flow, while avoiding the obstacle. We note that this simple example can be extended to other vehicle dynamics, including non-holonomic vehicles [83], and to the multi-obstacle case by considering other types of target hybrid systems [83], [138], [139]. In such cases, the target hybrid decision-making dynamics (51) will be modified, but the structure and stability properties of the hybrid set-seeking dynamics (53) can be studied using similar tools.

Seeking with Momentum and Resets

Reset control [140]–[142] is a well-known technique used to improve transient performance in dynamical systems that incorporate integrators in the feedback loop. The main idea behind the incorporation of resets is to dissipate energy at appropriate times to decrease overshoots and improve transient performance [142]. Resets can also be used to model restarting methods [113], [114], commonly employed in optimization routines. By leveraging tools from hybrid systems, set-seeking algorithms with momentum and restarting can also be designed to reduce overshoots and improve transient performance [69], [90], [116]. To illustrate

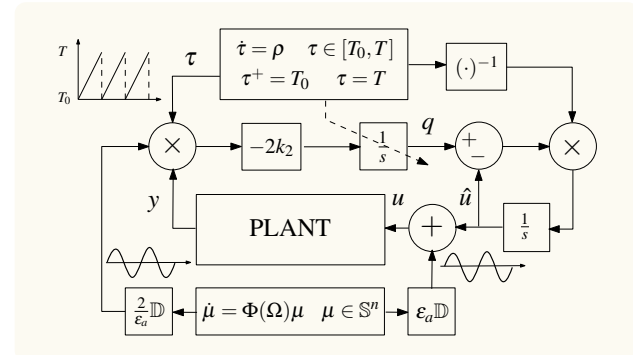


FIGURE 22 Block diagram representation of the hybrid set-seeking system with momentum, with (88) as target hybrid decision-making dynamics with $k_1 = 0$. Here, the low-pass filter is omitted.

this idea, we can consider the following target hybrid decision-making dynamics with state $(\hat{u}, q, \tau) \in \mathbb{R}^n \times \mathbb{R}^n \times \mathbb{R}_{\geq 0}$ and data

$$C_{u,z} = \mathbb{R}^n \times \mathbb{R}^n \times [T_0, T] \quad (88a)$$

$$\hat{F}(\hat{u}, q, \tau) = \begin{pmatrix} \frac{2}{\tau}(q - \hat{u}) - k_1 \nabla J(\hat{u}) \\ -2k_2 \tau \nabla J(\hat{u}) \\ \rho \end{pmatrix}, \quad (88b)$$

$$D_{\mu,z} = \mathbb{R}^n \times \mathbb{R}^n \times \{T\} \quad (88c)$$

$$\hat{G}(\hat{u}, q, \tau) = \begin{pmatrix} \hat{u} \\ \alpha \hat{u} + (1 - \alpha)q \\ T_0 \end{pmatrix}, \quad (88d)$$

where $k_1 \geq 0$ and $T_0, T, k_2, \rho > 0$ are tunable parameters that satisfy $T > T_0$. The parameter $\alpha \in \{0, 1\}$ is selected *a priori* to indicate whether the state q is reset during jumps. In particular, when the timer τ satisfies $\tau = T$, the discrete-time dynamics (88d) reset the timer back to T_0 . If, additionally, the parameter α satisfies $\alpha = 1$, then the state q is also reset to the current value of \hat{u} . Figure 21 presents a block-diagram representation of the hybrid set-seeking dynamics (53) associated with 88 for the case $k_1 = 0$. The filter is omitted for simplicity.

Using the change of coordinates $s = \hat{u}$ and $q = s + \frac{1}{2}\tau(\dot{s} + k_1\nabla J)$, the flows of the above system are related to the second-order ordinary differential equation

$$\ddot{s} + \frac{(2+\dot{\tau})}{\tau} \dot{s} + 4k_2 \nabla J(s) + k_1 \left(\nabla^2 J(s)^\top \dot{s} + \frac{\dot{\tau}}{\tau} \nabla J(s) \right) = 0,$$

which has been studied in the context of accelerated optimization algorithms under different choices of τ and parameters k_1, k_2 [93], [114], [143]–[145]. For example, when $k_1 = 0$ the above dynamics can also be written in state-space representation using $s_1 = s$ and $s_2 = \dot{s}$, leading to

$$\dot{s}_1 = s_2, \quad \dot{s}_2 = -\frac{c_1}{\tau} s_2 - c_2 \nabla J(s_1), \quad \dot{\tau} = \rho, \quad (89)$$

for suitable constants $c_1, c_2 > 0$. Note that when $\nabla J = \xi$, the system (89) has a structure similar to (58a) when $\hat{F}_\delta = \xi$. To avoid the issues discussed in Example 9, we can consider the flow and jump sets described in (88c) and (88a), respectively,

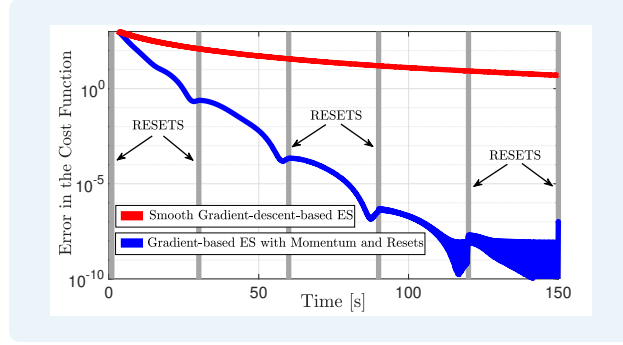


FIGURE 23 Trajectories \hat{u} generated by hybrid set-seeking dynamics with momentum and resets, compared to those of (3).

and the jump map

$$s_1^+ = s_1, \quad s_2^+ = (1 - \alpha)s_2, \quad \tau^+ = T_0, \quad (90)$$

which has a similar structure as (58b), with $s_1 = \hat{u}$, $\hat{z} = \tau$, $s_2 = \xi$, and $\hat{G}_\delta = (s_1, T_0)$ and $G_\xi = (1 - \alpha)s_2$. Therefore, this system can be viewed as a target hybrid decision-making system equipped with a hybrid filter that incorporates jumps to periodically reset the momentum to zero. Under a suitable choice of parameters, this hybrid set-seeking system can stabilize the set of minimizers of a convex functions J using only measurements. In particular, the following proposition follows from the results in [69], and illustrates the role of Theorem 4 in a slightly modified version of system (58) with nonlinear τ -dependent damping.

Proposition 6 (Seeking with Momentum and Resets)

Suppose that J is strictly convex and its unique minimizer is given by u^* , ∇J is globally Lipschitz and $\rho = \frac{1}{2}$. If $\alpha = 0$, then the HDS with flow and jump sets given by (88a) and (88c), and flow and jump maps given by (89) and (90), satisfies all the items of Assumption 2 with $\hat{u} = s_1$, $\hat{z} = \tau$, $r = 1$, $\xi = s_2$, $\kappa = -1$, $C_{u,z} = \mathbb{R}^n \times [T_0, T]$, $D_{u,z} = \mathbb{R}^n \times \{T\}$, $\Lambda_{\xi,c} = \Lambda_{\xi,d} = \mathbb{R}^n$, $\mathcal{O} = \{u^*\}$, $\Psi_z = [T_0, T]$, and $\Psi_f = \{0\}$. If $\alpha = 1$, and J is also strongly convex, then Assumption 2 also holds for T sufficiently large and in this case the set \mathcal{A} is UGES.

Figure 23 shows the performance of the hybrid set-seeking constructed with (88) as the target decision-making system, compared to the standard smooth gradient descent-based ES algorithm (3). As observed, the transient performance of the controller can be substantially improved under a suitable tuning of the resetting parameters $[T_0, T]$. For applications of similar ES algorithms in the context of traffic light systems, we refer the reader to [146].

The hybrid set-seeking dynamics (88) can be extended to multi-agent systems, as well as game theoretic settings where the goal is to converge to a Nash equilibrium [90], [147]. However, in these applications, the resets need to be coordinated to emulate the centralized "accelerated" performance observed in Figure 23, see [90]. Typically, such coordination mechanisms also need to

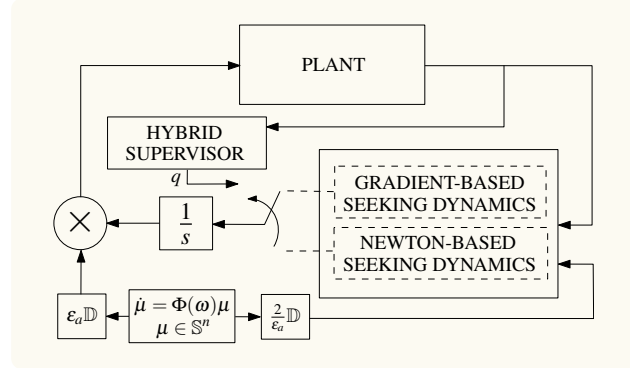


FIGURE 24 Scheme of hybrid set-seeking system that adaptively switches between gradient-based ES and Newton-based ES.

be set-valued to guarantee global convergence properties [148]. Adaptive resetting mechanisms that implement resets whenever state-dependent conditions are satisfied can also be considered for the design of hybrid set-seeking systems, see [94].

Seeking with Aggressive Gradient Exploration and Newton Fine-Tuning

When the cost function J is smooth and its Hessian matrix is positive definite, the decision-making problem (47) can be efficiently solved using Newton-like ES algorithms, which offer superior transient performance—allowing user-specified convergence rates—compared to traditional gradient-based ES methods [72], [116]. However, real-time estimation and inversion of the Hessian matrix in Newton-like ES algorithms can be highly sensitive to measurement noise and may lead to instabilities, particularly when the initial conditions are far from the minimizers of J . While increasing the frequency of the dither signals can help mitigate these challenges, it may require potentially unfeasible shorter sampling intervals to avoid aliasing during implementations. One potential solution to this issue is to use the more stable gradient-based ES algorithm when the system is far from the optimizer, and to switch to a Newton-like ES method for fine-tuning convergence near the optimum, a methodology that is not uncommon in standard optimization [149, pp. 23]. This idea can be formalized and implemented using hybrid set-seeking dynamics whenever a reasonable estimate of the optimal value of the cost J is known. To simplify our presentation, we focus on the 2-dimensional setting, and we incorporate a Hessian estimator into the flow map of (53b). Namely, instead of (53b), we let $\xi = (\xi_1, \xi_2)$ and consider a hybrid set-seeking system with feedback law (52), overall state $(x_{u,z}, \xi, \mu)$, and flow map

$$\dot{x} \in F(x) := \begin{pmatrix} \hat{F}(x_{u,z}, \xi) \\ -\frac{k_f}{\epsilon_f} \left(\xi_1 - \frac{2}{\epsilon_a} y \mathbb{D} \mu \right) \\ -\frac{k_h}{\epsilon_f} (y N(\mu) \xi_2 - y \mathbb{D} \mu) \\ \Phi(\omega) \mu \end{pmatrix}, \quad (91)$$

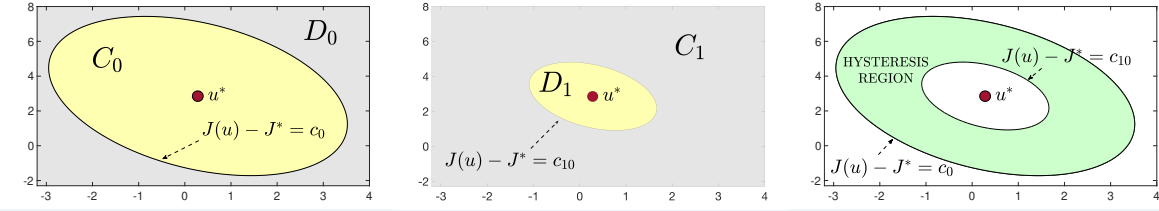


FIGURE 25 Representation of sets defined in (93) and (94), as well as the region of the space where hysteresis is induced in the switched controller.

where $x_{u,z} = (\hat{u}, \hat{z}) \in \mathbb{R}^3$, and

$$\hat{F}(x_{u,z}, \xi) = \begin{pmatrix} -\hat{z}\xi_1 - (1-\hat{z})\xi_2 \\ 0 \end{pmatrix}. \quad (92)$$

In this system, the auxiliary state $\hat{z} \in \mathcal{Q} := \{0, 1\}$ acts as a logic mode, and $\xi_2 \in \mathbb{R}^2$ can be seen as an estimate of the vector $\nabla^2 J^{-1} \nabla J$, where $\nabla^2 J$ is the Hessian of J [150], [151]. The matrix-valued function $N : \mathbb{R}^2 \rightarrow \mathbb{R}^{2 \times 2}$ can be designed as in [72], so that it has entries satisfying $N_{11} = \frac{16}{\varepsilon_a^2}(\mu_1^2 - \frac{1}{2})$, $N_{22} = \frac{16}{\varepsilon_a^2}(\mu_3^2 - \frac{1}{2})$, $N_{12} = \frac{4}{\varepsilon_a^2}\mu_1\mu_3$, and $N_{12} = N_{21}$. To define the sets C and D , we follow a uniting control approach [9], where the logic state \hat{z} indicates the current algorithm used by the controller. In particular, when the value of the cost J is sufficiently close to the optimal value J^* , we use $\hat{z} = 0$. On the other hand, when the value of J is greater than J^* , we use $\hat{z} = 1$. While this approach might require knowledge of J^* , for many ES applications where the cost to be minimized corresponds to some error function, it is known that $J^* = 0$. On the other hand, if J^* is unknown, a rough estimate can be used for the initial construction of the controller.

Building on these ideas, the switching zones for \hat{z} are defined using tunable thresholds specified by constants c_0 and c_{10} , with $c_0 > c_{10} > 0$. To characterize these thresholds, we define the sets

$$C_0 := \{\hat{u} \in \mathbb{R}^2 : J(\hat{u}) - J^* \leq c_0\}, \quad (93a)$$

$$C_1 := \overline{\mathbb{R}^2 \setminus \{\hat{u} \in \mathbb{R}^2 : J(\hat{u}) - J^* < c_{10}\}}, \quad (93b)$$

as well as the sets

$$D_0 := \overline{\mathbb{R}^2 \setminus \{\hat{u} \in \mathbb{R}^2 : J(\hat{u}) - J^* < c_0\}}, \quad (94a)$$

$$D_1 := \left\{ \hat{u} \in \mathbb{R}^2 : J(\hat{u}) - J^* \leq c_{10} \right\}. \quad (94b)$$

Using the constructions (93) and (94), the flow and jump sets for the state $x_{u,z}$ are given by

$$C_{u,z} := (C_0 \times \{0\}) \cup (C_1 \times \{1\}) \quad (95a)$$

$$D_{u,z} := (D_0 \times \{0\}) \cup (D_1 \times \{1\}). \quad (95b)$$

and the discrete-time dynamics of $x_{u,z}$ are given by

$$\hat{G}(x_{u,z}) = \begin{pmatrix} \hat{u} \\ 1 - \hat{z} \end{pmatrix}. \quad (96)$$

This scheme can be seen as using a "hybrid supervisor" to decide when to switch, while precluding Zeno behavior owing to the

hysteresis mechanism induced by the design of the flow and jump sets. A cartoon of the switching zones in \mathbb{R}^2 is shown in the left plot of Figure 25.

Proposition 7 (Switched Newton-Gradient Dynamics)

Consider the hybrid set-seeking dynamics (53), with $y = J(u)$, flow map (91), data (92)–(96), and feedback law (52). Then, item (a) of Assumption 1 holds with $r = 1$ and $\delta = 0$. Moreover, if J is smooth, radially unbounded and strongly convex, then item (b) also holds for the respective target hybrid decision-making dynamics with $\xi_1 = \nabla J$, $\xi_2 = \nabla^2 J^{-1} \nabla J$, $\mathcal{O} = \{u^*\}$ and $\Psi = \{0\}$. \square

We illustrate the Newton-Gradient Switched seeking dynamics using a simple two-dimensional numerical example for a quadratic cost function J , with the results shown in Figure 26. The figure depicts in color green a diverging trajectory that occurs when Newton-like ES dynamics are applied far from the optimal point using a moderate frequency ω . As shown by the blue trajectory, incorporating the hybrid uniting mechanism introduced in this section not only eliminates the instability but also significantly improves the transient performance of the controller—outperforming the more robust yet slower gradient-based ES dynamics, represented by the red trajectory. Figure 27

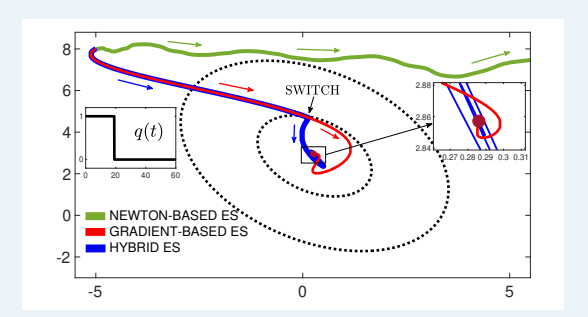


FIGURE 26 Trajectory \hat{u} of hybrid set-seeking system (shown in color blue) switching between Newton-based and gradient-based ES, compared to the trajectories obtained via standard gradient-based ES (shown in color red) and standard Newton-based ES (shown in color green).

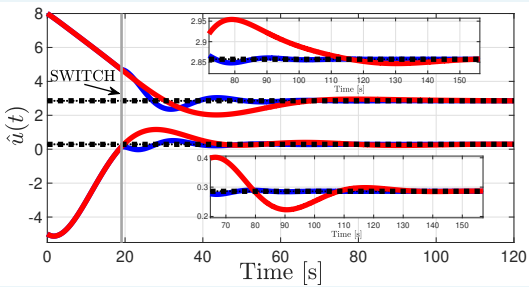


FIGURE 27 Evolution in time of trajectories \hat{u} for the hybrid set-seeking system switching between Newton-based and Gradient-based ES (shown in color blue). The red trajectory corresponds to the standard Gradient-based ES.

highlights this improvement in transient behavior, reducing the convergence time by more than half.

PART 3: HYBRID SET-SEEKING SYSTEMS FOR DYNAMIC PLANTS

In the previous section, we presented results and illustrative examples of hybrid set-seeking systems applied to plants modeled as static maps with output $y = J(u)$. In Part III, we extend these results to settings in which the plant exhibits dynamics. By leveraging singular perturbation results for hybrid inclusions (see Singularly Perturbed Hybrid Dynamical Systems), the standard methodology used to incorporate dynamic plants into smooth ES controllers can be naturally extended to the hybrid systems framework. This extension enables real-time set-seeking in dynamical systems.

Model of the Plant

Consider a plant with state $\theta \in \mathbb{R}^m$, input $u \in \mathbb{R}^n$ and output $y \in \mathbb{R}$, modeled by the constrained differential inclusion

$$\dot{\theta} \in P(\theta, u), \quad (\theta, u) \in \Lambda_\theta \times \mathbb{U}, \quad y = \varphi(\theta, u), \quad (104)$$

where $P : \mathbb{R}^m \times \mathbb{R}^n \rightrightarrows \mathbb{R}^m$ is a set-valued mapping, $\varphi : \mathbb{R}^m \times \mathbb{R}^n \rightarrow \mathbb{R}$ is an output function, θ evolves in the compact set $\Lambda_\theta := \lambda_\theta \mathbb{B} \subset \mathbb{R}^m$, $\lambda_\theta \in \mathbb{R}_{>0}$ can be taken arbitrarily large to encompass any solution of interest, and u evolves in the closed set $\mathbb{U} := \hat{\mathbb{U}} + \mathbb{B}$, where $\hat{\mathbb{U}} \subset \mathbb{R}^n$. The unitary inflation on $\hat{\mathbb{U}}$ is motivated by the fact that the control signal u will satisfy $u(t, j) \in \hat{\mathbb{U}} + \varepsilon_a \mathbb{B} \subset \mathbb{U}$ for all (t, j) in the domain of the solutions, where $\varepsilon_a \in (0, 1)$ is a tunable parameter.

To have enough regularity in the closed-loop system, we assume that $\hat{\mathbb{U}}$ is a closed set, that $P(\cdot, \cdot)$ is OSC, LB, and convex-valued relative to $\mathbb{R}^m \times \mathbb{U}$, and that $\varphi(\cdot, \cdot)$ is continuously differentiable. In this sense, the model (104) is quite general as it captures differential equations with a continuous right-hand side, as well as discontinuous plants modeled by their corresponding Krasovskii regularizations (see "Krasovskii Solutions of ODEs" in "Continuous-Time Set-Valued Dynamical Systems"). Common examples of plants with a discontinuous right-hand side include

mechanical systems with Coulomb friction [154, Chapter 12], systems arbitrarily switching between a finite number of continuous vector fields [8, Example 2.14], and plants with uncertain models and internal discontinuous feedback controllers, such as those based on sliding mode control [57].

Model-Free Feedback Optimization

For dynamic plants, the goal in ES is to regulate the input u towards the set of points that optimizes the steady-state input-to-output map of the plant. To ensure a well-defined optimization problem, we assume that the plant (104) exhibits suitable stability properties for each fixed input u . This can be achieved by first designing an inner controller that stabilizes (104) with respect to an external reference. Specifically, we assume that there exists a set-valued mapping $H : \mathbb{R}^n \rightrightarrows \mathbb{R}^m$ that is OSC and LB relative to \mathbb{U} , such that $H(\mathbb{U}) \subset \Lambda_\theta$, and for each $\rho > 0$ the compact set

$$\mathbb{M}_\rho := \{(\theta, u) : \theta \in H(u), u \in \mathbb{U} \cap \rho \mathbb{B}\} \quad (105)$$

is UGAS for the dynamics

$$(\theta, u) \in \Lambda_\theta \times (\mathbb{U}) \cap \rho \mathbb{B}, \quad \dot{\theta} \in P(\theta, u), \quad \dot{u} = 0. \quad (106)$$

In words, the above property establishes that for each fixed input u , the plant dynamics (104) have a well-defined (potentially set-valued) quasi-steady state, characterized by the set-valued mapping H . This property generalizes the classic assumptions made for ES in differential equations, e.g., [66, Assumptions 1 and 2], for the case that the plant under control is given by a constrained set-valued dynamical system.

Example 14 (Oscillator with Coulomb Friction)

Consider a simple harmonic oscillator with Coulomb friction and controllable velocity offset, given in open loop by the discontinuous dynamics

$$\dot{\theta}_1 = \theta_2 - u, \quad \dot{\theta}_2 = -\frac{B}{M} \operatorname{sgn}(\theta_2 - u) - \frac{K}{M} \theta_1, \quad \dot{u} = 0, \quad (107)$$

with $\Lambda_\theta = \lambda_\theta \mathbb{B} \subset \mathbb{R}^2$, $\mathbb{U} = \mathbb{R}$, $(B, K, M) \in \mathbb{R}_{>0}^3$, and $\lambda_\theta > \frac{B}{K} > 0$ is selected sufficiently large to characterize all the complete solutions of interest. The Krasovskii regularization of this system affects only the dynamics of θ_2 , and is given by

$$\dot{\theta}_2 \in P_2(\theta, u) = \begin{cases} -\frac{B}{M} - \frac{K}{M} \theta_1 & \text{if } \theta_2 > u \\ \left[-\frac{B}{M}, \frac{B}{M} \right] - \frac{K}{M} \theta_1 & \text{if } \theta_2 = u \\ \frac{B}{M} - \frac{K}{M} \theta_1 & \text{if } \theta_2 < u. \end{cases} \quad (108)$$

In this case, for each $\rho > 0$, system (106) renders the set $\mathbb{M}_\rho := \{(\theta, u) : \theta \in [-\frac{B}{K}, \frac{B}{K}] \times \{u\}, u \in \mathbb{R} \cap \rho \mathbb{B}\}$ UGAS [155, Section 3], thus satisfying the assumptions made on (104). \square

Example 15 (Fast Switching Plant)

Consider an open-loop switched linear system given by $\dot{\theta} = p_q(\theta, u) := A_q \theta + B_q u$, $\dot{u} = 0$, $\mathbb{U} := \mathbb{R}$, $(\epsilon, \lambda_\theta) \in \mathbb{R}_{>0}^2$, with matrices

$$A_q = \begin{bmatrix} -1 & \frac{3}{2} - \frac{5}{4}q \\ -\frac{9}{4} + \frac{5}{4}q & -1 \end{bmatrix}, \quad B_q = \begin{bmatrix} 1 \\ \frac{9}{4} - \frac{5}{4}q \end{bmatrix}, \quad (109)$$

Hybrid set-seeking systems can incorporate momentum with scheduled or adaptive restarting to accelerate convergence and reduce overshoots, while retaining robustness

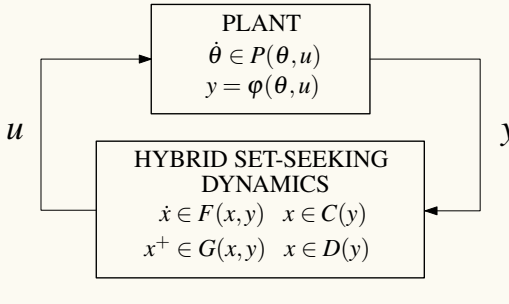


FIGURE 28 Dynamic plant interconnected with hybrid set-seeking dynamics for model-free feedback optimization.

where $q \in \{1, 2\}$. Under arbitrarily fast switching of q , this system is conveniently modeled by the differential inclusion

$$\dot{\theta} \in \{\alpha p_1(\theta, u) + (1 - \alpha)p_2(\theta, u), \alpha \in [0, 1]\}, \dot{u} = 0, \quad (110)$$

which is OSC, LB and convex-valued. For each $\rho > 0$ system (110) with flow set $\Lambda_\theta \times (\mathbb{U} \cap \rho\mathbb{B})$ renders UGAS the set $\mathbb{M}_\rho := \{(\theta, u) : \theta \in \{u\} \times \{0\}, u \in \mathbb{R} \cap \rho\mathbb{B}\}$, thus satisfying the required assumption. \square

To ensure a well-defined single-valued steady-state model-free optimization problem, we also assume that for each $u \in \mathbb{U}$ and any pair $\theta, \theta' \in H(u)$, the condition $\varphi(\theta, u) = \varphi(\theta', u)$ holds. In Example 14, any continuous output function $\varphi(\cdot, \cdot)$ that depends only on θ_2 in its first argument will satisfy this assumption. On the other hand, in Example 15, any continuous output function satisfies this assumption. If H is singled-valued, as in the traditional literature of ES, then this assumption is also satisfied.

We can now define the *response map* of the plant (104):

$$J(u) := \{\varphi(\theta, u) : \theta \in H(u)\}, \quad (111)$$

which is assumed to be continuously differentiable. As in the static case, the set-seeking problem is given by

$$\text{optimize } J(u), \quad \text{s.t. } u \in \hat{\mathbb{U}}. \quad (112)$$

For consistency, we denote again the set of solutions to (112) as $\mathcal{O} \subset \mathbb{R}^n$, which is assumed to be non-empty and compact.

Closed-Loop System and Stability Properties

To interconnect the plant (104) with the hybrid-set seeking dynamics (53) via the feedback law (52), a time-scale separation

usually needs to be induced between the flows of both systems. To achieve this separation, the flow map (53b) is multiplied by a small gain $k > 0$, leading to the following closed-loop hybrid system:

$$C := C_{u,z} \times \Lambda_\xi \times \mathbb{S}^n \times \Lambda_\theta, \quad (113a)$$

$$\dot{x} \in F(x) := \begin{pmatrix} k\hat{F}_\delta(x_{u,z}, \xi) \\ -k\frac{\varepsilon_f}{\varepsilon_f} \left(\xi - \frac{2}{\varepsilon_a} \varphi(\theta, \hat{u} + \varepsilon_a \mathbb{D}\mu) \cdot \mathbb{D}\mu \right) \\ k\Phi(\omega)\mu \\ P(\theta, \hat{u} + \varepsilon_a \mathbb{D}\mu) \end{pmatrix}, \quad (113b)$$

$$D := D_{u,z} \times \Lambda_\xi \times \mathbb{S}^n \times \Lambda_\theta, \quad (113c)$$

$$x^+ \in G(x) := \begin{pmatrix} \hat{G}_\delta(x_{u,z}) \\ \xi \\ \mu \\ \theta \end{pmatrix}, \quad (113d)$$

where $x := (x_{u,z}, \xi, \mu, \theta) \in \mathbb{R}^{r+4n+m}$, with tunable parameters $(k, \varepsilon_a, \varepsilon_f, \varepsilon_\omega)$. Figure 28 shows a high-level block diagram of the interconnection between the plant and the controller. The dependence of the hybrid dynamics on the output y highlights that the specific structure of the components is application-dependent.

To study the stability properties of the closed-loop system (113) via singular perturbation theory, we introduce a new continuous-time variable given by $s = kt$. Since $\frac{d}{dt}x = k\frac{d}{ds}x$, the continuous-time dynamics (113b) in the new s -time scale become

$$\frac{d}{ds}x \in F(x) := \begin{pmatrix} \hat{F}_\delta(x_{u,z}, \xi) \\ -\frac{\varepsilon_f}{\varepsilon_f} \left(\xi - \frac{2}{\varepsilon_a} \varphi(\theta, \hat{u} + \varepsilon_a \mathbb{D}\mu) \cdot \mathbb{D}\mu \right) \\ \Phi(\omega)\mu \\ \frac{1}{k}P(\theta, \hat{u} + \varepsilon_a \mathbb{D}\mu) \end{pmatrix}, \quad (114)$$

which, combined with (113a), (113c), and (113d) generates a singularly perturbed hybrid system of the form (S97) with $\varepsilon = k$ (see "Singularly Perturbed Hybrid Dynamical Systems"). We denote this system as \mathcal{H}_s to emphasize that the continuous-time dynamics evolve in the s -time scale. For this system, it follows that the reduced hybrid dynamics (S100) are precisely given by the hybrid-set seeking systems (53) with $y = J(u)$, whose stability properties were studied in Theorems 3-4. Since the boundary layer dynamics of \mathcal{H}_s are precisely given by the plant dynamics (106), we can use Theorem 6 (see "Singularly Perturbed Hybrid Systems") to obtain the following stability result for hybrid set-seeking systems with plants in the loop [91]:

Singularly Perturbed Hybrid Dynamical Systems

Stability properties of extremum seeking systems rely on multiple time-scale separations induced in the closed-loop system via appropriate tuning of the control parameters. Singular perturbation theory is a well-established field in the literature of differential equations that enables the study of systems for which certain states evolve in a faster time scale and converge to a quasi-steady state manifold, where the original system can be "reduced" [57], [58]. Here, we review some extensions of singular perturbations to hybrid systems [102], [152], [S1] that fit the models considered in this paper. Further details can be found in [S1].

Hybrid Systems with "Fast" and "Slow" States

Consider a hybrid system with states $(x, \theta) \in \mathbb{R}^{n_1} \times \mathbb{R}^{n_2}$ and the following dynamics:

$$(x, \theta) \in C := C_x \times \Theta, \quad \begin{cases} \dot{x} \in F_x(x, \theta) \\ \varepsilon \dot{\theta} \in F_\theta(x, \theta) \end{cases} \quad (\text{S97a})$$

$$(x, \theta) \in D := D_x \times \Theta, \quad (x^+, \theta^+) \in G(x, \theta), \quad (\text{S97b})$$

where the set-valued mappings $F_x : \mathbb{R}^{n_1} \times \mathbb{R}^{n_2} \rightrightarrows \mathbb{R}^{n_1}$ and $F_\theta : \mathbb{R}^{n_1} \times \mathbb{R}^{n_2} \rightrightarrows \mathbb{R}^{n_2}$ characterize the continuous-time dynamics of x and θ , respectively. Similarly, $G : \mathbb{R}^{n_1} \times \mathbb{R}^{n_2} \rightrightarrows \mathbb{R}^{n_1+n_2}$ describes the jump map of the system. The flow set C is comprised by the Cartesian product of the sets $C_x \subset \mathbb{R}^{n_1}$ and $C_\theta \subset \mathbb{R}^{n_2}$, while the jump set D is comprised of the sets $D_x \subset \mathbb{R}^{n_1}$ and $D_\theta \subset \mathbb{R}^{n_2}$. We make the assumption that system (S97) satisfies the hybrid basic conditions and that Θ is a compact set.

In system (S97), $\varepsilon \in \mathbb{R}_{>0}$ is a small parameter that induces a time-scale separation between the continuous-time dynamics of the state $x \in \mathbb{R}^{n_1}$ and the continuous-time dynamics of $\theta \in \mathbb{R}^{n_2}$. In particular, when ε is small, $x \in \mathbb{R}^{n_1}$ behaves as a "slow" state in the system, while $\theta \in \mathbb{R}^{n_2}$ behaves as a "fast" state. When the fast dynamics in system (S101) define a suitable "quasi-steady" state, the behavior of the state x can be approximately predicted by a *reduced system*. For example, this is the case when θ converges to a continuously differentiable quasi-steady state manifold $m : \mathbb{R}^n \rightarrow \mathbb{R}^m$, as is usually the case in the literature of differential equations. However, in the context of hybrid systems, it is common to have fast dynamics for which the quasi-steady state is actually characterized by a set-valued mapping $M : \mathbb{R}^n \rightrightarrows \mathbb{R}^m$. In such cases, we assume that M is outer-semicontinuous and locally bounded, and that for each $\rho > 0$ the set

$$M_\rho = \{(x, \theta) : \theta \in M(x), x \in \rho \mathbb{B}\} \quad (\text{S98})$$

is UGAS for the following *boundary layer dynamics*:

$$(x, \theta) \in (C_x \cap \rho \mathbb{B}) \times \Theta, \quad \dot{x} = 0, \quad \dot{\theta} \in F_\theta(x, \theta). \quad (\text{S99})$$

Note that in (S99), the state x is taken as constant from any initial condition on $C_x \cap \rho \mathbb{B}$.

Using the mapping M , the *reduced hybrid system*, with state $x_r \in \mathbb{R}^n$, can be defined using the following dynamics:

$$x \in C_x, \quad \dot{x} \in F_r(x) := \overline{\text{co}}\{f : f \in F_x(x, \theta), \theta \in M(x)\} \quad (\text{S100a})$$

$$x \in D_x, \quad x^+ \in G_r(x) := \{f_1 : (f_1, f_2) \in G_x(x, \theta), \theta \in \Theta\}. \quad (\text{S100b})$$

By construction, and by the assumptions on the data of system (S97), the reduced hybrid system (S100) satisfies the Hybrid Basic Conditions.

Theorem 6 (SGPAS in Singularly Perturbed HDS)

Suppose there exists a compact set $\mathcal{A} \subset \mathbb{R}^{n_1}$ that is UGAS for the reduced HDS (S100). Then, the singularly perturbed HDS (S97) renders the set $\mathcal{A} \times \Theta$ SGPAS as $\varepsilon \rightarrow 0^+$.

When the hybrid system (S97) possesses additional structure, stronger results such as UGAS or UGES can be established. For instance, in the context of hybrid extremum seeking with hybrid filters operating on a faster time scale, the flow and jump sets in (S97) take the form $C = C_x \times C_\theta$ and $D = D_x \times D_\theta$, where C_θ and D_θ are not necessarily compact. By imposing appropriate Lyapunov-based conditions on the reduced dynamics, boundary layer dynamics, and certain interconnection properties, UGAS or UGES can usually be established for these dynamics, provided that ε is sufficiently small [102, Sec. 5]. This approach mirrors the classical composite Lyapunov method based on quadratic-like Lyapunov functions used to analyze singularly perturbed differential equations [153].

Remark 1: Averaging using Singular Perturbations

There are close connections between averaging and certain models of singularly perturbed systems. For example, when the fast state in (S101) does not settle to a point, but instead oscillates, it is still possible to define a well-posed reduced hybrid system. For example, when the continuous-time dynamics in (S101) have the form

$$(x, \theta) \in C := C_x \times \Theta, \quad \begin{cases} \dot{x} = f_x(x, \theta) \\ \varepsilon \dot{\theta} = f_\theta(x, \theta) \end{cases} \quad (\text{S101})$$

and the jump map in (S97b) is of the form $G(x, \theta) = G_x(x) \times \{\theta\}$, we can define a hybrid reduced system using the data

$$\bar{x} \in C_x, \quad \dot{\bar{x}} = \bar{f}(\bar{x}), \quad (\text{S102a})$$

$$\bar{x} \in D_x, \quad \bar{x}^+ \in G(\bar{x}), \quad (\text{S102b})$$

where \bar{f} is a continuous function that satisfies

$$\left| \frac{1}{T} \int_0^T (f_x(x, \theta(s)) - \bar{f}(x, p)) ds \right| \leq \gamma_K(T), \quad (\text{S103})$$

for all $T \in \mathbb{R}_{\geq 0}$, all $x \in C_x \cap K$, all compact sets $K \subset \mathbb{R}^{n_1}$, and all solutions $\theta : [0, T] \rightarrow \mathbb{R}^{n_2}$ of the dynamics $\dot{\theta}(t) = f_\theta(x, \theta(t))$, where $\gamma_K(\cdot)$ is a continuous, non-increasing function that satisfies $\lim_{T \rightarrow \infty} \gamma_K(T) = 0$, and which is allowed to depend on K . Note that the definition of \bar{f} in (S103) is similar to the average map defined in (S44). Indeed, one can study oscillatory hybrid systems with fast states generated by time-invariant systems via averaging using the model (S102). This observation is important in order to exploit robustness properties in well-posed hybrid systems with compact attractors.

REFERENCES

[S1] R. G. Sanfelice, A. R. Teel, "On singular perturbations due to fast actuators in hybrid control systems", *Automatica*, Vol. 47, No. 4 pp. 692-701, 2011.

Theorem 7 (Stability Properties in Dynamic Maps)

Consider the HDS \mathcal{H}_s , and suppose that Assumption 1 holds for the hybrid reduced set-seeking dynamics (53). Then, the set $\mathcal{A} \times \Lambda_\xi \times \mathbb{S}^n \times \Lambda_\theta$ is SGPAS as $(\delta, \varepsilon_f, \varepsilon_a, \varepsilon_\omega, k) \rightarrow 0^+$.

Based on Theorem 7 and the material presented in Parts II-III of this article, several comments are in order:

- » The semi-global practical stability properties of Theorem 7 are established with respect to compact sets, where the main state $x_{u,z}$ is steered towards a neighborhood of $\mathcal{A} = \mathcal{O} \times \Psi$, i.e., \hat{u} converges to a neighborhood of the optimal solution of problem (112). Since the actual input u is defined via the feedback law (52), it will also converge to a neighborhood of order ε_a of the set \mathcal{O} , which is consistent with the classic results in ES.
- » It is possible to refine the convergence statement for the state θ , such that $\theta(t, j) \rightarrow H(\mathcal{O})$ as $(t, j) \rightarrow \infty$. Without additional structure or regularity conditions, this property holds only if jumps do not dominate the hybrid system's dynamics—that is, the system must not exhibit Zeno behavior or purely discrete solutions. Such pathological behaviors can be ruled out by applying any of the temporal regularization strategies discussed in Part 2 using dynamic timers, which impose dwell-time or average dwell-time constraints on the jump times.
- » Similarly to the static map case, the result of Theorem 7 asserts suitable \mathcal{KL} bounds of the form (42) for all solutions of the system. In this sense, we do not insist on the uniqueness of solutions for any of the proposed controllers. Instead, we ask that every solution satisfies the desired property. When multiple solutions exist, the practitioner can select the most meaningful solution for the application of interest based on application-dependent considerations.
- » As discussed in Part II, the result of Theorem 7 can be extended to cover set-seeking systems that use hybrid filters and hybrid dither generators as part of the feedback loops. Similarly, more complex plants can also be incorporated by using averaging tools for hybrid systems that exhibit hybrid boundary layer dynamics. Due to space constraints, we do not elaborate on these extensions here, and instead we refer readers interested in these subjects to the references [156], [102], [157], [158], and [108].

We finish this section with a numerical example in the context of Nash equilibrium seeking problems, and by highlighting the fact that the stability results presented in Theorems 3, 4 and 7 are amenable to standard discretization techniques, such as (consistent) Euler methods or Runge-Kutta methods (c.f., Corollary 2). This follows by the fact that the proposed hybrid controllers are robust to small perturbations, including those that emerge when the flow map is discretized. For further details on this subject, we refer the reader to [159] and [69, Sec.4].

Example 16 (Nash-Seeking with Intermittent Updates)

Consider a two-player noncooperative game, where each player $i \in \{1, 2\}$ is characterized by a switching plant with state $\theta_i = (\theta_{i,1}, \theta_{i,2})$, and dynamics of the form (109), that is

$$\dot{\theta}_{i,1} = -\theta_{i,1} + \left(\frac{3}{2} - \frac{5}{4} p_i \right) \theta_{i,2} + u_i, \quad (115)$$

$$\dot{\theta}_{i,2} = -\theta_{i,2} + \left(-\frac{9}{4} + \frac{5}{4} p_i \right) \theta_{i,1} + \left(\frac{9}{4} - \frac{5}{4} p_i \right) u_i, \quad (116)$$

where $p_i : \text{dom}(q) \rightarrow \{1, 2\}$ is the switching signal, which, for simplicity, is assumed to be the same for both players. Each player has a quadratic output function φ_i that depends on the first state of each player, i.e., $y_i = \varphi_i(\tilde{\theta}_1) = \tilde{\theta}_1^\top Q_i \tilde{\theta}_1 + \tilde{\theta}_1^\top b_i + c_i$, where $\tilde{\theta}_1 = (\theta_{1,1}, \theta_{2,1})$, $Q_i \in \mathbb{R}^{2 \times 2}$, $b_i \in \mathbb{R}^2$ and $c_i \in \mathbb{R}$ are selected as in [91, Sec.6.3]. The goal of the players is to individually maximize their own steady-state input-to-output cost function (111) using only individual output measurements y_i . However, unlike traditional Nash-seeking problems where players continuously update their actions [51], [107], we study the scenario where the inputs to the player dynamics are updated only sporadically, which is common under computational or communication constraints. To model this behavior, we assign to each player a logic state $q_i \in \{0, 1\}$ that multiplies the dynamics of the player's states \hat{u}_i , $i \in \{1, 2\}$. In particular, we consider the simple Nash-seeking rule $\dot{\hat{u}}_i = q_i \xi_i$, where ξ_i is generated by an individual low-pass filter implemented by each player. Figure 29 shows a block-diagram representation of the closed-loop system of each player $i \in \{1, 2\}$ under the seeking dynamics with switching logic states q_i , and switching plant with logic states p_i . To study the stability properties of the overall switching system, we let $\ell \in \{1, 2, 3, 4\}$ be a logic state that indexes the four possible combinations of the pair (q_1, q_2) , where $\ell = 1$ corresponds to $q_1 = q_2 = 1$. Using $\ell \in Q = \{1, 2, 3, 4\}$ as a logic state, and $Q = Q_s \cup Q_u$ where $Q_s = \{1\}$ and $Q_u = \{2, 3, 4\}$, we impose an average dwell-time bound of the form (76) on the jump times of ℓ^+ using the hybrid automaton (75), and an average activation bound (78) using the hybrid monitor (78). Additionally, since the switching plant admits a common Lyapunov function, we leverage proposition (1) and consider the differential inclusion (71) obtained from the two modes of the plant. The resulting system has the form (113), with main states $x_{u,z} = (\hat{u}, \ell, \tau_1, \tau_2)$. Figure 30 shows the trajectories of the state variables θ_1 for the players under the Nash-seeking dynamics with intermittent updates. The red shaded regions indicate time intervals during which player 2 does not update its action, while the blue shaded region corresponds to periods when player 1 does not update \hat{u}_1 . As observed, for a moderate value of η_2 , the trajectories still converge to a neighborhood of the Nash equilibrium, indicated by the dotted lines. However, the convergence time increases as $\eta_2 \rightarrow 1$. For related results in scenarios where q_i is allowed to take negative values—causing the nominal Nash-seeking dynamics to become unstable for bounded periods of time (i.e., in the presence of adversarial players)—we refer the reader to [91, Sec.6.3].

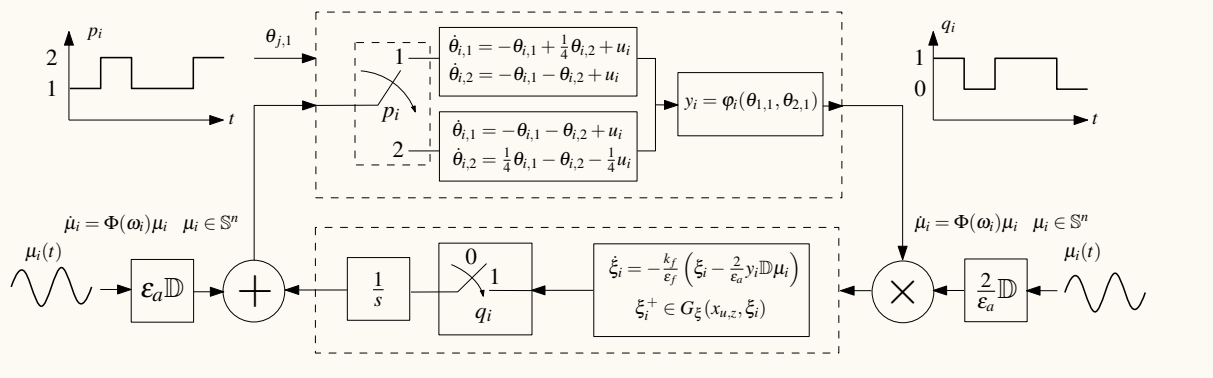


FIGURE 29 Block diagram representation of Nash-seeking dynamics under intermittent updates for players characterized by switching dynamical systems. The logic mode q_i indicates if the dynamics \hat{u}_i are inactive ($\hat{u}_i = 0$) or active ($\hat{u}_i = \xi$).

CONCLUDING REMARKS

Hybrid set-seeking systems extend traditional continuous-time extremum-seeking algorithms by enabling feedback schemes, algorithms, and plants that incorporate both continuous-time and discrete-time dynamics, and whose stability properties are studied with respect to general sets as opposed to equilibrium points. These systems naturally arise in applications that require switching between multiple controllers to meet stringent transient or steady-state specifications that cannot be achieved with smooth feedback alone. They are also relevant for "intelligent" controllers that use "if-then" rules. Hybrid set-seeking systems may also emerge when the seeking dynamics are smooth, but the plant under control exhibits hybrid behavior, such as jumps or impacts. Other potential applications include developing general, real-time, model-free optimization algorithms for cyber-physical systems, where digital components are integrated into physical plants, such as in sampled-data systems and event-triggered control. The analytical development of hybrid set-seeking systems builds on the traditional tools used for extremum-seeking control: averaging and singular perturbation theory. By extending these tools to hybrid systems, new families of model-free hybrid set-seeking systems can be constructed to emulate model-based hybrid decision-making algorithm. In this sense, working with hybrid time domains and dynamics that satisfy appropriate regularity conditions allows for the property of "closeness of solutions", which is crucial in the study of smooth ES systems, to be established for hybrid set-seeking systems as well. By leveraging both this property and the uniform stability of the target dynamics, semi-global stability can be demonstrated for general hybrid set-seeking dynamics.

The examples of hybrid set-seeking systems presented in this paper only begin to reveal the broad potential of hybrid extremum seeking and hybrid set-seeking in model-free control and optimization. These approaches open the door to novel controllers and algorithms capable of incorporating "if-then" logic through hybrid systems tools. Furthermore, such algorithms are expected to benefit from techniques developed in related fields, including

computer science, signal processing, and communications.

The approaches studied in this paper rely on conventional averaging techniques, often referred to as "first-order" averaging. However, over the past decade, a rich body of work in extremum seeking has emerged based on Lie-bracket and second-order averaging techniques, see [48], [95], [133], [144], [151], [160]–[162]. These methods are often better suited for applications involving geometric constraints, such as systems evolving on manifolds or non-holonomic systems. For a monograph on Lie-bracket-based extremum seeking with applications to model-free stabilization, we refer the reader to [163]. For hybrid tools similar to those discussed in this paper, which are applicable to Lie-bracket averaging-based systems, we refer the readers to [103], [164].

Finally, in addition to the development of these novel algorithms, several open problems remain in the context of hybrid seeking systems. These include the development of a comprehensive stability framework for seeking systems that incorporate stochastic behaviors during flows and jumps, as well as developing tools for interconnected networked seeking systems, i.e., "open extremum-seeking systems"—an under-explored area with numerous potential applications in complex engineering, biological, and socio-technical systems where multiple individual agents implement different adaptation and optimization algorithms for real-time decision making.

ACKNOWLEDGMENTS

Many of the developments reported in this article are a result of research supported by the Air Force Office of Scientific Research under grant number FA9550-22-1-0211, and the National Science Foundation under grant numbers CNS 1947613, ECCS CAREER 2305756, and CMMI 2228791.

AUTHOR INFORMATION

Jorge I. Poveda (poveda@ucsd.edu) received B.S. degrees in Electronics Engineering and Mechanical Engineering, both from the University of Los Andes, Bogotá, Colombia, in 2012. He

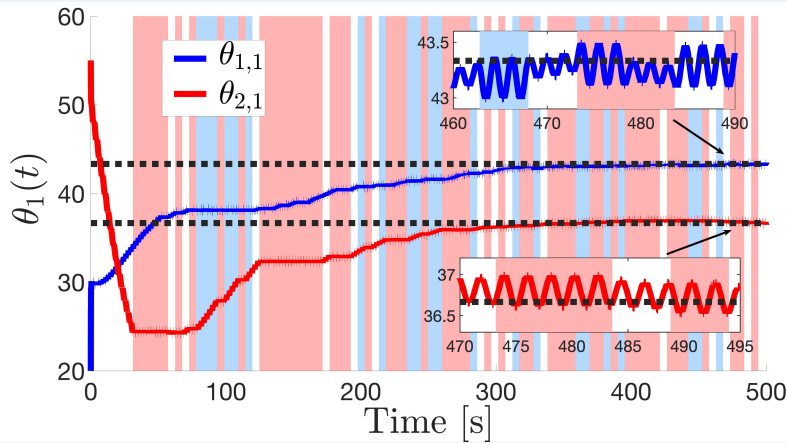


FIGURE 30 Evolution in time of the states $\theta_{i,1}$, for each player $i \in \{1, 2\}$, under intermittent updates of the Nash seeking dynamics. The colors (light blue and light red) of the shaded regions indicate times when $q_i = 0$ for each player i .

received M.Sc. and Ph.D. degrees in Electrical and Computer Engineering from the University of California, Santa Barbara, in 2016 and 2018, respectively. Subsequently, he was a Postdoctoral Fellow at Harvard University in 2018 and Assistant Professor at the University of Colorado (Boulder). Since 2022, he has been with the Department of Electrical and Computer Engineering at the University of California, San Diego, where he is currently Associate Professor. He is the recipient of the CRII and CAREER awards from NSF, the Young Investigator awards from AFOSR and SHPE, the 2023 Donald P. Eckman Award from AACC, the 2023 Best Paper Award from IEEE Transactions on Control of Network Systems, and the 2013 CCDC Outstanding Scholar Fellowship and 2020 Best Ph.D. Dissertation award from UCSB. Furthermore, he is an advisor for students selected as finalists for the Best Student Paper award at the 2024 American Control Conference and as winners of the Young Author Award at the 2024 IFAC Conference on Analysis and Design of Hybrid Systems. He was also a finalist for the Best Student Paper Award at the IEEE Conference on Decision and Control in 2017 (as a student) and 2021 (as a co-author). He has served as Associate Editor for Automatica, Nonlinear Analysis: Hybrid Systems, and IEEE Control Systems Letters.

Andrew R. Teel (teel@ucsb.edu) received his A.B. degree in Engineering Sciences from Dartmouth College in Hanover, New Hampshire, in 1987 and his M.S. and Ph.D. degrees in Electrical Engineering from the University of California, Berkeley, in 1989 and 1992, respectively. After receiving his Ph.D., he was a postdoctoral fellow at the Ecole des Mines de Paris in Fontainebleau, France. In 1992 he joined the faculty of the Electrical Engineering Department at the University of Minnesota, where he was an assistant professor until 1997. Subsequently, he joined the faculty of the Electrical and Computer Engineering Department at the University of California, Santa Barbara, where he is currently a Distinguished Professor and director of the Center

for Control, Dynamical systems, and Computation. His research interests are in nonlinear and hybrid dynamical systems, with a focus on stability analysis and control design. He has received NSF Research Initiation and CAREER Awards, the 1998 IEEE Leon K. Kirchmayer Prize Paper Award, the 1998 George S. Axelby Outstanding Paper Award, and was the recipient of the first SIAM Control and Systems Theory Prize in 1998. He was the recipient of the 1999 Donald P. Eckman Award and the 2001 O. Hugo Schuck Best Paper Award, both given by the American Automatic Control Council, and also received the 2010 IEEE Control Systems Magazine Outstanding Paper Award. In 2016, he received the Certificate of Excellent Achievements from the IFAC Technical Committee on Nonlinear Control Systems. In 2020, he and his co-authors received the HSCC Test-of-Time Award. He is Editor-in-Chief for Automatica, and a Fellow of the IEEE and of IFAC.

REFERENCES

- [1] A. M. Farid, “A hybrid dynamic system model for multimodal transportation electrification,” *IEEE Transactions on Control Systems Technology*, vol. 25, no. 3, pp. 940–951, 2016.
- [2] D. E. Ochoa, F. Galarza-Jimenez, F. Wilches-Bernal, D. A. Schoenwald, and J. I. Poveda, “Control systems for low-inertia power grids: A survey on virtual power plants,” *IEEE Access*, vol. 11, pp. 20560–20581, 2023.
- [3] A. D. Ames and I. Pouliquen, *Hybrid zero dynamics control of legged robots*. Butterworth-Heinemann Oxford, UK, 2017.
- [4] M. Senesky, G. Eirea, and T. J. Koo, “Hybrid modelling and control of power electronics,” in *International Workshop on Hybrid Systems: Computation and Control*. Springer, 2003, pp. 450–465.
- [5] D. Stewart, “Rigid-body dynamics with friction and impact,” *SIAM Rev.*, vol. 42, pp. 3–39, 2000.
- [6] B. Lennartson, M. Tittus, B. Egardt, and S. Pettersson, “Hybrid systems in process control,” *IEEE control systems magazine*, vol. 16, no. 5, pp. 45–56, 2002.
- [7] D. L. Pepyne and C. G. Cassandras, “Optimal control of hybrid systems in manufacturing,” *Proceedings of the IEEE*, vol. 88, no. 7, pp. 1108–1123, 2002.
- [8] R. Goebel, R. G. Sanfelice, and A. R. Teel, *Hybrid Dynamical Systems: Modeling, Stability, and Robustness*. Princeton University Press, 2012.
- [9] R. Sanfelice, *Hybrid Feedback Control*. Princeton, 2021.

[10] J. Lygeros, C. Tomlin, S. Sastry *et al.*, "Hybrid systems: modeling, analysis and control," *Electronic Research Laboratory, University of California, Berkeley, CA, Tech. Rep. UCB/ERL M*, vol. 99, p. 6, 2008.

[11] T. A. Henzinger, "The theory of hybrid automata," in *Proceedings 11th Annual IEEE Symposium on Logic in Computer Science*. IEEE, 1996, pp. 278–292.

[12] J. Lygeros, K. H. Johansson, S. N. Simic, J. Zhang, and S. S. Sastry, "Dynamical properties of hybrid automata," *IEEE Transactions on automatic control*, vol. 48, no. 1, pp. 2–17, 2003.

[13] L. Tavernini, "Differential automata and their discrete simulators," *Nonlinear Analysis: Theory, Methods & Applications*, vol. 11, no. 6, pp. 665–683, 1987.

[14] A. R. Teel and D. Popović, "Solving smooth and nonsmooth multivariable extremum seeking problems by the methods of nonlinear programming," *Proc. of the American Control Conference*, pp. 2394–2399, 2001.

[15] T. Pan, Z. Ji, and Z. Jiang, "Maximum power tracking of wind energy conversion systems based on sliding mode extremum seeking control," in *Proc. of the IEEE Energy Conference, Atlanta*, pp. 1–5, 2008.

[16] N. J. Killingsworth and M. Krstic, "PID tuning using extremum seeking: online, model-free performance optimization," *IEEE Control Systems Magazine*, vol. 26, no. 1, pp. 70–79, 2006.

[17] J. Cochran, E. Kanso, S. D. Kelly, H. Xiong, and M. Krstić, "Source seeking for two nonholonomic models of fish locomotion," *IEEE Trans. on Robotics*, vol. 25, pp. 1166–1176, 2009.

[18] H. Yu and U. Ozguner, "Extremum-seeking control strategy for ABS system with time delay," in *Proc. of American Control Conference*, pp. 3753–3758, 2002.

[19] M. Benosman, "Multi-parametric extremum seeking-based auto-tuning for robust input-output linearization control," *Int. Journal of Robust and Nonlinear Control*, vol. 26, no. 18, 2016.

[20] B. Ren, P. Frihauf, R. J. Rafac, and M. Krstic, "Laser pulse shaping via extremum seeking," *Control Engineering Practice*, vol. 20, no. 7, pp. 674–683, 2012.

[21] Z. Zhi-dan, H. Hai-bo, Z. Xin-jian, C. Guang-yi, and R. Yuan, "Adaptive maximum power point tracking control of fuel cell power plants," *Journal of Power Sources*, vol. 176, no. 1, pp. 259–269, 2008.

[22] M. Benosman and J. I. Poveda, "Robust source seeking and formation learning-based controller," *US Patent 10,915,108 B2*, 2019.

[23] Y. Li and E. Seem, "Extremum seeking control with actuator saturation control," *Patent: US 2010/0106331 A1*, 2010.

[24] A. Subbaraman and M. Benosman, "Extremum seeking-based iterative learning model predictive control (esilc-mpc)," in *12th IFAC Workshop on Adaptation and Learning in Control and Signal*, 2016, pp. 193–198.

[25] M. Abdelgalil, Y. Aboelkassem, and H. Taha, "Sea urchin sperm exploit extremum seeking control to find the egg," *Physical Review E*, vol. 106, no. 6, p. L062401, 2022.

[26] D. E. Ochoa and J. I. Poveda, "High-performance optimal incentive-seeking in transactive control for traffic congestion," *European Journal of Control*, vol. 68, p. 100696, 2022.

[27] H. Yu, S. Koga, T. R. Oliveira, and M. Krstic, "Extremum seeking for traffic congestion control with a downstream bottleneck," *Journal of Dynamic Systems, Measurement, and Control*, vol. 143, no. 3, p. 031007, 2021.

[28] A. A. Elgohary and S. A. Eisa, "Extremum seeking for controlled vibrational stabilization of mechanical systems: A variation-of-constant averaging approach inspired by flapping insects mechanics," *IEEE Control Systems Letters*, 2025.

[29] R. Suttner, "Extremum-seeking control for a class of mechanical systems," *IEEE Transactions on Automatic Control*, vol. 68, no. 2, pp. 1200–1207, 2022.

[30] ———, "Extremum seeking control for a class of nonholonomic systems," *SIAM Journal on Control and Optimization*, vol. 58, no. 4, pp. 2588–2615, 2020.

[31] S. Z. Khong, D. Nešić, Y. Tan, and C. Manzie, "Unified framework for sampled-data extremum seeking control: Global optimisation and multi-unit systems," *Automatica*, vol. 49, pp. 2720–2733, 2013.

[32] Y. Zhu, E. Fridman, and T. R. Oliveira, "Sampled-data extremum seeking with constant delay: a time-delay approach," *IEEE Transactions on Automatic Control*, vol. 68, no. 1, pp. 432–439, 2022.

[33] A. Scheinker, "100 years of extremum seeking: A survey," *Automatica*, vol. 161, p. 111481, 2024.

[34] Y. Tan, W. H., C. Manzie, D. Nešić, and I. Mareels, "Extremum seeking from 1922 to 2010," *Proceedings of the 29th Chinese Control Conference*, pp. 14–26, 2010.

[35] J. Sternby, "A review of extremum control," 1979.

[36] K. J. Astrom and B. Wittenmark, *Adaptive control*. Addison-Wesley Longman Publishing Co., Inc., 1994.

[37] M. Leblanc, "Sur l'electrification des chemins de fer au moyen de courants alternatifs de frequence elevee," *Rev. Gen. Electr.*, 1922.

[38] I. S. Morosanov, "Method of extremum control," *Automatic and Remote Control*, vol. 18, pp. 1077–1092, 1957.

[39] S. M. Meerkov, "Asymptotic methods for investigating quasi-stationary states in continuous systems of automatic optimization," *Automatic and Remote Control*, vol. 11, pp. 1726–1743, 1967.

[40] ———, "Averaging of trajectories of slow dynamic systems," *Differentsial'nye Uravneniya*, vol. 9, pp. 1609–1617, 1973.

[41] A. Krasovskii, "Dynamics of continuous self-tuning systems," *Moscow: Fizmatgiz*, 1963.

[42] P. Chinaev, "Self-tuning systems handbook," *Automn. Remote Control*, vol. 22, pp. 1–12, 1969.

[43] K. J. Astrom and B. Wittenmark, *Adaptive Control*. Addison-Wesley Publishing Company, 1989.

[44] M. Krstić and H.-H. Wang, "Stability of extremum seeking feedback for general nonlinear dynamic systems," *Automatica*, vol. 36, no. 4, pp. 595–601, 2000.

[45] K. B. Ariyur and M. Krstić, *Real-Time Optimization by Extremum-Seeking Control*. Wiley, 2003.

[46] C. Zhang and R. Ordóñez, *Extremum-Seeking Control and Applications: A Numerical Optimization Based Approach*. Springer, 2012.

[47] A. Scheinker and M. Krstic, *Model-Free Stabilization by Extremum Seeking*. Springer, 2017.

[48] H. Dürr, M. Stanković, C. Ebenbauer, and K. H. Johansson, "Lie bracket approximation of extremum seeking systems," *Automatica*, vol. 49, pp. 1538–1552, 2013.

[49] W. H. Moase and C. Manzie, "Fast extremum-seeking for Wiener-Hammerstein plants," *Automatica*, vol. 48, pp. 2433–2443, 2012.

[50] M. Benosman, *Learning-Based Adaptive Control: An Extremum Seeking Approach - Theory and Applications*. Cambridge, MA: Butterworth-Heinemann, 2016.

[51] P. Frihauf, M. Krstic, and T. Basar, "Nash equilibrium seeking in noncooperative games," *IEEE Transactions on Automatic Control*, vol. 57, no. 5, pp. 1192–1207, 2012.

[52] S. Dougherty and M. Guay, "An extremum-seeking controller for distributed optimization over sensor networks," *IEEE Transactions on Automatic Control*, vol. 62, no. 2, pp. 930–933, 2017.

[53] J. Poveda and N. Quijano, "Distributed extremum seeking for real-time resource allocation," in *Proc. of American Control Conference*, pp. 2772–2777, 2013.

[54] J. Feiling, S. Koga, M. Krstić, and T. R. Oliveira, "Gradient extremum seeking for static maps with actuation dynamics governed by diffusion pdes," *Automatica*, vol. 95, pp. 197–206, 2018.

[55] S. Liu and M. Krstic, "Stochastic Nash equilibrium seeking for games with general nonlinear payoffs," *SIAM J. Control Optim.*, vol. 49, no. 4, pp. 1659–1679, 2011.

[56] F. Verhulst, *Nonlinear Differential Equations and Dynamical Systems*. Springer, 1996.

[57] H. K. Khalil, *Nonlinear Systems*. Prentice Hall, 2002.

[58] P. Kokotović, H. K. Khalil, and J. O'Reilly, *Singular Perturbation Methods in Control: Analysis and Design*. Academic Press, 1986.

[59] A. R. Teel, L. Moreau, and D. Nešić, "A Unified Framework for Input-to-State Stability in Systems With Two Time Scales," *IEEE Trans. Autom. Control*, vol. 48, pp. 1526–1544, 2003.

[60] F. Lamnabhi-Lagarrigue, A. Annaswamy, S. Engel, A. Isaksson, P. Kharagonekar, R. M. Murray, H. Nijmeijer, T. Samad, D. Tilbury, and P. V. den Hof, "Systems & Control for the future of humanity, research agenda: Current and future roles, impact and grand challenges," *Annual Reviews in Control*, vol. 43, pp. 1–64, 2017.

[61] R. G. Sanfelice, *Analysis and design of cyber-physical systems: a hybrid control systems approach*. Boca Raton, FL, USA: CRC Press, 2016, ch. Cyber-physical systems: From theory to practice, pp. 3–31.

[62] J. C. Luxat and L. H. Lees, "Stability of peak-holding control systems," *IEEE Transactions on Industrial Electronics and Control Instrumentation*, no. 1, pp. 11–15, 1971.

[63] S. J. Moura and Y. A. Chang, "Lyapunov-based switched extremum seeking for

photovoltaic power maximization," *Control Engineering Practice*, vol. 21, no. 7, pp. 971–980, 2013.

[64] D. Nešić, Y. Tan, C. Manzie, A. Mohammadi, and W. Moase, "A Unifying Framework for Analysis and Design of Extremum Seeking Controllers," in *Proc. of IEEE Chinese Control and Decision Conference*, pp. 4274–4285, 2012.

[65] D. Nešić, Y. Tan, W. H. Moase, and C. Manzie, "A unifying approach to extremum seeking: Adaptive schemes based on estimation of derivatives," *49th IEEE Conference on Decision and Control*, pp. 4625–4630, 2010.

[66] Y. Tan, D. Nešić, and I. Mareels, "On non-local stability properties of extremum seeking controllers," *Automatica*, vol. 42, no. 6, pp. 889–903, 2006.

[67] N. Mimmo, L. Marconi, and G. Notarstefano, "Uniform non-convex optimisation via extremum seeking," *IEEE Transactions on Automatic Control*, 2024.

[68] A. R. Teel and L. Praly, "A smooth Lyapunov function from a Class-KL estimate involving two positive semidefinite functions," *ESAIM: Control, Optimisation and Calculus of Variations*, pp. 313–367, 2000.

[69] J. I. Poveda and N. Li, "Robust hybrid zero-order optimization algorithms with acceleration via averaging in continuous time," *Automatica*, vol. 123, 2021.

[70] X. Chen, J. I. Poveda, and N. Li, "Continuous-time zeroth-order dynamics with projection maps: Model-free feedback optimization with safety guarantees," *IEEE Transactions on Automatic Control*, vol. 70, pp. 5005–5020, 2025.

[71] J. Poveda and N. Quijano, "A shahshahani gradient based extremum seeking scheme," in *Proc. of Conference on Decision and Control (CDC)*, pp. 5104–5109, 2012.

[72] A. Ghaffari, M. Krstić, and D. Nešić, "Multivariable newton-based extremum seeking," *Automatica*, vol. 48, pp. 1759–1767, 2012.

[73] M. Ye, Q.-L. Han, L. Ding, and S. Xu, "Distributed Nash equilibrium seeking in games with partial decision information: A survey," *Proceedings of the IEEE*, vol. 111, no. 2, pp. 140–157, 2023.

[74] R. Goebel, R. G. Sanfelice, and A. R. Teel, "Hybrid dynamical systems," *IEEE Control Systems Magazine*, vol. 29, no. 2, pp. 28–93, 2009.

[75] R. K. Goebel, *Set-Valued, Convex, and Nonsmooth Analysis in Dynamics and Control: An Introduction*. SIAM, 2024.

[76] D. Liberzon, *Switching in Systems and Control*. Boston, MA.: Birkhäuser, 2003.

[77] G. Bianchin, J. I. Poveda, and E. Dall'Anese, "Feedback optimization of switched linear systems via continuous-time and hybrid accelerated gradient flows," *Automatica*, 2022.

[78] W. M. Haddad, V. Chellaboina, and S. G. Nersesov, *Impulsive and Hybrid Dynamical Systems: Stability, Dissipativity, and Control*. NJ, Princeton: Princeton University Press, 2006.

[79] K. Astrom and B. Bernhardsson, "Comparison of periodic and event based sampling for first order stochastic systems," in *Proc. IFAC World Conf.*, pp. 301–306, 1999.

[80] J. Hespanha and A. Morse, "Stability of switched systems with average dwell-time," *38th IEEE Conf. Decision Control*, vol. 3, pp. 2655–2660, 1999.

[81] H. Hajieghrary, D. Mox, and M. A. Hsieh, "Information theoretic source seeking strategies for multiagent plume tracking in turbulent fields," *Journal of Marine Science and Engineering*, vol. 5, 2017.

[82] N. Ghods and M. Krstić, "Multi-agent deployment around a source in one dimension by extremum seeking," *2010 American Control Conference*, pp. 4794–4799, 2010.

[83] J. I. Poveda, M. Benosman, A. R. Teel, and R. G. Sanfelice, "Robust coordinated hybrid source seeking with obstacle avoidance in multivehicle autonomous systems," *IEEE Transactions on Automatic Control*, vol. 67, no. 2, pp. 706–721, 2021.

[84] C. Zhang, A. Siranosian, and M. Krstić, "Extremum seeking for moderately unstable systems and for autonomous vehicle target tracking without position measurements," *Automatica*, pp. 1832–1839, 2007.

[85] A. Morse, "Supervisory control of families of linear set-point controllers-part I: Exact matching," *IEEE Trans. Autom. Control*, vol. 41, pp. 1413–1431, 1996.

[86] M. Baradaran and A. R. Teel, "Omega-limit sets and robust stability for switched systems with distinct equilibria," *IFAC-PapersOnLine*, vol. 53, no. 2, pp. 2039–2044, 2020.

[87] R. T. Rockafellar and R. J. Wets, *Variational Analysis*. Springer, 1998.

[88] D. Popović, *Topics in Extremum Seeking*, PhD Thesis. CA, USA: University of California, Santa Barbara, 2004.

[89] S. Z. Khong, Y. Tan, C. Manzie, and D. Nesic, "Multi-agent source seeking via discrete-time extremum seeking control," *Automatica*, vol. 50, no. 9, pp. 2312–2320, 2014.

[90] D. Ochoa and J. I. Poveda, "Momentum-based Nash equilibrium seeking over networks via multi-time scale hybrid inclusions," *IEEE Transactions on Automatic Control*, vol. 69, pp. 4245–4260, 2024.

[91] J. I. Poveda and A. R. Teel, "A framework for a class of hybrid extremum seeking controllers with dynamic inclusions," *Automatica*, vol. 76, pp. 113–126, 2017.

[92] ———, "The heavy-ball ODE with time-varying damping: Persistence of excitation and uniform asymptotic stability," in *Proc. of American Control Conference, to appear*, pp. 773–778, 2020.

[93] J. I. Poveda and N. Li, "Inducing uniform asymptotic stability in time-varying accelerated optimization dynamics via hybrid regularization," *58th IEEE Conference on Decision and Control*, pp. 3000–3005, 2019.

[94] A. R. Teel, J. I. Poveda, and J. Le, "First-order optimization algorithms with resets and hamiltonian flows," in *2019 IEEE 58th Conference on Decision and Control (CDC)*. IEEE, 2019, pp. 5838–5843.

[95] M. Abdelgalil and J. I. Poveda, "Initialization-free lie-bracket extremum seeking," *Systems & Control Letters*, vol. 191, p. 105881, 2024.

[96] R. Suttner, "Extremum seeking control with an adaptive dither signal," *Automatica*, vol. 101, pp. 214–222, 2019.

[97] M. Weber, B. Gharesifard, and C. Ebenbauer, "Inferring global exponential stability properties using lie-bracket approximations," *IEEE Conference on Decision and Control*, pp. 6274–6279, 2024.

[98] J. Sanders and F. Verhulst, *Averaging Methods in Nonlinear Dynamical Systems*. New York, NY: Springer-Verlag, 1985.

[99] A. R. Teel and D. Nešić, "Averaging theory for a class of hybrid systems," *Dynamics of Continuous, Discrete and Impulsive Systems*, vol. 17, pp. 829–851, 2010.

[100] W. Wang, A. R. Teel, and D. Nešić, "Averaging in singularly perturbed hybrid systems with hybrid boundary layer systems," in *2012 IEEE 51st IEEE Conference on Decision and Control (CDC)*. IEEE, 2012, pp. 6855–6860.

[101] W. Wang, D. Nesic, and A. R. Teel, "Input-to-state stability for a class of hybrid dynamical systems via averaging," *Mathematics of Control, Signals, and Systems volume*, vol. 23, pp. 223–256, 2012.

[102] M. Abdelgalil, D. E. Ochoa, and J. I. Poveda, "Multi-time scale control and optimization via averaging and singular perturbation theory: From odes to hybrid dynamical systems," *Annual Reviews in Control*, vol. 56, p. 100926, 2023.

[103] M. Abdelgalil and J. I. Poveda, "On Lie-Bracket averaging for a class of hybrid dynamical systems with applications to model-free control and optimization," *IEEE Transactions on Automatic Control*, vol. 70, pp. 4655–4670, 2025.

[104] R. Kutadinata, W. H. Moase, and C. Manzie, "Dither re-use in nash equilibrium seeking," *IEEE Trans. Autom. Control*, vol. 60, pp. 1433–1438, 2015.

[105] M. Stanković, K. H. Johansson, and D. M. Stipanović, "Distributed seeking of Nash equilibria with applications to mobile sensor networks," *IEEE Transactions on Automatic Control*, vol. 57, no. 4, pp. 904–919, 2012.

[106] J. I. Poveda and N. Quijano, "Shahshahani gradient-like extremum seeking," *Automatica*, vol. 58, pp. 51–59, 2015.

[107] J. I. Poveda, M. Krstić, and T. Başar, "Fixed-time nash equilibrium seeking in time-varying networks," *IEEE Transactions on Automatic Control*, vol. 68, no. 4, pp. 1954–1969, 2022.

[108] J. I. Poveda, R. Kutadinata, C. Manzie, D. Nešić, A. R. Teel, and C. Liao, "Hybrid extremum seeking for black-box optimization in hybrid plants: An analytical framework," *57th IEEE Conference on Decision and Control*, pp. 2235–2240, 2018.

[109] W. Moase, Y. Tan, D. Nešić, and C. Manzie, "Non-local stability of a multi-variable extremum-seeking scheme," in *Proc. of IEEE Australian Control Conference*, pp. 38–43, 2011.

[110] E. D. Sontag, "Stability and stabilization: discontinuities and the effect of disturbances," in *Nonlinear analysis, differential equations and control*. Springer, 1999, pp. 551–598.

[111] T. Strizic, J. I. Poveda, and A. R. Teel, "Hybrid gradient descent for robust global optimization on the circle," *56th IEEE Conference on Decision and Control*, pp. 2985–2990, 2017.

[112] D. Ochoa and J. I. Poveda, "Robust global optimization on smooth compact manifolds via hybrid gradient-free dynamics," *Automatica*, vol. 171, p. 111916, 2025.

[113] O'Donoghue and E. J. Candes, "Adaptive restart for accelerated gradient schemes," *Foundations of Computational Mathematics*, vol. 15, no. 3, pp. 715–

[114] W. Su, S. Boyd, and E. Candes, "A differential equation for modeling Nesterov's accelerated gradient method: Theory and insights," *Journal of Machine Learning Research*, vol. 17, no. 153, pp. 1–43, 2016.

[115] F. Galarza-Jimenez, J. I. Poveda, R. Kutadinata, L. Zhang, and E. Dall'Anese, "Self-optimizing traffic light control using hybrid accelerated extremum seeking," in *2021 60th IEEE Conference on Decision and Control (CDC)*. IEEE, 2021, pp. 1941–1946.

[116] F. Galarza, J. I. Poveda, G. Bianchi, and E. Dalleneise, "Extremum seeking under persistent gradient deception: A switching systems approach," *IEEE Control Systems Letters*, pp. 133–138, 2021.

[117] J. I. Poveda and M. Krstic, "Fixed-time newton-like extremum seeking," in *Proc. of IFAC World Congress*, pp. 1–6, 2020.

[118] W. Sandholm, *Population Games and Evolutionary Dynamics*. The MIT Press, 2010.

[119] F. H. Clarke, *Optimization and Nonsmooth Analysis*. Philadelphia: SIAM, 1990.

[120] F. H. Clarke, Y. S. Ledyaev, R. J. Stern, and P. R. Wolenski, "Nonsmooth analysis and control theory," *Graduate Texts in Mathematics*, Springer-Verlag, New York, vol. 178, 1998.

[121] C. Henry, "An existence theorem for a class of differential equations with multivalued right-hand side," *J. Math. Anal. Appl.*, vol. 41, no. 1, pp. 179–186, 1973.

[122] F. Galarza-Jimenez, J. Poveda, and E. Dall'Anese, "Sliding-seeking control: Model-free optimization with safety constraints," in *Learning for Dynamics and Control Conference*. PMLR, 2022, pp. 1100–1111.

[123] J. I. Poveda and M. Krstic, "Fixed-time seeking and tracking of time-varying extrema," in *2021 60th IEEE Conference on Decision and Control (CDC)*. IEEE, 2021, pp. 108–113.

[124] J. Poveda and M. Krstic, "Non-smooth extremum seeking control with user-prescribed convergence," *IEEE Transactions on Automatic Control*, vol. 66, pp. 6156 – 6163, 2021.

[125] R. Kamalapurkar, J. A. Rosenfeld, A. Parikh, A. R. Teel, and W. E. Dixon, "Invariance-like results for nonautonomous switched systems," *IEEE Transactions on Automatic Control*, vol. 64, no. 2, pp. 614–627, 2018.

[126] A. Bhaya and E. Kaszkurewicz, *Control perspectives on numerical algorithms and matrix problems*. SIAM, 2006.

[127] R. Olfati-Saber and R. Murray, "Consensus problems in networks of agents with switching topology and time-delays," *IEEE Transactions on Automatic Control*, vol. 49, pp. 1520–1533, 2004.

[128] J. I. Poveda, M. Benosman, and A. R. Teel, "Distributed extremum seeking in multi-agent systems with arbitrary switching graphs," *IFAC World Congress*, vol. 50, no. 1, pp. 735–740, 2016.

[129] P. Lin, W. Ren, and J. A. Farrell, "Distributed continuous-time optimization: nonuniform gradient gains, finite-time convergence, and convex constraint set," *IEEE Transactions on Automatic Control*, vol. 62, no. 5, pp. 2239–2253, 2016.

[130] C. Cai, A. R. Teel, and R. Goebel, "Smooth Lyapunov functions for hybrid systems. part II: (pre)asymptotically stable compact sets," *IEEE Transactions on Automatic Control*, vol. 53, no. 3, pp. 734–748, 2008.

[131] F. Galarza-Jimenez, G. Bianchin, J. I. Poveda, and E. Dall'Anese, "Online optimization of LTI systems under persistent attacks: Stability, tracking and robustness," *Nonlinear Analysis: Hybrid Systems*, 2022.

[132] A. Scheinker and M. Krstic, "Extremum seeking-based tracking for unknown systems with unknown control directions," in *2012 IEEE 51st IEEE Conference on Decision and Control (CDC)*. IEEE, 2012, pp. 6065–6070.

[133] C. Labar, C. Ebenbauer, and L. Marconi, "ISS-like properties in Lie-bracket approximations and application to extremum seeking," *Automatica*, vol. 136, p. 110041, 2022.

[134] M. Jankovic, M. Santillo, and Y. Wang, "Multiagent systems with CBF-based controllers: Collision avoidance and liveness from instability," *IEEE Transactions on Control Systems Technology*, vol. 32, no. 2, pp. 705–712, 2023.

[135] M. Marley, R. Skjetne, and A. R. Teel, "Hybrid control barrier functions for continuous-time systems," *IEEE Transactions on Automatic Control*, 2024.

[136] D. E. Koditschek and E. Rimon, "Robot navigation functions on manifolds with boundary," *Advances in applied mathematics*, vol. 11, no. 4, pp. 412–442, 1990.

[137] R. G. Sanfelice, M. J. Messina, S. E. Tuna, and A. R. Teel, "Robust hybrid controllers for continuous-time systems with applications to obstacle avoidance and regulation to disconnected set of points," in *Proc. of American Control Conference*, pp. 3352–3357, 2006.

[138] S. Berkane, A. Bisoffi, and D. V. Dimarogonas, "Obstacle avoidance via hybrid feedback," *IEEE Transactions on Automatic Control*, vol. 67, no. 1, pp. 512–519, 2021.

[139] M. Sawant, I. Polushin, and A. Tayebi, "Hybrid feedback control design for non-convex obstacle avoidance," *IEEE Transactions on Automatic Control*, 2024.

[140] P. Jain and P. Kar, "Non-convex optimization for machine learning," *Foundations and Trends in Machine Learning*, 2017.

[141] D. Nesic, A. R. Teel, and L. Zaccarian, "Stability and performance of siso control systems with first-order reset elements," *IEEE Transactions on Automatic Control*, vol. 56, no. 11, pp. 2567–2582, 2011.

[142] G. Zhao, D. Nešić, Y. Tan, and C. Hua, "Overcoming overshoot performance limitations of linear systems with reset control," *Automatica*, vol. 101, pp. 27–35, 2019.

[143] J. Zhang, A. Mokhtari, S. Sra, and A. Jadbabaie, "Direct Runge-Kutta discretization achieves acceleration," *Advances in neural information processing systems*, vol. 31, 2018.

[144] S. Michalowsky and C. Ebenbauer, "The multidimensional n-th order heavy ball method and its application to extremum seeking," in *53rd IEEE Conference on Decision and Control*. IEEE, 2014, pp. 2660–2666.

[145] M. Laborde and A. Oberman, "A Lyapunov analysis for accelerated gradient methods: From deterministic to stochastic case," in *International Conference on Artificial Intelligence and Statistics*. PMLR, 2020, pp. 602–612.

[146] H. Yu, S. Koga, and T. Oliveira, "Extremum seeking for traffic congestion control with a downstream bottleneck," *Journal of Dynamic Systems, Measurement, and Control*, vol. 143, 2021.

[147] S. Krilašević and S. Grammatico, "Learning generalized nash equilibria in monotone games: A hybrid adaptive extremum seeking control approach," *Automatica*, vol. 151, p. 110931, 2023.

[148] J. I. Poveda and A. R. Teel, "Hybrid mechanisms for robust synchronization and coordination of multi-agent networked sampled-data systems," *Automatica*, vol. 99, pp. 41–53, 2019.

[149] J. Martens and I. Sutskever, "Training deep and recurrent networks with hessian-free optimization," in *Neural Networks: Tricks of the Trade: Second Edition*. Springer, 2012, pp. 479–535.

[150] H. Attouch and P. Redont, "The second-order in time continuous newton method," in *Approximation, optimization and mathematical economics*. Springer, 2001, pp. 25–36.

[151] C. Labar, E. Garone, M. Kinnaert, and C. Ebenbauer, "Newton-based extremum seeking: A second-order lie bracket approximation approach," *Automatica*, vol. 105, pp. 356–367, 2019.

[152] W. Wang, A. Teel, and D. Nešić, "Analysis for a class of singularly perturbed hybrid systems via averaging," *Automatica*, vol. 48, no. 6, 2012.

[153] A. Saberi and H. Khalil, "Quadratic-type Lyapunov functions for singularly perturbed systems," *IEEE Transactions on Automatic Control*, vol. 29, pp. 542–550, 1984.

[154] Y. V. Orlov, *Discontinuous Systems, Lyapunov Analysis and Robust Synthesis under Uncertainty Conditions*. Springer, 2009.

[155] D. Shevitz and B. Paden, "Lyapunov stability theory of nonsmooth systems," *IEEE Trans. Autom. Control*, vol. 39, pp. 1910–1914, 1994.

[156] W. Wang, A. R. Teel, and D. Nešić, "Averaging in singularly perturbed hybrid systems with hybrid boundary layer systems," *51st IEEE Conference on Decision and Control*, pp. 6855–6860, 2012.

[157] R. J. Kutadinata, W. Moase, and C. Manzie, "Extremum-seeking in singularly perturbed hybrid systems," *IEEE Transactions on Automatic and Control*, vol. 62, no. 6, pp. 3014–3020, 2017.

[158] R. Kutadinata, W. Moase, C. Manzie, L. Zhang, and T. Garoni, "Enhancing the performance of existing urban traffic light control through extremum-seeking," *Transportation Research Part C: Emerging Technologies*, vol. 62, pp. 1–20, 2016.

[159] R. Sanfelice and A. R. Teel, "Dynamical properties of hybrid systems simulators," *Automatica*, vol. 46, no. 2, pp. 239–248, 2010.

[160] V. Grushkovskaya, H.-B. Durr, C. Ebenbauer, and A. Zuyev, "Extremum seeking for time-varying functions using lie bracket approximations," *IFAC-Papers Online*, vol. 50, pp. 5522–5528, 2017.

[161] C. Labar, C. Ebenbauer, and L. Marconi, "Extremum seeking with intermittent measurements: A Lie-brackets approach," *IEEE Transactions on Automatic Control*, vol. 67, no. 12, pp. 6968–6974, 2022.

[162] V. Grushkovskaya, A. Zuyev, and C. Ebenbauer, "On a class of generating

vector fields for the extremum seeking problem: Lie bracket approximation and stability properties," *Automatica*, vol. 94, pp. 151–160, 2018.

[163] A. Scheinker and M. Krstić, "Non- c^2 lie bracket averaging for nonsmooth extremum seekers," *ASME. J. Dyn. Sys., Meas., Control*, vol. 136, no. 1, 2013.

[164] M. Abdelgalil and J. I. Poveda, "Hybrid minimum-seeking in synergistic Lyapunov functions: Robust global stabilization under unknown control directions," *arXiv preprint arXiv:2408.04882*, 2024.